Transport Effects on Calorimetry of Porous Wildland Fuels

Christopher F. Schemel

Doctor of Philosophy

The University of Edinburgh

2008

This dissertation and Ph.D. are dedicated to all who suffer cancer and offered in solidarity with those unable to fulfil their dreams.

DECLARATION

I declare that the overall research project direction, experimental design and the thesis document including all conclusions were the sole work of Christopher F. Schemel. Over the course of the research project many experiments were conducted with aid and advice provided by Juan de Dios Rivera, Ph.D. and Albert Simeoni Ph.D. both of whom were willing supporters of the work and granted permission for their contribution to be used as part of this research project. I made a substantial contribution to all group work as evidenced by being first author on the published papers pertaining to the joint work. This work was done under the supervision of Professor Jose L. Torero. This work has not been submitted for any other degree or professional qualification.

_____

Christopher F. Schemel
University of Edinburgh

ABSTRACT

Wildland fire is a natural part of the earth's phenomenological pattern and like most natural phenomena has presented a challenge to human activity and engineering science. Wildfire presents Fire Safety Engineering with the task of developing fundamental research and designing analysis tools to address fire on a scale where interactions with atmospheric and terrestrial conditions dominate fire behavior. The research work presented in this thesis addresses a fundamental research issue involving transport processes in porous wildland fuel beds. This research project had the specific goal of developing an understanding of how transport processes affected the combustion of wildland fuels that were in the form of a porous bed. No detailed study could be found in the literature that specifically addressed how the fuel structure affected the combustion process in these types of fuels. To this end, a series of experiments were designed and carried out that approached the understanding of this problem using commonly available fire testing equipment, specifically the cone calorimeter and the FM Global Fire Propagation Apparatus. The goal of this research study and the basis for the novel and relevant contribution to the field of engineering was to conduct an experimental test series, analyze the data and examine the scalability of the results, to determine the effect of transport processes on the Heat Release Rate (HRR) of porous wildland fuels. The project concluded that flow dominates HRR in fires involving the wildland fuels tested. A dimensionless analysis of the fuel sample baskets showed consistency with well established mass transfer, fluid flow and chemical kinetic relationships. The dimensionless analysis also indicates that the experimental results should be scalable to similar configurations in larger fuel beds. One conclusion of this study was that wildland fire modeling efforts should invest in understanding flow conditions in fuel beds because this behavior dominates over the chemical kinetics of combustion for predicting HRR which is an important parameter in fire modeling.

ACKNOWLEDGEMENTS

This dissertation and Ph.D. program would not have been undertaken nor successfully completed without the insightful leadership and inspired teaching of my supervisor Professor Jose L. Torero, the vision for engineering excellence and commitment to employee development of Ken Packer and Charlotte Sartain of Packer Engineering, Inc., and the unshakable support and belief in my dreams offered by my beautiful loving wife Shannon. My two sons, Zachariah and Elijah, strengthened me with their love and have been a constant reminder that the work of this generation only derives enduring meaning if serving the well being of the next.

Albert Simeoni played an essential role in teaching me how to engage only the most exacting standards of detail and consistency when conducting an experimental program. Juan de Dios Rivera inspires as a committed professional who maintains passion for his family and enthusiasm for life. Guillermo Rein gave meaningful guidance at critical points of this program, advancing me and my research. I also thank all of the people of the Fire Safety Engineering Group at the University of Edinburgh. Their support went beyond all my expectations.

I owe a great personal debt to Vincent Van Brunt, who for over 10 years mentored and taught me what it means to be an engineer.

I am enormously grateful to the cancer care givers and researchers at the University of Maryland, especially Aaron Rapoport, Michael Garofalo and Susan Hodges. Without their professional commitment this document and degree program never would have been finished. Additionally, Father Bill, Chaplin at the University of Maryland Medical Centre, is a constant reminder that as science and technology advance to better serve human welfare, it is only through our connections with one another and faith in God's love that we can offer hope to sorely felt need, and realize the promise that our troubles can transform to joy.

TABLE OF CONTENTS

LIST OF FIGURES

LIST OF TABLES

NOMENCLATURE

A	Cross-sectional area of the exhaust duct, m^2
E	Energy release per unit mass, kJ/kg
K	Pitot tube coefficient
k	Reaction constant, s (or) s^{-1}
k_B	Boltzmann's constant
k_g	Mass transfer coefficient
M	Molecular weight, $g.mol^{-1}$
m	Mass, kg
$\dot{m}$	Mass flow rate, $kg.s^{-1}$
n	Number of moles
P	Pressure, N/m^2
P_t	Absolute pressure, N/m^2
ΔP	Pressure drop in the Pitot tube, Pa
$\dot{q}$	Heat Release Rate, kW
R	Gas Constant, J K^{-1} mol^{-1}
T	Temperature, K
t	Time, s
t_1	Time at 28.3% of reaction
t_2	Time at 63.2% of reaction
u	Velocity, m/s
$\dot{V}$	Volumetric Flow Rate, m^3/s
χ	Conversion of fuel
Y	Molar fraction

Greek Symbols

α	Expansion factor
ρ	Density, $kg.m^{-3}$
ϕ	Oxygen depletion
τ	Time constant, s
μ	Viscosity, cP

Dimensionless Groups

Da	Damköhler Number
Re″	Reynolds Number

Subscripts

a	Incoming gas
c	Combustion
e	Exhaust gas

Species Subscripts

O_2	Oxygen
H_2O	Water
N_2	Nitrogen

Superscript

A	Measured analyzer value
0	Initial conditions

Acronyms

ANOVA	Analysis of Variance
CFD	Computational Fluid Dynamics
FPA	Fire Propagation Apparatus
HRR	Heat Release Rate
PIV	Particle Image Velocimetry

1.0 INTRODUCTION

Wildland fire is a natural part of the earth's phenomenological pattern and like most natural phenomena has presented a challenge to human activity. Wildland fire and human interaction usually manifests with undesirable outcomes involving the loss of life and property, use of expensive resources for fire mitigation, and systemic forest mismanagement. As with most threats from natural phenomenon, wildland fire presents an opportunity for engineering science to address the overlap of nature and human activity. Engineered systems can be designed to modify the outcome of natural phenomenon by minimizing detrimental consequences to people and providing better management of natural resources.

Wildfire presents Fire Safety Engineering with the task of designing protection and suppression schemes, developing building designs, creating applicable analysis tools and producing other engineered systems that address fire on several scales. Interactions with atmospheric and terrestrial conditions dominate the wildland fire behavior from a global perspective. These large scale conditions establish the large scale boundary conditions of the wildland fire problem; however, the physical problem of combustion takes place on the molecular level. Both of these scales must be addressed in any wildfire analysis method.

A challenge exists in developing experimental methods of analysis that effectively address wildfire systematically. Small scale fire experiments need to be designed so that they allow a particular phenomenon to be studied under conditions that are relevant to fire behavior on a larger scale. Experimental designs must break down global wildland fire conditions into elements that can be studied in meaningful ways with control over parameters of interest and measurement of useful variables.

The research project presented in this thesis was designed consistent with the idea of segmenting wildland fire behavior at the macro level by identifying a large

scale physical phenomenon of interest with a mechanism of behavior controlled at the micro level. In particular, this research project examined how transport processes effected the burning of two varieties of pine needles. The transport processes in this study were defined by air flow and the combustion processes involved the movement of matter and energy around the surfaces of a bed of pine needles. Air flow conditions in wildland fuel beds are dominated by wind and other large scale features that take place on a global scale, but transport and combustion inside fuel beds is dependant on a length scale of mm or less.

The pine needles studied in this project were *Pinus pinaster* and *Pinus halepensis* and were chosen for a few reasons. Pine needles have a consistent overall structure and other physical characteristics that provide for good comparison, contrast of test conditions and potentially repeatable testing conditions. This made them good candidates for an experimental program. Additionally, when pine needles are found on the forest floor, they comprise a porous fuel bed. A porous wildland fuel bed has a structure that creates void spaces of gas between solid fuel particles. A third consideration was that pine needles present a significant fire hazard because of the continuous nature of the fuel matrix across a forest floor. Most fire spread in wildland fires is the result of forest floor fuels [1,2].

In flaming wildland fires, the transport processes of concern are generally highly dependant on the flow of gases. In wildland fire the flow conditions external to the fuel bed are generally controlled by meteorological conditions and characterizing how these flow effect internal flow conditions in the fuel beds is one of the most difficult problems in predicting wildland fire [3]. Transport processes supply oxygen to the fuel bed that can lead to propagation of the combustion reaction, in addition to transporting energy away from the combustion reaction zone. Porous fuels allow fresh air, driven by wind and affected by topographical conditions, to enter the fuel matrix created by the porous structure of the fuel. This flow containing mass and heat generated by the combustion and

pyrolysis reactions, in turn, moves away from the fuel bed, leading to fire spread and fire damage.

Fire Safety Engineering can provide many design tools for application to wildland fire analysis. One class of analysis tools that requires further development, but can potentially provide tremendous support in wildland fire analysis, are predictive fire growth models. One area that requires research to develop better wildland fire growth models involves the analysis of transport processes in porous fuels under wildland fire conditions. In wildland fire modeling it is important to have an accurate understanding of and how transport affects the Heat Release Rate (HRR) of the fuel for different conditions. HRR is one of the most important parameters in fire analysis because it defines fire size and is extensively used in fire modeling [4]. To further develop wildland fire modeling, at least with respect to fire spread in porous fuels, detailed experimental studies need to be conducted to examine the effect of transport on HRR in porous fuel beds. As will be illustrated in the Background Section of this thesis, very little data exists on how air flow and, in turn, transport processes affects HRR in porous fuel bed s.

The details of this research project are presented in this thesis. The background section builds the relevance for the work presented. The experimental design and results with analysis are described in detail. A dimensionless analysis of the fuel beds and test conditions is presented. Finally, conclusions are offered that show the effect of transport processes in porous wildland fuels. The test series conducted indicated that transport process have a significant effect on the combustion of the fuels tested. The presence of different types of flow in the porous fuel beds influenced the combustion reaction regime and determined both kinetically and flow controlled conditions. The dimensionless analysis of the test conditions indicates consistency with the HRR results and that the results should be scalable to larger fuel beds. The results of this test series has implications in what mechanisms need to be understood to effectively model wildland fire spread in porous fuels. In particular, this finding has significant impact on how fluid

dynamics modeling of wildland fire involving porous fuel beds needs to be addressed.

2.0 BACKGROUND AND RESEARCH GOALS

The testing program presented here has identified two forest floor fuels, relevant to many regions throughout the world, and analyzed them to better understand their combustion characteristics. This section offers a brief background on the development of wildland fire spread modeling. An emphasis was placed on developments in understanding forest floor fuels and how they behave as permeable fuel beds during heating, ignition, and burning. Additionally, the general trend in forest fuel calorimetry research was presented. The review of literature was intended to provide a perspective and add relevance to the current research. The goal of this research project is then stated.

2.1 Background

A review of wildland fire research shows many perspectives on the science and application of the science. Fundamental work in the field of porous fuel beds with application to wildland fire modeling begin in the 1960's and many landmark contributions have been made that provide the basis for many of the wildland fire models currently used [5,6]. However, the development of analytical tools that apply physical and chemical principles to prediction of large scale wildland fire behavior, to the degree necessary for reliable engineering applications, is still in its infancy. This research project hopes to aid in defining the parameters of importance with respect to transport processes in porous fuel beds.

Most fire prediction tools in regular use by forest managers, policy makers and fire fighters are very limited in scope and handicapped by a lack of knowledge regarding fundamental fire behavior. In addition, most loss prevention professionals working with wildland fire risk assessment have no engineered tools that they apply regularly to problem solving [7]. To help manage the increasing risks that wildland fire imposes on human activity and better understand wildland management issues, improved assessment tools that address wildland fire

behavior need to be developed. To intelligently develop engineering tools for wildland fire management, fundamental research into the behavior of wildland fuels must be designed and conducted in a manner consistent with developing data that allows application of experimental analysis into engineering tools.

As stated, the precision of wildland fire assessment tools is limited by the understanding of many key parameters that dictate fire behavior. The understanding of the fuel dependent behavior and other parameters affecting combustion are of great importance. HRR and ignition requirements of a given fuel are among the most important parameters for understanding the combustion process, fire characteristics and fire propagation rates. HRR serves to define parameters such as flame geometry and temperature fields and is one of the most used properties of a fuel given to classify its fire hazard [4]. HRR is also extensively used as a descriptive fire parameter in most fire modeling [8].

Spatial depiction of wildland fire characteristics, such as severity, intensity and pattern, are indispensable in fire management [9]. To provide useful and timely wildland fire behavior information, computer codes have been applied to the problem of modeling wildland fire spread in a practical way since 1972 [5]. Rothermel developed the first widely accepted complete spread model for wildland fires for the U.S. Forestry Service. At the core of the model, Rothermel used an equation that described fire spread in a porous fuel bed as a function of the fuel heat release rate, fuel bed depth, effective heat of combustion of the fuel and the mass of the fuel burned [6]. Rothermel's method for predicting fire spread, although complete for a set of underling assumptions, was restricted to a homogenous fuel bed and a quasi-steady state and a fully developed line fire. The use of a quasi-steady state implies that the rate of change in the bed was dominated by the rate of spread of fire with respect to the time dependence of other variables. The method did not include the chemical kinetics of the combustion process, and transport processes were empirically derived for specific fuel geometries. Wind effects are a derived multiplier to an already spreading fire

and the model will not predict the rate of spread when wind is required for successful spread [10].

The foundation laid by Rothermel was the basis for the FARSITE and BEHAVE fire model packages in use by the U.S. Forest Service today [11,12]. Rothermel's model is the most widely used fire behavior model in wildland fire research and management [13]. The FARSITE and BEHAVE packages have limitations with respect to predicting fire spread and require further development with respect to the transfer of energy from the fire to the surroundings and flame structure, in addition to other predictive capabilities [14]. Rothermel's model is sensitive to input parameters, and natural fuel variations can lead to a big error in the results [13]. In addition, the model requires continued improvement in order to model behavior of fire in mixed fuels [15].

As part of the effort to improve the state of wildland fire modeling, new, more complete wildland fire models are being developed within the European Community. Many scientific disciplines have contributed and continue to study many aspects of porous media combustion with a wide range of goals. Much of the information in this area come from research into coal [16], waste management [17], and some very detailed work on modeling of char particles in packed beds [18].

The latest generation of wildland fire models can take advantage of ongoing related research and more advanced computer power to solve more complex evaluation schemes. Complete model frameworks use an approach consisting of heat, mass and momentum conservation equations, along with chemical kinetics models of the combustion process. Solutions for sets of these equations are done in control volumes containing both solid and gas and are incorporated into Computational Fluid Dynamics (CFD) models [19].

Fuels found on the forest floor are generally arranged to form a porous media and have different burning characteristics collectively than they do as individual solid

fuel elements. A porous fuel bed is a hybrid arrangement of a solid fuel with relatively large open gas spaces and will undergo significant internal flows during combustion. Characterizing combustion in this complex environment is one of the most difficult problems in predicting wildland fires [20].

Pinus halepensis and *Pinus pinaster* thermal degradation pathways have been studied under analytical methods such as differential scanning calorimetry, mass spectrometry, and thermal galvanometric analysis. *Pinus halepensis* and *Pinus pinaster* are of special interest in forest fire research because of their high flammability, their contribution to the spread of fire, and for environmental reasons as well [1,2].

One-dimensional fire spread in pine needles for different airflow conditions have been studied [21]. Many studies have examined the open burning of pine needles in bulk and measured various parameters of the combustion process [22,23,24]. These studies all emphasize the importance of understanding pine needle fire behavior for advancing fire spread modeling.

The current study strives to better understand how flow conditions effect burning of porous fuel beds. Multiple experimental studies have shown that combustion in porous media can be greatly influenced by the prevailing flow through the media [6,10,19,25]. In a porous media at high oxidant flow rates surface reactions and gas-phase reactions compete for the available oxidant [26]. Empirical data and analytical evidence indicate that with higher rates of fluid flow, fire spread through a porous fuel will be enhanced [27]. Developing and validating improved CFD sub-grid models for fire spread in forest floor fuels requires a detailed understanding of the physical phenomenon which dominate combustion processes under fire conditions.

The cone calorimeter has been used for a long time to help understand how particular fuels burn. The cone calorimeter has been applied to define forest fuel combustibility by several researchers. Some of these studies take into account

several aspects of the fuel's physical configuration, but mainly examine heat release effects by vegetation type [28] and growth conditions [29].

Much work in the past has developed how the physical arrangement of wildland fuel affects fire spread on a global level. The understanding of how solid fuels make up the forest floor and form porous fuel beds is still developing within wildland fire research [30]. Some recent studies examine how solid fuels breakdown [31]; however, further research efforts are needed to develop an understanding of breakdown of porous fuel beds and how they form flammable mixtures. Relatively little work could be found that details the relationship between transport processes and chemical kinetics in forest floor fuels.

Models under development will require a more complete understanding of how porous fuel beds decompose under fire conditions, ignite and spread fire. The flow effects of heat and mass transfer during combustion are the subject of interest for the current study. The research hopes to define flow regimes where fluid transport through the fuel bed and fluid composition within the fuel bed control combustion. The first step in this process involves the tests described in the following section.

2.2 Research Goals

This research project had the specific goal of developing an understanding of how transport processes affected the combustion of wildland fuels that were in the form of a porous bed. No detailed study could be found in the literature that specifically addressed how the fuel structure affected the combustion process with respect to flow in the fuel matrix. To this end, a series of experiments were designed and carried out that approached the understanding of this problem using commonly available fire testing equipment, specifically the cone calorimeter and the FPA. The goal of this research study and the basis for the novel and relevant contribution to the field of engineering was to conduct an experimental test series,

analyze the data and examine the scalability of the results, to determine the effect of transport processes on the HRR of porous wildland fuels.

3.0 EXPERIMENTAL METHODOLOGY

The test program described in this research project was undertaken to help build an understanding of how porous wildland fuels burn in conditions relevant to wildland fires and natural fuel beds. The research was centered on the hypothesis that transport processes play a fundamental role in the burning process and dominate the measured Heat Release Rate of porous wildland fuels. The work presented here was done to test this hypothesis and establish an experimental methodology for obtaining consistent HRR data for porous wildland fuels.

The analysis method for HRR used in this project was oxygen consumption calorimetry. The method is generally well accepted for determining the HRR of fuels under fire conditions and uses standard test equipment capable of producing repeatable results. Obtaining repeatable calorimetry data for wildland fuels using oxygen consumption calorimetry, or by other methods, is difficult because of the number of parameters that significantly affect uncertainty associated with the measurement of HRR [32]. HRR uncertainty has been examined from several perspectives for a variety of species [33]. Controlling and understanding uncertainty was a large driving force in this experimental program.

The experimental design used a proof of concept test series to then develop a full test series using a full factorial design with 3 replications. Several of the measured variables were analyzed at discrete, relevant values using t- tests and an Analysis of Variance (ANOVA). The time dependent behavior of the data was also analyzed and described. This section provides a brief background of oxygen depletion calorimetry and then a detailed explanation of the experimental design and analysis methods used in this testing program.

3.1 Calorimetry Calculations

Oxygen consumption calorimetry is a convenient and widely used method for measuring the amount of heat release for a laboratory scale fire test [34]. The use of the HRR from a fire can be calculated from the amount of O_2 consumed by the combustion process [35]. The HRR for a fuel is calculated using Equation 3.1.

$$\dot{q} = E_{O_2} \left(\dot{m}^0_{O_2} - \dot{m}_{O_2} \right) \qquad (3.1)$$

The HRR ($\dot{q}$) is calculated by multiplying an energy factor (E_{O_2}) by the mass of oxygen consumed during the burning of a fuel, calculated by the diffecance in the mass of oxygen at the inlet and post combustion ($\dot{m}^o_{O_2} - \dot{m}_{O_2}$).

In general, several simplifying assumptions are associated with the calculation of HRR by oxygen consumption calorimetry; one key assumption is that all gases are considered to behave as ideal. The apparatus used for the HRR calculations in the test series presented in this paper were conducted at atmospheric pressure lending validity to this assumption. It is also assumed that the amount of energy released by complete combustion of an organic fuel per unit mass of O_2 consumed (E_{O_2}) was constant at 13.1 $kJ.g^{-1}$ [36]. Combustion air was assumed to contain only O_2, H_2O, CO_2, and N_2. All inert gases were assumed to have the same properties as nitrogen. Water vapor production during combustion was not considered in the calorimetry calculation.

Prior to measurement in the experimental apparatus, the combustion exhaust gases were dried. The mole fraction (Y_{O_2} or Y_{H_2O}) of O_2 (CO_2, CO, Total Hydrocarbon) in the exhaust flow is different from the one measured in the analyzer ($Y^A{}_{O_2}$) , it is calculated by Equation 3.2.

$$Y_{O_2} = \left(1 - Y_{H_2O}\right) Y_{O_2}^{A} \qquad (3.2)$$

The only exhaust gases considered were O_2, H_2O, CO_2, CO and N_2. They were assumed to represent over 99% of the exhaust gases in all of the tests [37]. Nitrogen does not participate in the combustion reaction and was assumed to be conserved, allowing the following assumption outlined in Equation 3.3 in that ($\dot{n}_{N_2}$) does not change.

$$\dot{n}_{N_2} = \dot{n}_{N_2}^{0} \qquad (3.3)$$

The flow rate was measured by a Pitot tube. It is evaluated by Equation 3.4

$$\dot{V}_e = K\, A \sqrt{\frac{2\,\Delta P}{\rho_e}} \qquad (3.4)$$

The volumetric flow rate ($\dot{V}_e$) is given by the standard relationship of the square root of the pressure drop across the device over the fluid density (ρ_e) in the exhaust stream. The overall flow rate is proportional to the flow coefficient (K) and the cross sectional area (A) of the Pitot tube.

The density of the exhaust (ρ_e) stream is given by Equation 3.5.

$$\rho_e = \frac{P_{duct}}{RT_e} M_e \qquad (3.5)$$

The pressure measured in the exhaust duct (P_e) and the molecular weight of the gas (M_e) are divided by the ideal gas constant (R) and the measured temperature in the exhaust duct (T_e).

The parameter ϕ is defined as the depletion factor. It is the fraction of the incoming air that is fully depleted of its oxygen during the combustion process. This parameter is defined in Equation 3.6.

$$\phi = \frac{\dot{n}_{O_2}^0 - \dot{n}_{O_2}}{\dot{n}_{O_2}^0} = \frac{Y_{O_2}^{A^0}\left(1 - Y_{CO_2}^A - Y_{CO}^A\right) - Y_{O_2}^A\left(1 - Y_{CO_2}^{A^0}\right)}{Y_{O_2}^{A^o}\left(1 - Y_{O_2}^A - Y_{CO_2}^A - Y_{CO}^A\right)} \qquad (3.6)$$

This equation represents the ratio of the number of moles of oxygen consumed ($\dot{n}_{O_2}^0 - \dot{n}_{O_2}$) over the number of moles of oxygen in the inlet air stream ($\dot{n}_{O_2}^o$). This ratio can also be defined in terms of the mole fraction of oxygen consumed (Y_{O_2}) over the mole fraction of oxygen in the incoming air stream (Y_{O_2}).

α is the expansion factor. During a combustion reaction, a fraction of the incoming air is depleted of its oxygen and is replaced by an equal or larger number of moles of combustion products. The expansion factor is the ratio of these two molar quantities. To simplify the calculation, an average value for the expansion factor α is assumed to be equal to 1.105 with a maximum relative error of 10% [30]. The HRR can also be corrected using CO measurements. The heat of formation per kg of CO present in the exhaust gas is subtracted from the heat released by oxygen consumption [38].

3.2 Experimental Design: Concept Testing

The experimental design was developed to determine if a transport driven effect on a fuels HRR could be identified in a systematic way using standard fire testing apparatuses and wildland fuels of interest. Two fire test apparatuses were evaluated for this application, the cone calorimeter and the Factory Mutual Fire Propagation Apparatus (FPA). These devices were used because they are known and well understood fire testing apparatuses.

The driving force behind the research was that wildland fuels in porous beds pose the great threat as a fire hazard. Standard test methods do not account for the porous nature of this class of wildland fuels when determining HRR for use in fuel hazards assessments and fire modeling. A new design of the fuel sample holder for use in both fire test devices was developed that allowed the permeability of the fuel bed and fuel layer to participate during the burn testing. Providing mechanisms for the permeability of the fuel to influence a combustion test allows important information to be captured on how transport processes in the fuel bed effect the combustion process.

The methods of controlling flow in the experiments were constrained by the design of the cone calorimeter and the FPA. The cone calorimeter was designed to allow for natural convection during burning, the FPA allows the combustion sample to have different flow rates and gases flow around the sample. The methods developed in this test program account for the porous nature of the fuel beds. The sample basket was designed and constructed with holes in the exterior surface area to allow for air to flow through into the fuel sample. These baskets were developed for use in both the cone calorimeter and the FPA.

The cone calorimeter as a fire analysis tool was first established in 1982. An excellent history of the development and infiltration of the cone calorimeter as a fire analysis tool was presented by Babrauskas [39]. A schematic as detailed by Babrauskas of the cone is presented in Figure 3.1. The schematic shows the equipment layout as used in this test series.

The design intent of the baskets included functioning under both natural draft and forced flow conditions and to establish different flow conditions inside the porous fuel. The natural draft condition was created during normal combustion of the porous fuel sample inside the basket. Air was drawn by natural convection through the sample basket holes and into the fuel. Under forced flow conditions a fraction of a prevailing air stream established outside of the basket in the FPA combustion chamber would be allowed to flow into the basket and through the

fuel. The size of the opening on the outside of the baskets would act as an orifice to regulate to flow.

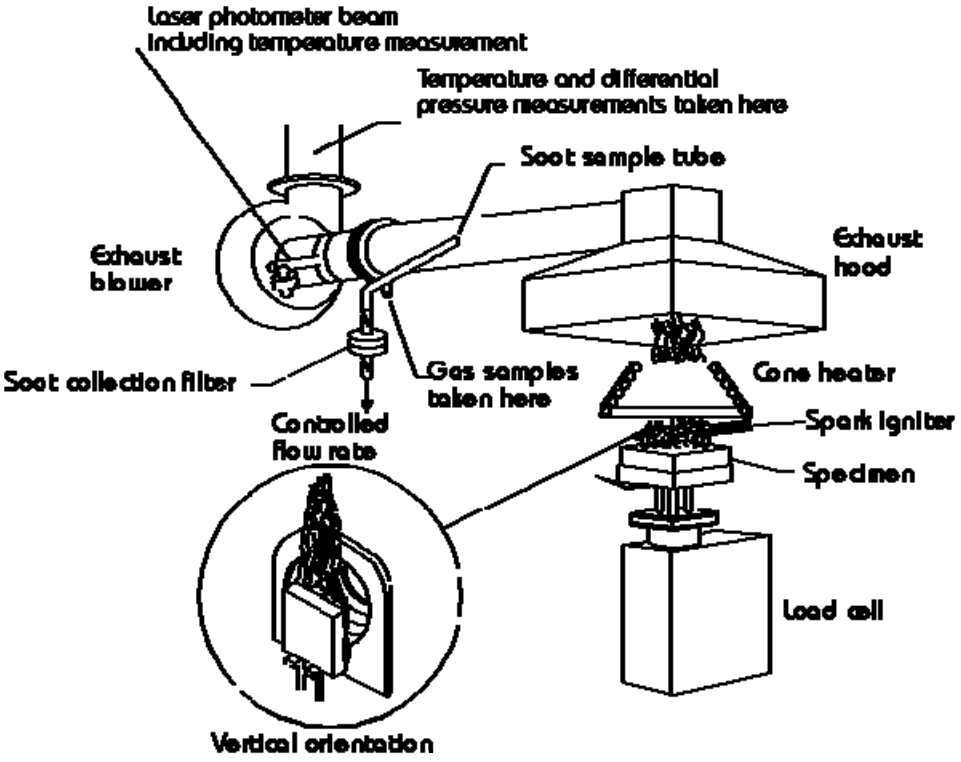

Figure 3. 1 Schematic of Cone Calorimeter [39]

Different sized holes, accounting for different percent openings, were used on the surface of the baskets. The open walls were intended to capture the mechanisms of transport that develop in a natural fuel layer by allowing air to flow through the sample at a rate determined by either natural convection or a forced flow simulating the effect of wind. The percent openings of the sample baskets ranged from 0 to 76%. This allowed both effects to be seen where the wall permeability affected the experiment and where fuel permeability affected the experiment.

Other than being permeable and cylindrical, the baskets differed from the standard sample holder in the cross sectional area. The permeability of the open mesh basket was expressed as the percent opening of the outer surface area. The open basket was made of steel wire mesh or perforated stainless steal. The cylindrical

sample baskets were also lined with foil to establish 0% permeability. The standard cone sample holder was considered to have 0% permeability. The details of both sample holders are presented in Table 3.1 and pictured in Figure 3.2.

Table 3. 1. Main Dimensions of Sample Holders

Type	Horizontal dimension, cm	Area, cm^2	Depth, cm
76, 63, 26 and 0 Basket	12.6 diameter	125	3.1
Standard, non-permeable	10.0 by 10.0	100	5.0

(a) (b)

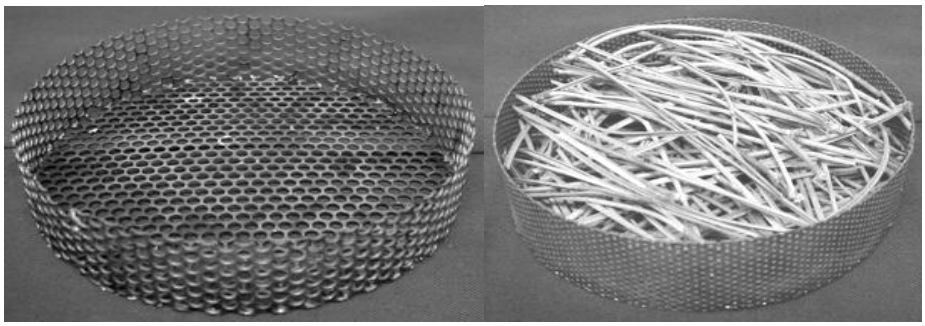

Figure 3. 2. Sample Baskets; a) 63% Open Basket, b) 26% Open Basket with *Pinus pinaster*

The two fuels studied in this test series, *Pinus pinaster* and *Pinus halepensis,* were collected from Mediterranean wildland areas. This fuel was provided by Institute National de Recherché Agronomique. Pine needles were selected because they form a consistent porous fuel bed with a general randomness to the beds structure. These two fuels offered several good properties for testing the significance of the new sample holder design.

An ultimate analysis provided the elemental components of *Pinus halepensis* and allowed calculating the heat of combustion for the fuel: ΔH_c = 185,000 kJ/kg.

Pinus halepensis and *Pinus pinaster* have very similar heats of combustion and chemical compositions, including the ash content which varies by several percent by mass [40].

The key difference from the perspective of this study was the surface to volume ratio of the two fuels. The measurement of surface to volume ratio for *Pinus pinaster* has been reported as 4,600 m^{-1} to 4,990 m^{-1} and for *Pinus halepensis* 7,970 $^{-1}$ to 11,110 m^{-1} [41]. The variability in the surface to volume ratio measurements come from measurement method and geographical area of the sample. Most measurements were taken at more than one place on the needle and averaged.

The surface to volume ratio established a different internal structure to the fuel beds by creating different void fractions of the fuel beds. *Pinus halepensis* packed tighter in the sample baskets and created less void fraction. The void fraction is the area of the packed fuel bed that does not contain fuel, only open space (air or combustion products). The void fraction was critical in establishing different flow behavior within the fuel beds. The two needles created significantly different porous fuel structures, but had relatively similar combustion characteristics and fuel chemistries [42]. This allowed the transport properties of the fuel bed to be studied by examining the HRR of these fuels when burned in the similar prevailing flow conditions performed during this testing program.

As mentioned, tests were performed in both the cone calorimeter and the FPA. The standard cone calorimeter used was a Stanton Redcroft machine with oxygen, carbon monoxide and carbon dioxide analyzers, a load cell and a spark igniter. The cone calorimeter tests presented here used the standard cone sample holder and the 76% open basket. The sample masses used in the cone tests were between 8 and 13 grams for the open mesh sample holder and 10 to 15 grams for the standard holder. The external heat flux used in the cone was 25 kW/ m^2 for all tests. This heat flux was consistent with ignition fluxes found for similar fuels in large scale fire testing.

The needles were dead and not conditioned prior to testing. The pine needles moisture was at equilibrium with the ambient air. The moisture remained fairly constant during the testing period, between 8 and 9 percent. The moisture levels of the needles were determined by oven drying of a sample for 24 hours at 60 degrees Celsius.

3.3 Experimental Design: Parametric Analysis

The FPA was used to conduct a series of tests to analyze three parameters that influence flow in the fuel beds. The basic layout of the FPA is presented in Figure. 3.3 [38]. The FPA operates on a similar concept to a cone calorimeter, however, the FPA allows for some control of the combustion environment. A fuel sample was positioned in the combustion chamber and radiated and an ignition source provided. The combustion chamber and the sample holder for the FPA are cylindrical. The sample holder fits inside the combustion chamber and is positioned on a balance. A picture of the sample basket is presented in Figure 3.2. The mass loss rate of the sample is measured and the exhaust gases are analyzed for composition, temperature, optical obscuration and pressure drop across an orifice plate. As mentioned, one key difference with the FPA in comparison to the cone calorimeter was that the combustion chamber for the sample allows for a controlled environment with respect to gas flow rate and composition.

The experiments in the FPA were designed to test each pine needle species in three sample holders allowing different airflows. The airflows were established for both natural convection and forced combustion air conditions. The fuel samples were 15 g and were distributed to fill the volume of the basket. The needle species provided one experimental factor, surface to volume ratio as described in the Methodology Section. The baskets were a second experimental design factor (porosity) with three levels (0, 26 and 63% opening).

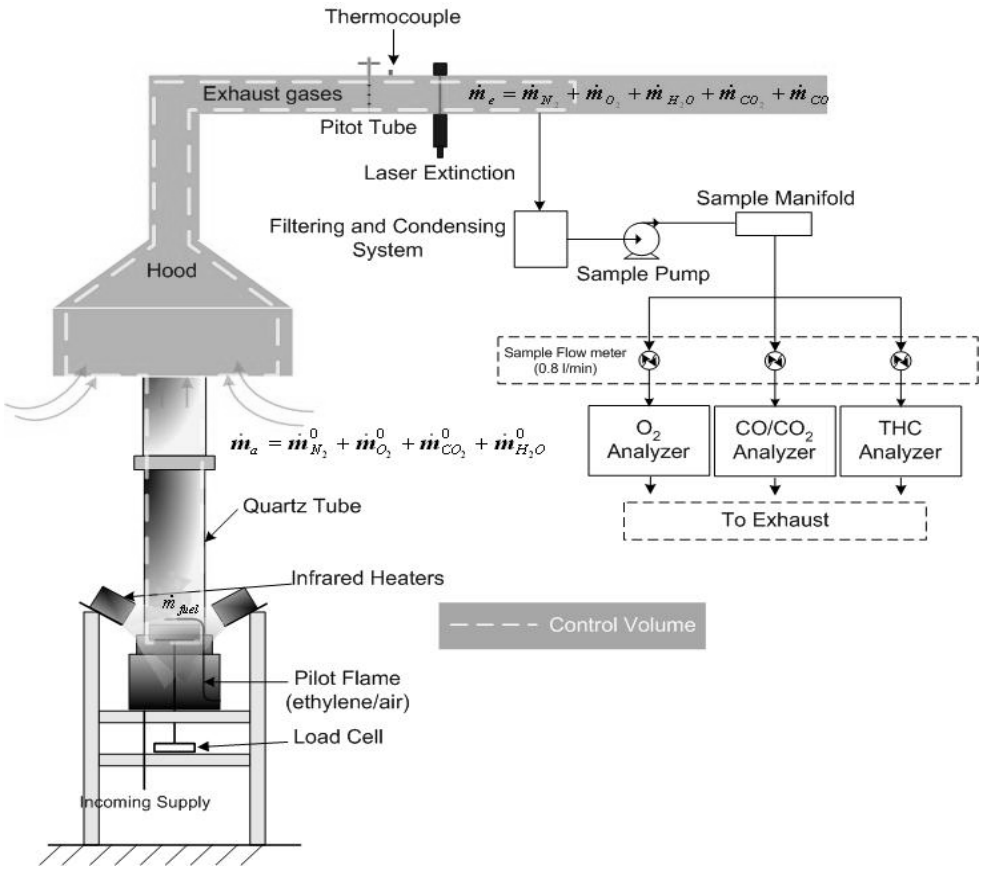

Figure 3. 3. Overview of the FPA System

A third experimental design factor was flow of air to the combustion chamber. The flow control allowed for two levels to the fuel sample; natural convection (defined as the no-flow condition) and forced combustion air (defined as the flow condition). A single value of 200 l/min for the forced air flow was used and supplied to the combustion chamber. The precise value of the flow through the fuel bed samples was not directly measured during the tests. A camera was positioned to observe the behavior of the pine needle bed during combustion. Each test condition was repeated three times for a total of thirty six test runs. The test matrix is presented in Table 3.2.

Table 3. 2. Experimental Design

Test Number	Fuel Type	Sample Basket Percent Opening	Combustion Air Condition
1-3	*Pinus pinaster*	0%	Natural Convection
4-6	*Pinus halepensis*	0%	Natural Convection
7-9	*Pinus pinaster*	26%	Natural Convection
10-12	*Pinus pinaster*	26%	Forced Flow
13-15	*Pinus halepensis*	26%	Natural Convection
16-18	*Pinus halepensis*	26%	Forced Flow
19-21	*Pinus pinaster*	63%	Natural Convection
22-24	*Pinus pinaster*	63%	Forced Flow
25-27	*Pinus halepensis*	63%	Natural Convection
28-30	*Pinus halepensis*	63%	Forced Flow
31-33	*Pinus pinaster*	0%	Forced Flow
34-36	*Pinus halepensis*	0%	Forced Flow

3.4 Analysis Methodology

The test series presented in Table 3.2 is a full factorial design with three replications. This test design offers many advantages in the analysis methods that can be applied to the data and allows for some clear cut answers to be obtained from test data. The hypothesis testing presented in Section 4 used t-tests and an ANOVA to determine significance. The analysis was done using the statistical package SYSTAT [43]. The results are presented in Section 4 and a sample ANOVA result is presented in Appendix A. The goal of the experimental design and analysis methods were to optimize the information that could be obtained from the test results while minimizing and characterizing uncertainty. Many

uncontrolled parameters exist in fire testing in general and in wildland fuels. This experimental design and analysis method helps to reduce the influence of these parameters [44].

Using the t-test in this analysis provided a method of hypothesis testing that allowed comparison of the mean values of the discrete variables measured during the test runs. For example, the mean peak HRR measured over the three replicated test runs, tests 19-21 from Table 3.2, were compared (or tested) with the mean value for the replicated tests 25-27 from Table 3.2. The t-test quantitatively examines the hypothesis that the change in fuel surface to volume ratio (difference between *Pinus pinaster* and *Pinus halepensis*) had a statistically significant effect (95% confidence was used for these tests) on the measured average peak HRR for each set of the test runs.

The t-test examines the variance in two mean distributions using the t distribution and calculating a value called the p statistic. The p statistic represents the probability that the two mean values of peak HRR for the two test conditions are from the same population. Significance is usually placed at $p = 0.1$ (90% confidence) or $p = 0.05$ (95% confidence). The hypothesis is true in this case if the p statistic is less then 0.05. There was then a 95 percent chance that the two mean values were not from the same general population. This then proves that the change made in the experimental condition (use of *Pinus pinaster* or *Pinus halepensis*) was, in fact, responsible for the difference in the measured peak HRR.

The ANOVA test method is similar to a t-test, but this method can be used to compare more than two means and more than one measured variable. The ANOVA allows insight into the interaction of controlled variables on the measured variables. This methodology is a very good analysis method when many uncontrolled variables may exist in the experiments. All of the details of the analysis methods for ANOVA are explained in references [43 and 44].

The ANOVA produces many calculations. Two used in this analysis included the F- ratio and the p statistic. The p statistic in this case is based on the standard F distribution. Between these two variables, the degree of interaction of several variables on a calculated mean can be determined. This analysis method was used to examine the test results for each of the three test conditions alone and in combination. This analysis method uses the F-ratio to establish a relationship between and within the variances of the measured variables with respect to the test conditions. The test conditions are limited to specific levels as described in the experimental design. The effects that were tested at each level and combination of levels to calculate a p statistic are much like the t-test. This p statistic was then used to determine if the degree of significance was then reached to conclude that a factor, or test condition, had an effect on the measured variables.

The results and analysis are presented in Section 4. The combination of the experimental design and analysis methods used allowed for clear cut relationships to be seen in the test conditions that controlled transport in the sample fuel beds and the combustion characteristics of the fuel beds. As with the t-test, references [43 and 44] offer a detailed explanation of the methods.

4.0 EXPERIMENTAL RESULTS AND ANALYSIS

The experiments performed during this project used the cone calorimeter and the FPA. The experimental program tested porous wildland fuel samples. Tests were conducted to determine if a new design for a sample holder could be used in the cone calorimeter and FPA to determine if flow effects could be separated and tested using these two experimental devices. Once this proof of concept was complete, a full experimental design was conducted using the FPA to determine the effect of transport using combustion air flow, porous fuel samples with significantly different void fraction and the new permeable sample holder. The results and analysis of these experiments are presented in this section.

4.1 Induced Flow Effects: Descriptive Statistics

The first set of test results involved the cone calorimeter and used the standard cone sample holder and the 76% open mesh basket. The goal of this test series was to separate the effect of an induced flow in the fuel sample during a standard cone calorimetry test. Descriptive statistical tests, HRR plots and some basic chemical kinetics analysis were performed. Many of the general results presented in Section 4.1 were first presented in [45].

The variables tested were common calorimetry discrete measured variables. These were the time to ignition, total mass lost during the test, the peak mass loss curve and the peak HRR. The descriptive statistics for the test runs are presented in Table 4.1. These are broken into three sets; set (A) presents the complete data set for all tests, set (B) presents the data for the test run using the open basket type sample holder, and set (C) presents the data collected using the standard cone sample holder.

As shown in Table 4.1 eight tests with the basket sample holder and 9 tests using the standard sample holder were analyzed. The hypothesis test was done using

two-sample t-tests. Table 4.2 (A-C) illustrates the results of several t-test runs on the experimental data. The analysis was intended to determine if the mean value measured for one of the measured parameters was significantly different for each sample holder type.

Table 4. 1. Descriptive Statistics for Cone Calorimeter Tests

A. All Cone Tests (n=17)

	Time to Ignition (s)	Mass Loss (g)	Peak dm/dt (g/s)	Peak HRR (kW/m^2)
Minimum	11.000	6.420	0.146	206.491
Maximum	63.000	12.210	0.733	673.190
Arithmetic Mean	20.059	8.865	0.441	425.967
Standard Deviation	12.755	2.174	0.185	190.962

B. Open Basket Sample Holder (n =8)

	Time to Ignition (s)	Mass Loss (g)	Peak dm/dt (g/s)	Peak HRR (kW/m^2)
Minimum	11.000	6.420	0.517	516.983
Maximum	63.000	12.210	0.733	673.190
Arithmetic Mean	24.750	9.092	0.614	617.316
Standard Deviation	17.903	2.534	0.084	56.986

C. Results for the Standard Sample Holder (n = 9)

	Time to Ignition (s)	Mass Loss (g)	Peak dm/dt (g/s)	Peak HRR (kW/m^2)
Minimum	14.000	6.880	0.146	206.491
Maximum	20.000	11.650	0.409	312.859
Arithmetic Mean	15.889	8.663	0.287	255.878
Standard Deviation	1.833	1.933	0.078	30.498

Table 4. 2. t-Test Results for Cone Calorimeter tests

A. Maximum HRR, kW/m^2

Test Group	N	Mean HRR, (kW/m^2)	Standard Deviation, (kW/m^2)
Open Holder	8	617.316	56.986
Standard	9	255.878	30.498

B. Percent mass loss, m_f/m_i

Test Group	N	Mean Mass Loss, %	Standard Deviation, %
Basket	8	0.859	0.041
Standard	9	0.688	0.118

C. Time to Ignition, s

Test Group	N	Mean Ignition Time, sec	Standard Deviation, sec
Basket	16	12.805	17.372
Standard	18	8.288	7.921

The t-tests results indicate that the sample holder type had a significant effect on the mean differences for HRR and the percent mass loss during the burn. The means of time to ignition for the two sample holders differed by ~4.5 seconds. However, the distribution of values for each sample holder indicates that these means are not significantly different.

An interesting point here was that two of the open basket test runs did produce outliers for time to ignition. As can be see in the table, the average time to ignition for a basket type sample holder was ~13 seconds. However, two tests had extended times to ignition, one 63 seconds and the other 40 seconds. Time to ignition was an interesting parameter in many ways during this test program. In the cone calorimeter the times to ignition indicated the effect of distribution on the air flowing through the fuel bed and the fuels ability to form a flammable concentration of pyrolysis gases above it.

4.1.2 Induced Flow Effects: Bed Dynamics

The next step in the analysis was to determine if the sample holder had an effect on time dependent aspects of the burning process. This was first done by examining the HRR as a function of time for the fuel types and the two types of sample holders. The HRR was calculated from measurements in the cone using three methods, oxygen consumption, oxygen consumption with CO_2 and CO correction and by CO_2 Generation. Figure 4.1 shows a plot of a typical HRR curve for the standard cone sample holder. Figure 4.2 shows a typical HRR curve for a basket type sample holder.

As the plots indicate, the effect of the sample holder appears to be significant on HRR for the entire duration of the combustion of the fuel bed. The basket type sample holder reaches a peak HRR that was three times higher than the standard sample holder achieved. In addition, the HRR process was faster with the basket sample holder.

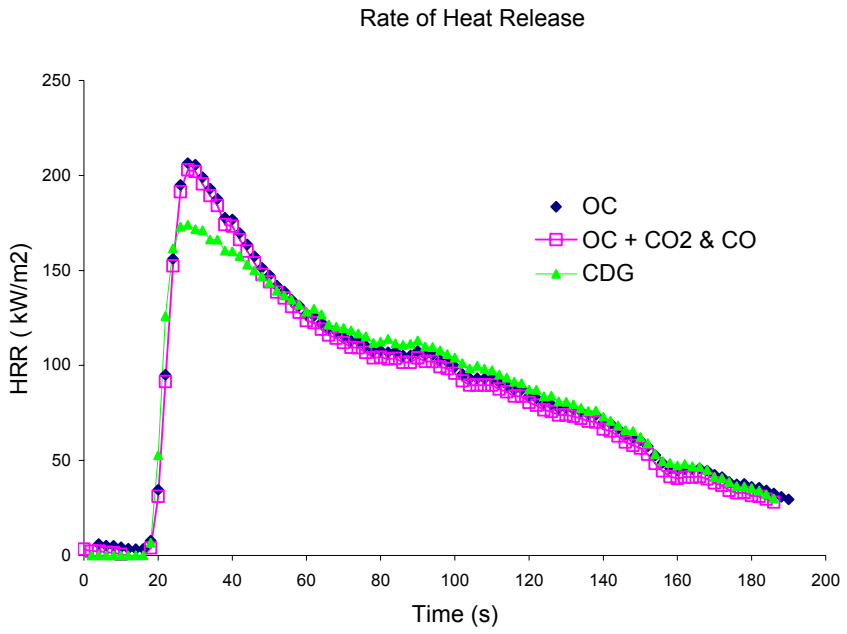

Figure 4. 1. HRR vs. Time for the Standard Holder
OC- Oxygen Calorimetry, OC+CO_2 & CO – Oxygen Calorimetry with Carbon Generation Correction, CDG – Carbon Generation Calorimetry.

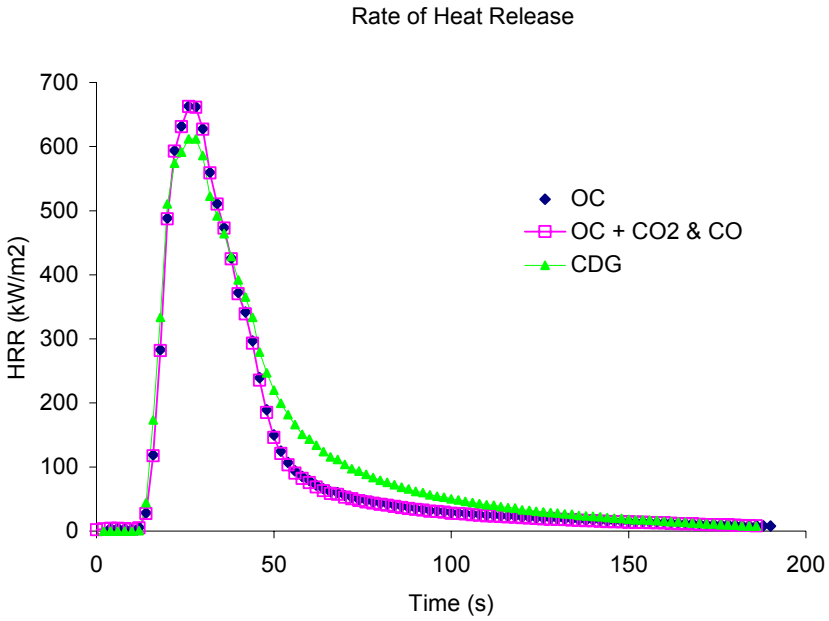

Figure 4. 2. HRR vs. Time for the Open Basket Sample Holder

The standard sample holder reaches its peak value and then drops off more slowly over a longer period of time. This includes both the flaming and smoldering combustion portions of the tests. For the standard sample holder, flaming to some degree on some portion on the fuel sample was maintained over most of the test.

The rate of mass loss of the sample during the combustion process is the best indicator of extent and rate of reaction during this type of calorimetry test. Examining the mass loss also provided a method to determine the order of the combustion reaction using the experimental data for the two sample holder types.

Mass loss was normalized to better understand the process because different initial masses were used for several test runs. The normalized mass was also used to define the concentration of fuel in the basket that was available for reaction. This was defined as χ as related in Equation 4.1 and represented the extent of fuel conversion by using the value of mass at any time (mass(t)) over the initial mass in the sample holder.

$$\chi = \frac{mass(t)}{mass_i} \qquad (4.1)$$

χ was examined for all tests for each sample holder type. Two typical plots are presented here that reflect the case for the standard and open mesh sample holders. The relationship of χ in time for each sample holder is presented in Figure 4.3. As can be seen in the graph, the mass loss for the basket type sample holder is much faster than for the standard sample holder. This indicates that the reaction was occurring more quickly in the open basket sample holders where natural convection was allowed to move incoming air into the burning fuel samples. This seems to have facilitated mass transport according to these plots.

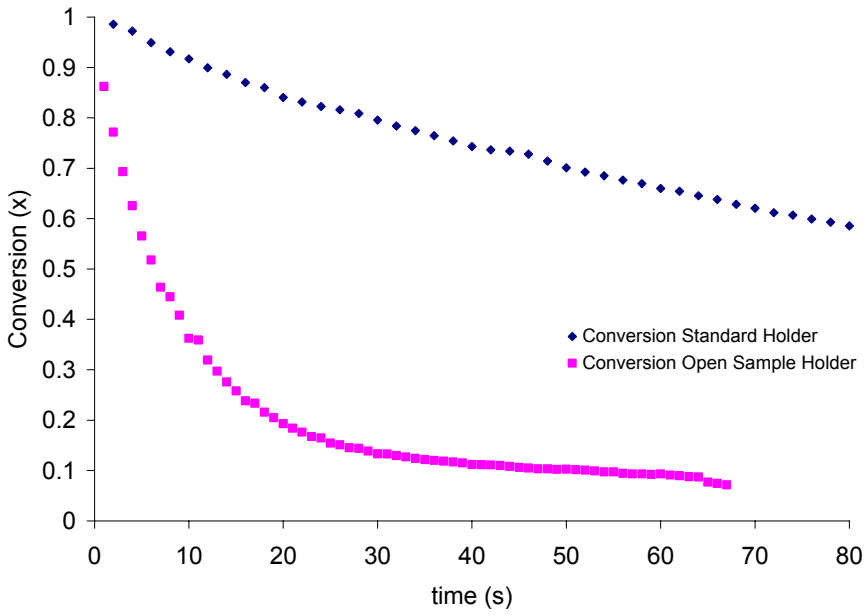

Figure 4. 3. Conversion vs. Time Post Ignition

As mentioned, the mass loss of the fuel bed during the test is a good measure of the extent and the rate of the burning reaction taking place. Conversion can also be used to help determine the kinetics for the decomposition reaction of the fuel bed and the order of the reaction. The order of a reaction refers to the power to which the concentrations are raised in the kinetic rate law. A standard first order

chemical reaction for fuel (A) reacting into combustion products (B) is presented in equation 4.2.

$$A \rightarrow B \qquad (4.2)$$

A common form of the kinetic rate law applied to the combustion of the fuel in the sample baskets in this case is presented in equation 4.3.

$$-r_A = k\chi \qquad (4.3)$$

The reaction rate ($-r_A$) is dependent on the reaction constant (k) and the conversion (χ) of the fuel. For a second order reaction presented in equation 4.4, 2 moles of the fuel are reacted into products of combustion.

$$2A \rightarrow B \qquad (4.4)$$

The reaction rate equation for a second order reaction takes the form of equation 4.5 where in this case the conversion is raised to the second power.

$$-r_A = k\chi^2 \qquad (4.5)$$

A standard method for determining first order reaction kinetics from experimental data for this application can be described by equation 4.6.

$$\ln(\chi) = -kt \qquad (4.6)$$

The experimental reaction data can be plotted as $\ln(\chi)$ vs. time. If the data forms a line then the reaction can be considered first order with the slope being equal to a reaction constant, k. The experimental data can be plotted as $1/\chi$ vs. time. If this plot of the experimental data forms a line then the reaction can be considered

second order with the slope being equal to –k and the intercept being $1/\chi_o$. Second order reaction kinetics can be described as equation 4.7:

$$\frac{1}{\chi_O} - \frac{1}{\chi_t} = kt \qquad (4.7)$$

The data from both sample holders during flaming combustion was plotted using both methods. Again, typical individual test runs were plotted because any averaging of the data created responses that lost time dependent features of the experiments.

Both sample holders appear to be second order in kinetics. This is shown in Figures 4.4-4.7. These plots presented an interesting result. The order of the decomposition reaction was the same in both cases for the different sample holders. The rate of reaction, however, was much faster for the open mesh sample holder than for the standard sample holder.

Figure 4.4 was an attempt to fit a linear trend line to the data for a standard sample holder for first order kinetics. As mentioned, the standard sample holder showed flaming combustion at least in some locations on the fuel bed during most of the test run. This presents a case where both flaming and smoldering combustion kinetics are being represented in the mass loss of the fuel sample.

Figure 4.5 is a linear trend line for $1/\chi$ and this fits the data very well. This indicates that the degradation process is second order for the standard sample holder.

Figure 4.6 plots conversion the data for the basket type sample holder. The trend line for the $\ln(\chi)$ data does not seem to fit well. As can be seen in Figure 4.7 the fit to $\ln(\chi)$ is much better. This indicates, again, second order kinetics for the degradation process of the fuel.

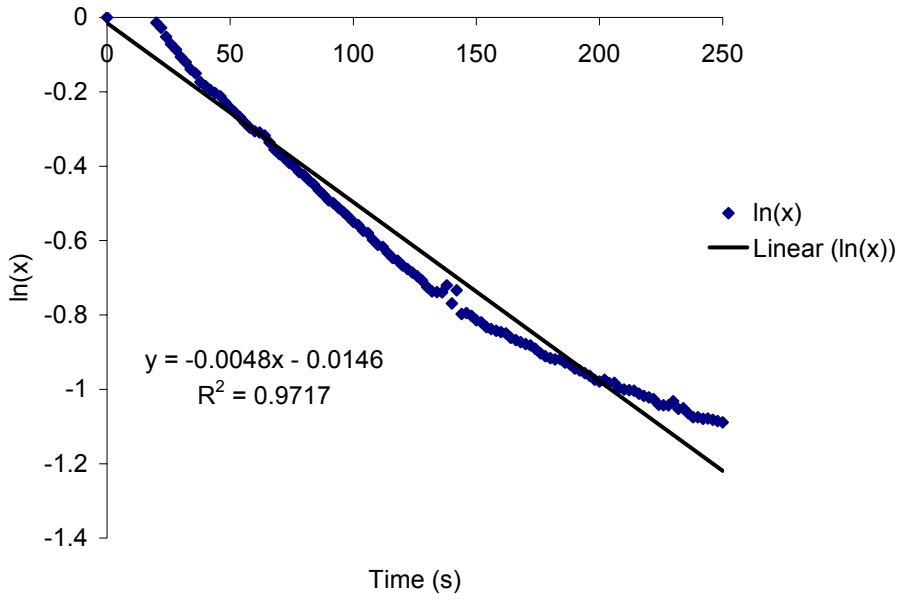

Figure 4. 4. Linear Fit to ln(χ) vs. Time for a Standard Sample Holder

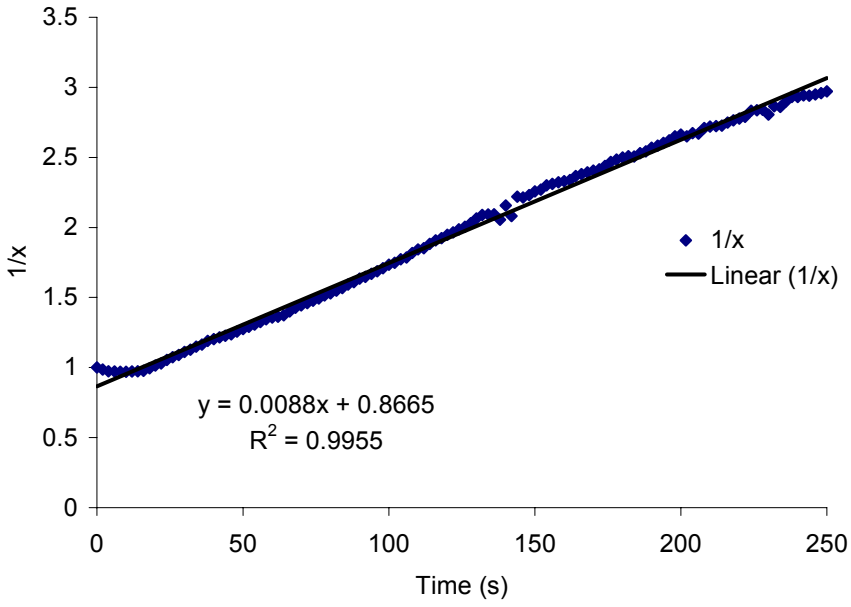

Figure 4. 5. Linear Fit to 1/χ vs. Time for the Standard Sample Holder

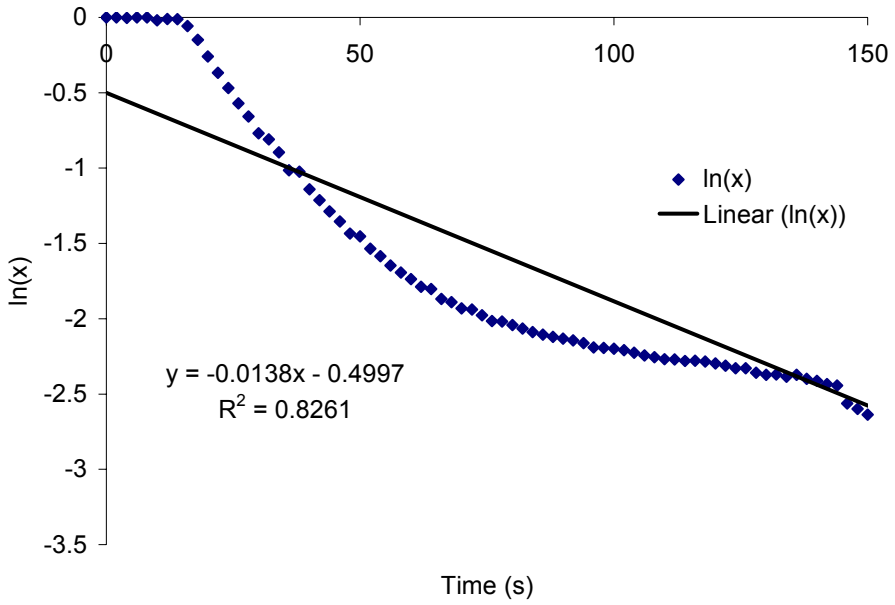

Figure 4. 6. Linear Fit to ln(χ) vs. Time for the Open Mesh Sample Holder

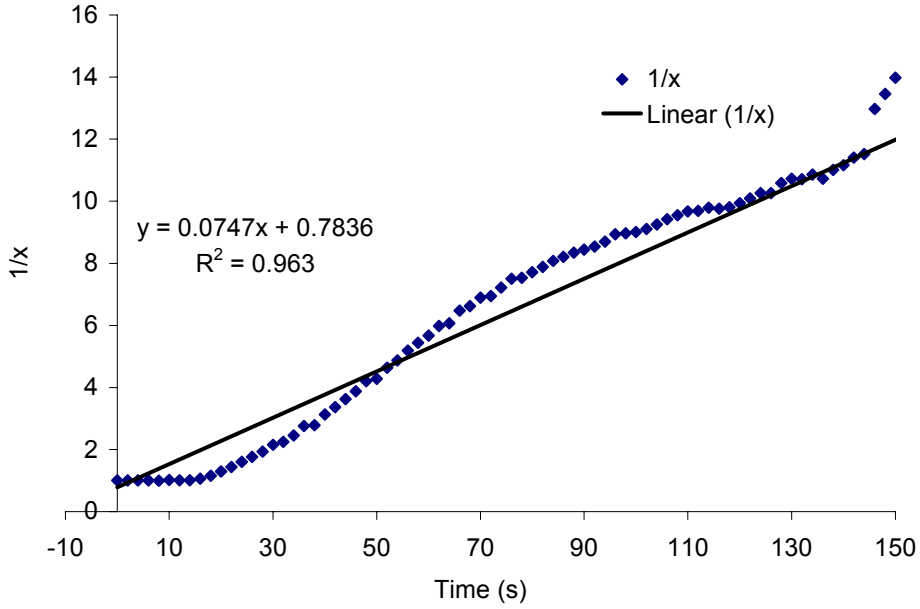

Figure 4. 7. Linear Fit to 1/χ vs. Time for the Open Mesh Sample Holder

A description of the progression of the open mesh basket tests provides some perspective on the plots for the open mesh holder. After ignition, the subsequent burning was very intense in the open baskets during flaming combustion. During all tests the open mesh basket became ignited and spread fire across the top of the fuel bed in less then 5 seconds. The downward spread in the basket was done in less than 7 seconds after the top spread was completed. The open mesh bed was fully involved in flame (fire supported from the top to the bottom of the fuel bed) for no more then 30 seconds in any test.

In some cases there was a flash of flame supported for ~1 second shortly after the initial extinction. At the current level of resolution, the normalized CO_2 curve for the open mesh holder seems to have distinct responses at each point in the fuel beds evolution in time with respect to the combustion process. The standard holder supported flaming combustion that started somewhat rigorous and then steadily dropped off during the test. Spread across the top and downward in the fuel bed for the standard sample holder was difficult to determine with any precision. Therefore, no similar description of the bed burning behavior could be provided.

4.2 Initial FPA Tests

Tests were run to determine how the sample holders would perform and, could best be used, in the FPA. The test data gathered during these initial FPA tests also helped to develop the test protocol used for many FPA burn tests using non-solid or powder fuels. In addition to identifying the physical and mechanical design issues of using the basket sample holders in the FPA, the potential consistency of data obtained using the sample baskets needed to be determined.

The new sample basket designs had the same cylindrical geometry of the regular FPA sample holders, but they were larger in all dimensions. This created some issues with positioning in the combustion chamber and required designing a new basket holder to fit in the balance of the FPA.

This data illustrates the general trends and the repeatability of the sample basket holders in the FPA. The trends for O_2, consumption during test runs with both the 26% and 63% sample baskets were consistent with O_2 consumption curves found in the cone calorimeter. Figure 4.8 shows the oxygen consumption for several tests run in the FPA. The results for the oxygen were consistent with all of the gas measurements.

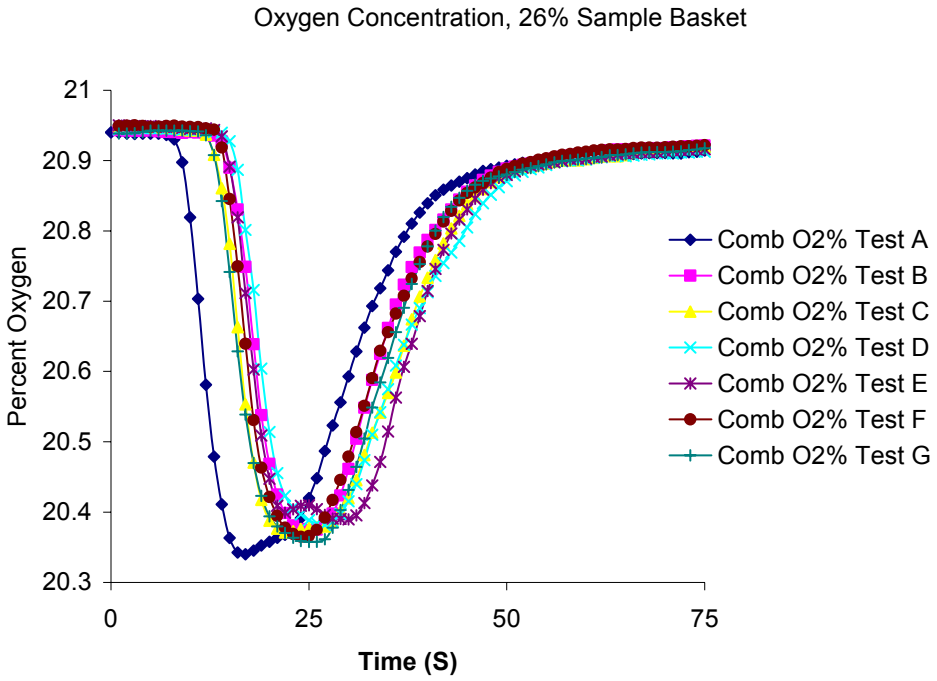

Figure 4. 8 Oxygen Concentration for the 26% Sample Holder in the FPA

As mentioned, these test runs were used to develop a test method for the FPA. One aspect of data analysis learned during this test series was that the use of averaged results when analyzing the time series data tended to lose interesting characteristics, such as inflection points, that were smoothed over during the time series averaging process.

The consistency of the tests, run to run was very encouraging as a performance indicator of the new sample baskets. The general time series data behavior was observed for each measured variable, the sample baskets were considered to be

performing in an acceptable manner. One interesting factor that was noted during these initial tests in the FPA was how the position of the igniter above the fuel bed influenced the ignition of the bed. During the pyrolysis of the fuel beds, prior to ignition, the gases could be observed evolving off of the fuel bed. The formation of a flammable cloud above the fuel bed was required for ignition. The position of the igniter in the radial and axial directions could be seen to impact the ignition behavior. Based on the goals of the testing for this program a detailed study of this phenomenon was not conducted, however, the observation is noted as being present. The FPA apparatus as it existed at the time of these tests did not have a good mechanism to measure igniter position relative to the fuel bed.

These initial tests in the FPA had limited, but very important goals: 1) Determining applicability of the basket sample holders application in the FPA; 2) See if repeatable data could be obtained from wildland fuels in the FPA, a consistent problem with cone calorimetry in literature data [46]; 3) Develop a test protocol for use in further testing with wildland fuels for the FPA; and 4) Provide experience with the wildland fuels in the FPA to aid in the experimental design of the Phase III test series. Once all of these goals were realized, a more comprehensive test program could be developed to examine the transport process effects.

4.3 Complete FPA Test Series

This test series was the most comprehensive test series performed as part of this research project. The goal of the test series was to prove or disprove the hypothesis that transport processes and not chemical kinetics were the dominant factor in determining the rate of burning in this type of porous wildland fuel configuration.

As described in the Experimental Methodology section of this report, a full factorial experimental design with three replications was used. With the test

parameters of fuel type, sample holder and combustion air flow condition, this created a total of 36 test runs.

The experimental design allowed for an analysis taking full advantage of an ANOVA methodology. The tests were intended to determine if a clear effect could be established between transport processes within a porous wildland fuel bed and the burning characteristics of the porous fuel beds. The transport processes were defined and controlled by the experimental factors of combustion air, fuel sample holder percent opening and fuel surface to volume ratio. The burning characteristics were measured by HRR, mass loss, products of combustion, time to ignition and duration of burning.

As an example to the analysis methodology, the first test results presented and analyzed in this section are the ANOVA results for the test conditions and the effect on one discrete measured variable, peak HRR. This was done to provide an explanation of how the ANOVA was applied in the overall analysis. For the overall analysis a multivariable ANOVA was run to determine the complete interaction of the experimental parameters with the measured results. The full ANOVA results are presented in Appendix A.

After the first ANOVA is presented several graphs showing the time dependent behavior of measured variables are presented. This was done also to illustrate the results that were obtained during the testing and to provide some ideas on how the analysis was conducted. After these sections, the two analysis methods are used to develop discussion around some of the most relevant findings of the experimental program.

4.3.1 Discrete Variables Analysis

The discrete variables used in this analysis were peak HRR, time to ignition of the sample, time to reach peak HRR and time of flaming combustion of the fuel sample. All of these variables were measured for each test condition and, as

stated, each test condition repeated three times. The distributions for each of these measured variables are presented in Figure 4.9.

As the figure illustrates, the distributions for these variables are normal in trend when plotted as distribution density functions about a mean. The normal distribution of the variables indicates the randomness of the errors associated with the experimental apparatus and measurement techniques [47]. This allowed for standard statistical analysis techniques to be applied.

The values for the discrete measured variables used all 36 data points. The table provides the minimum and maximum values measured for each variable. The range of each measured value was also provided as it provides a feel for the 95% confidence intervals which are also provided for each variable.

It is important to keep in mind that the point of these tests was to determine the differences between the various test conditions that were run, and in some respect providing descriptive statistics on this type of data set provides limited value. However, the type of analysis performed in this research program looks at differences in experimental values with what may be considered subtle changes in experimental parameters. For that reason the overall measured values for the variables presented in Table 4.3 are of interest to the bulk behavior of these two varieties of pine needles when specific burning conditions may not be known or of interest. Therefore, presenting this data has value in not only comparing these overall results to specific test conditions presented later in this section, but the data may also have value to other research projects not envisioned as part of this study.

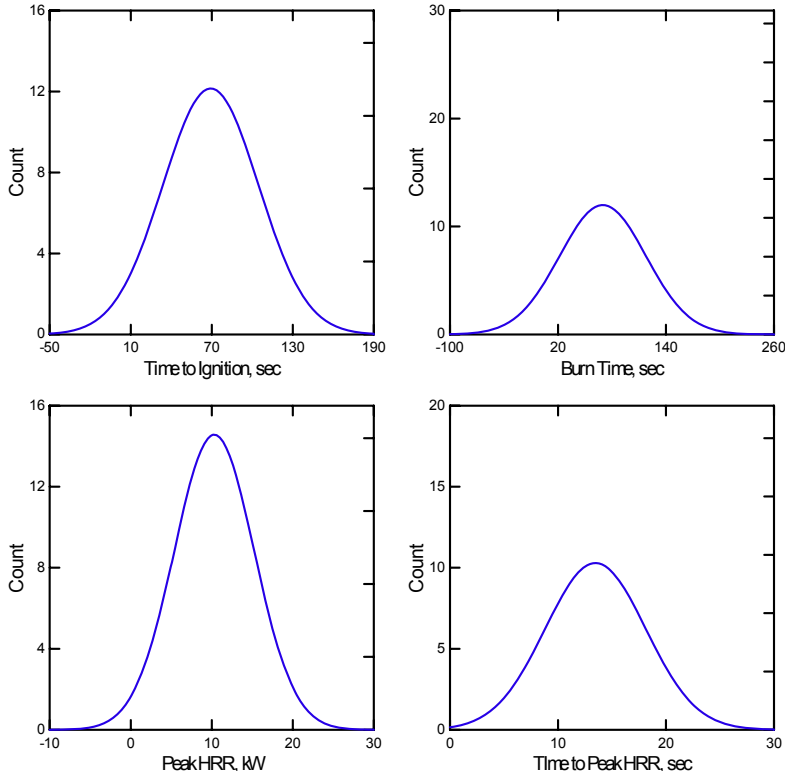

Figure 4. 9. Distributions of Measured Discrete Variables

Table 4. 3. Descriptive Statistics for Discrete Variables Analysis (n=36)

	Time to Ignition, sec	Burn Time, sec	Peak HRR, kW	Time to Peak HRR, sec
Minimum	22.000	23.000	2.369	7.000
Maximum	151.000	226.000	18.096	24.000
Range	129.000	203.000	15.727	17.000
Arithmetic Mean	69.250	69.833	10.309	13.472
95.0% Lower Confidence Limit	57.257	53.609	8.642	11.899
95.0% Upper Confidence Limit	81.243	86.058	11.975	15.046
Standard Deviation	35.446	47.951	4.926	4.651

Table 4.4 contains the classically reported results for an ANOVA test. The full ANOVA for each factor, fuel type, sample holder opening and combustion air flow condition and the effect of peak HRR is presented here. The first column lists the experimental parameter or factor being examined. This is referred to as the source of the variance in the distribution of the results. The second column lists the sum of squares for the regression, the third is the degrees of freedom (d.f.) for the parameter, the mean squares is presented in the forth column. In addition, the F-ratio and the p-value are provided in the last two columns.

The F-Ratio is a statistic that is calculated from the ratio of the two variances being compared and the p-value provides the confidence level for the estimate (see Experimental Method Section for details on these test parameters). In this study a 95% or $p<0.05$ was used to determine a significant result in a test effect.

Table 4. 4. ANOVA for Peak HRR with All Test Conditions

Analysis of Variance

Test Parameter(s)	Type III Sum of Squares	d.f.	Mean Squares	F-ratio	p-value
Fuel Type	4.041	1	4.041	7.715	0.010
Sample Holder	556.658	2	278.329	531.420	0.000
Flow Condition	79.480	1	79.480	151.753	0.000
Fuel Type with Sample Holder	2.812	2	1.406	2.684	0.089
Fuel Type with Flow Condition	27.519	1	27.519	52.542	0.000
Sample Holder with Flow Condition	158.218	2	79.109	151.045	0.000
Fuel Type with Sample Holder with Flow Condition	7.939	2	3.970	7.579	0.003
Error	12.570	24	0.524		

This result of this ANOVA shows that a significantly different HRR (95% confidence level, $p<0.05$) was calculated for each test condition except Fuel Type with Sample Holder ($p=0.089$). Each of these influences will be examined in

detail and a description of how they relate to the analysis provided in this section. The first parameter examined was the fuel type, *Pinus pinaster* or *Pinus halepensis*, and the effect on Peak HRR.

As Table 4.5 indicates, the mean values for Peak HRR are very close for each set of test conditions, but the difference in the calculated mean values was still significantly different for the two fuel types. It is important to remember that these average values are calculated for all test conditions and a significant difference in the mean values for the two fuels was found. This was an important finding for a test of this type and design. For the means to be relatively close in magnitude, both very near 10 kW in addition to the standard error of the estimate being only 0.171 kW, represents a strong indication of the degree of the repeatability and consistency among similar test runs. Consistency in test results for HRR is a problem in wildland fuels [28].

Table 4. 5. ANOVA for Peak HRR with Fuel Type (n=18)

Least Squares Means of Peak HRR (SEE=0.171)

Fuel Type	Mean of Peak HRR, kW
Pinus halepensis	9.974
Pinus pinaster	10.644

The graphical representation of the HRR result includes the error bars and illustrates the differences between the test conditions and the two measured variables. This is presented in Figure 4.10.

The sample holder percent opening was a test parameter that influenced the flow from the prevailing combustion air stream in the FPA's combustion chamber that was allowed to enter the fuel bed. The openings created a boundary condition for the fuel bed that was intended to affect this air flow. The air flow effect ranged from no air entry into the fuel bed with the 0% basket to a relatively high flow of air for the 63% basket. Later in this section a description of the flow conditions created in the fuel beds based on a flow study of the baskets in the FPA

combustion chamber is provided. Tests were included in the experimental design to flow air past the 0% baskets. Table 4.6 presents the data on how the sample holder opening affected the Peak HRR for each sample holder tested.

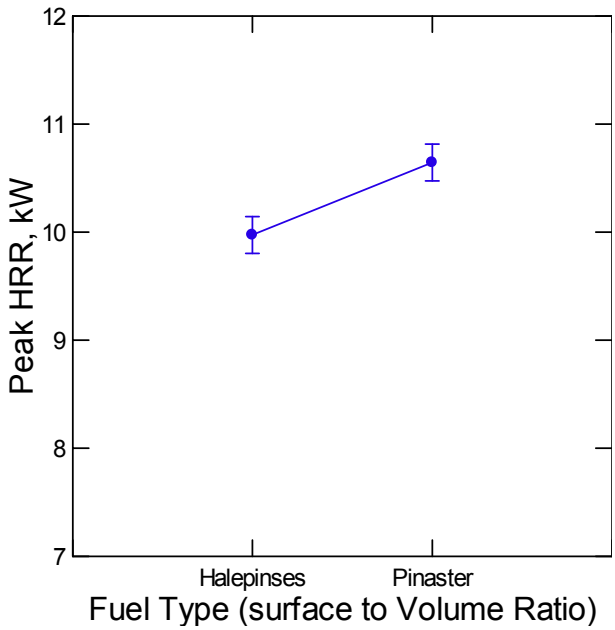

Figure 4. 10. Peak HRR with Fuel Type

The results from these tests show how the existence of an opening in the sample holder had an effect on Peak HRR. This was illustrated very clearly in the graphical output for this test as presented in Figure 4.11. As can be seen in the figure, the effect exists between having an opening (the 26 and 63% sample holders) and not having an opening (the 0% sample holder). The real effect on Peak HRR could not be established at a given percent opening in the sample holder from this testing and analysis method, just the fact that an opening existed and once air flow was established, an effect on Peak HRR could be noted.

As mentioned, tests were run both without and with air flowing around the 0% sample holder. This was an important experimental design issue and leads strength to this data set and the argument that the combustion air flow condition affected what was taking place in the fuel bed during the burning process and that the air did not have a significant effect on the flame with respect to HRR. Again,

this supports the idea that the transport process inside the fuel bed is controlling the HRR. The graphical representation of the data in Figure 4.11 appears to indicate that the 26% open sample holder seemed to have surpassed some minimum critical opening for the overall combustion air flow used in the tests to establish this flow condition inside the fuel bed.

Table 4. 6. Fuel Sample Holder and Peak HRR

Least Squares Means (n=12, SEE=0.209)	
Sample Basket	**Mean Peak HRR, kW**
0%	4.749
26%	12.998
63%	13.179

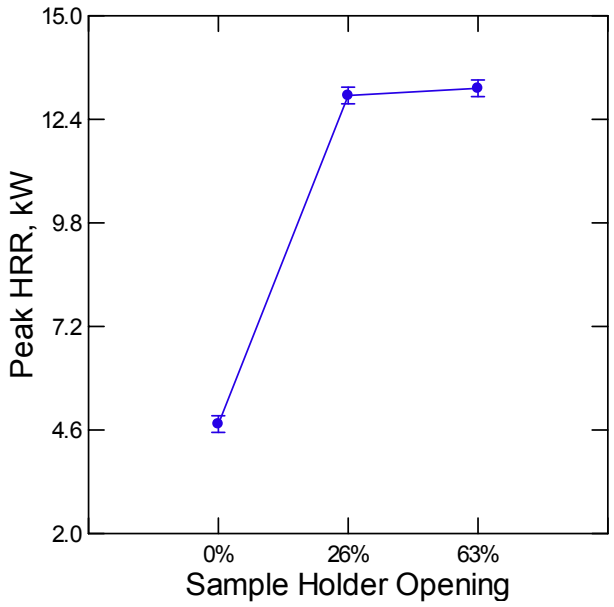

Figure 4. 11. Peak HRR and Sample Holder Opening

The last single test parameter examined here was the combustion air flow versus no flow condition. The result of the ANOVA for this test parameter supported the basket opening finding, in that the effect for flow in the fuel sample was

consistent with increasing the Peak HRR in all cases tested. Table 4.7 presents the values at each test condition and Figure 4.12 illustrates the differences.

Table 4. 7. Combustion Air and Peak HRR (n=18, SEE=0.171)

Combustion Air Condition	Mean of Peak HRR, kW
Flow	11.795
No	8.823

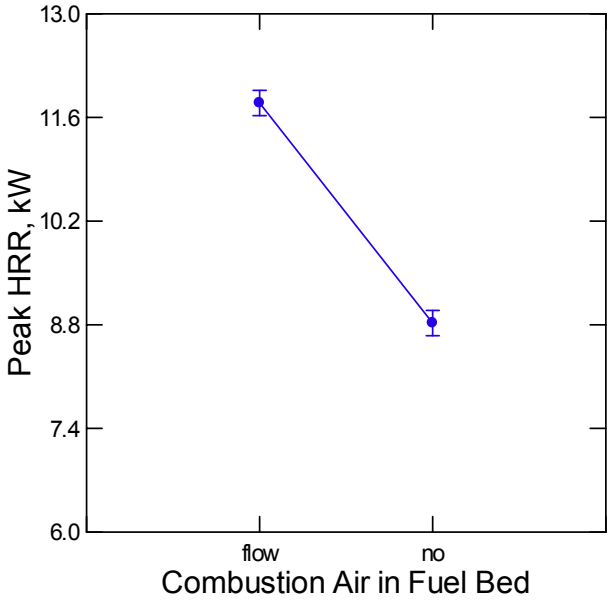

Figure 4. 12. Peak HRR with Combustion Air Flow

The error bars are very tight around the mean values shown on the graph. Again, this result shows a consistency from test to test that allows for meaningful conclusions to be made about the test parameters and how they affected the measured test result of Peak HRR.

The next step for the ANOVA was to analyze the effect of combinations of the test parameters on the measured value of Peak HRR. As was indicated in

Table 4.4 each test combination, except fuel type with sample holder, had a significant effect on the Peak HRR. Table 4.8 shows how the interaction of the fuel type and the sample holder affected the Peak HRR. The graphs presented in Figure 4.13 illustrate the results clearly and to help visualize the tabulated results. The mean Peak HRR was very close for several fuel and sample holder combinations. When the error was considered, no conclusion that the two test parameters consistently created significantly different results in Peak HRR could be established. The graphs clearly show the error bars overlapping.

Table 4. 8. Peak HRR with Fuel and Sample Holder (n=6)

Least Squares Means, Standard Error = 0.295

Fuel and Sample Holder Combination	Mean for Peak HRR, kW
Halepensis*0%	4.028
Halepensis*26%	12.781
Halepensis*63%	13.113
Pinaster*0%	5.469
Pinaster*26%	13.216
Pinaster*63%	13.246

Only for the 0% opening sample holder was a significant difference in the Peak HRR found for the two fuel types. The *Pinus halepensis* with a 0% holder had an average Peak HRR of 4.028 kW +/- 0.059 and *Pinus pinaster* was a Peak HRR of 5.469 kW +/- 0.59. At 95% confidence these were different. This shows an interesting interaction of surface to volume ratio when no air was free to flow through the bed, either by forced convection or natural convention. The *Pinus pinaster* needles had a larger surface to volume ratio; almost double that of the *Pinus halepensis* needles. When all mechanical methods for flow to the bed are restricted, the fuel bed with the least resistance to internal flow, highest void fraction created by the surface to volume ratio, had the highest Peak HRR.

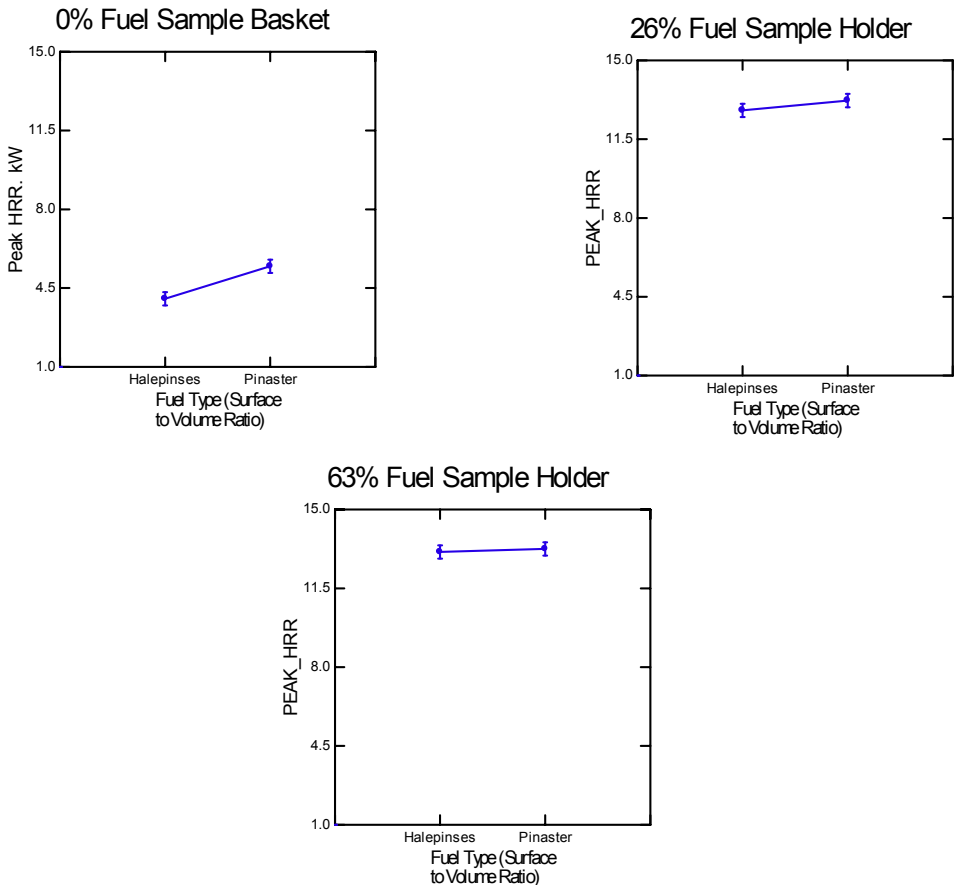

Figure 4. 13. Fuel Type and Fuel Sample Holder Effect on Peak HRR

The remaining combinations of test parameters all had a significant effect on the Peak HRR of the fuel beds. Table 4.9 and Figure 4.14 provide illustration of the effects for Fuel Type with Combustion Air. These results were of particular interest in the time dependent analysis of HRR presented later in this section.

Table 4. 9. Fuel Type with Combustion Air (n=9, SEE=0.241)

Fuel, Combustion Air Flow Combination	Mean for Peak HRR, kW
Halepensis*air flow	12.334
Halepensis*no air flow	7.614
Pinaster*air flow	11.255
Pinaster*no air flow	10.032

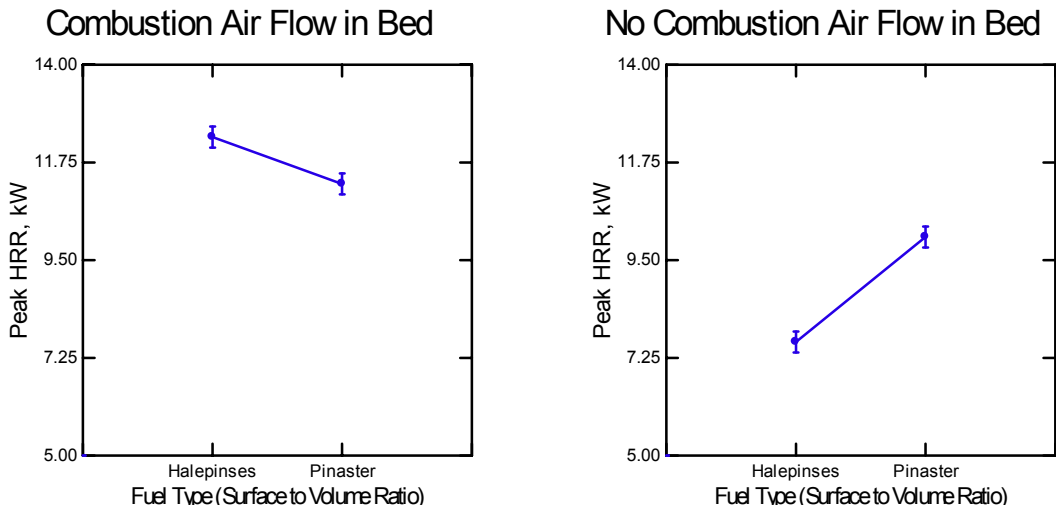

Figure 4. 14. Fuel Type with Combustion Air Flow effect on Peak HRR

These results were interesting, with air flow in the bed during combustion the fuel producing the higher Peak HRR changed. With no air flow in the bed, the *Pinus pinaster* had a higher Peak HRR. With air flow in the bed during combustion the result changes and the *Pinus halepensis* has the higher Peak HRR. As noted, *Pinus pinaster* has a smaller surface to volume ratio, about half of *Pinus halepensis*. The resulting void fractions in the two fuel beds create a condition more favorable for natural convection in the *Pinus pinaster*.

This was the first result that provided proof that the internal dynamics of the flow in the fuel bed had a significant impact on Peak HRR. The earlier results showed that flow itself had a significant impact on Peak HRR, but in this case it was shown that the surface to volume ratio affects the Peak HRR.

Once flow was established in the fuel bed at some critical velocity (as of now not determined), the parameters that controlled HRR change. During the no combustion air flow case, the ability of the fuel beds void fraction to allow internal flow determined which fuel had the larger Peak HRR. When a forced combustion air flow was established in the fuel beds (again at some unknown critical value), the fuel bed with more fuel surface area produced a higher Peak HRR.

The next set of tests that had an effect was the sample baskets with the combustion air flow condition. These results are presented in Table 4.10 and Figure 4.15. This set of test conditions addresses flow conditions at various rates.

Table 4. 10. Sample Holder with Combustion Air Effect on Peak HRR (n=6 and Standard Error=0.295)

Sample Basket, Combustion Air Flow Combination	Mean for Peak HRR (kW)
0%*flow	3.287
0%*no	6.210
26%*flow	16.237
26%*no	9.760
63%*flow	15.860
63%*no	10.499

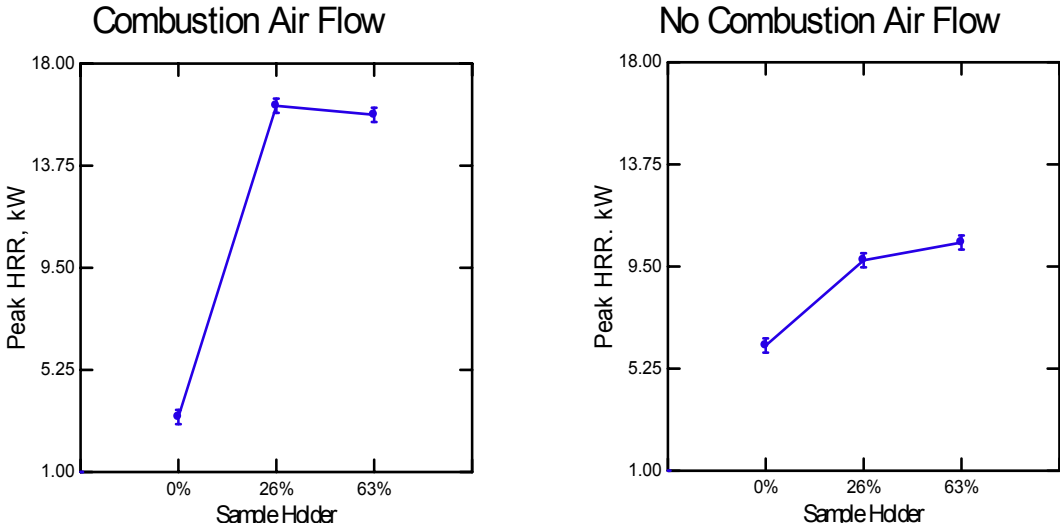

Figure 4. 15. Sample Holder with Combustion Air Effect on Peak HRR

As the trend in the analysis has been indicating, the presence of a forced combustion air increases the Peak HRR for a set of test conditions. An interesting result indicated by the combination of sample holder type and presence of combustion air flow was that the 26% open sample holder had a higher Peak HRR

than the 63% sample holder. As mentioned earlier in this section, the 26% opening seems to have been at near some ideal value for flow with some of the test conditions. The experimental design and test equipment used in this study did not provide sufficient details to address this result further than to observe it.

For the no combustion air flow condition the trend in Peak HRR followed with the other test results indicating that with no forced air flow in the bed, natural convection and the fuel beds internal void space effected the Peak HRR reached for a given test condition.

The last combination of the Peak HRR ANOVA was for each test condition to be analyzed for an effect. This part of the analysis provided perspective on the repeatability of each test condition. The analysis, as presented in Table 4.11 and Figure 4.16, indicates that each condition had a significant effect on Peak HRR.

Table 4. 11. All Test Conditions, Fuel Type, Sample Holder and Combustion Air Effect on Peak HRR (n=3, Standard Error=0.418)

Fuel, Sample Basket, Combustion Air Flow Combination	Peak HRR (kW)
Halepensis*0%*flow	2.783
Halepensis*0%*no flow	5.274
Halepensis*26%*flow	17.298
Halepensis*26%*no flow	8.263
Halepensis*63%*flow	16.921
Halepensis*63%*no flow	9.304
Pinaster*0%*flow	3.792
Pinaster*0%*no flow	7.146
Pinaster*26%*flow	15.176
Pinaster*26%*no flow	11.256
Pinaster*63%*flow	14.798
Pinaster*63%*no flow	11.694

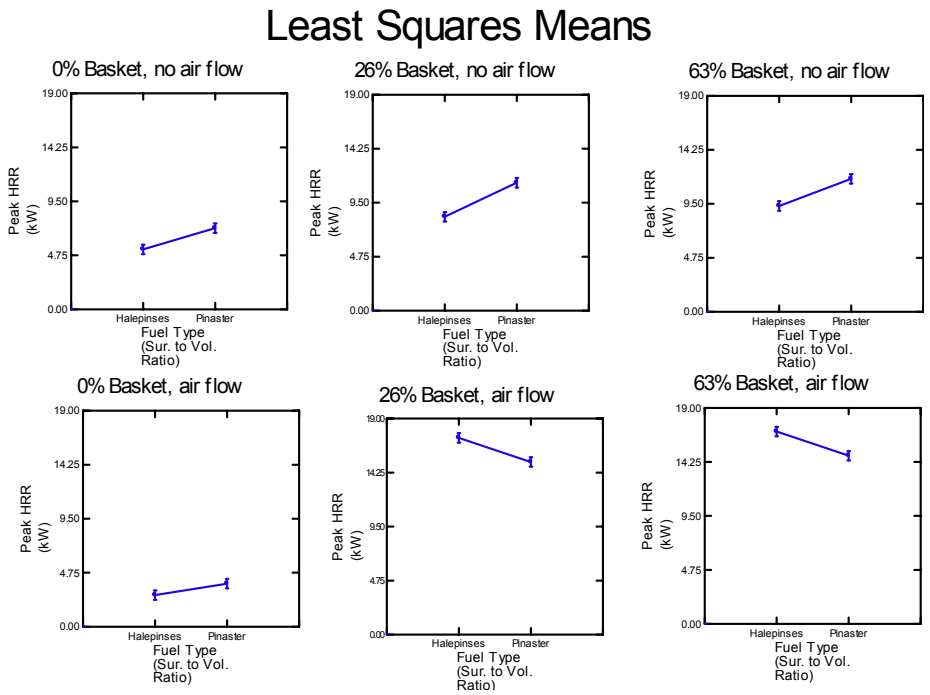

Figure 4. 16. All 12 Test Conditions and the Effect on Peak HRR

As mentioned, additional ANOVA's were run with each of the measured discrete variables to determine how each test condition affected the value. The process for this was similar to the one for Peak HRR. Several interesting results were found with the other variables. The ANOVA for time to ignition showed that each test condition had a significant effect except when all grouped together. This was an interesting result and shows the degree of variability in the ignition time. The time to ignition analysis provides the best perspective on how long it took for flammable gas concentrations to build over the fuel bed during pyrolysis. Figures 4.17 – 4.19 show the average time to ignition for the three test conditions. The main finding was that as the ability of the fuel bed to have an air flow through it increased, so did the time to ignition.

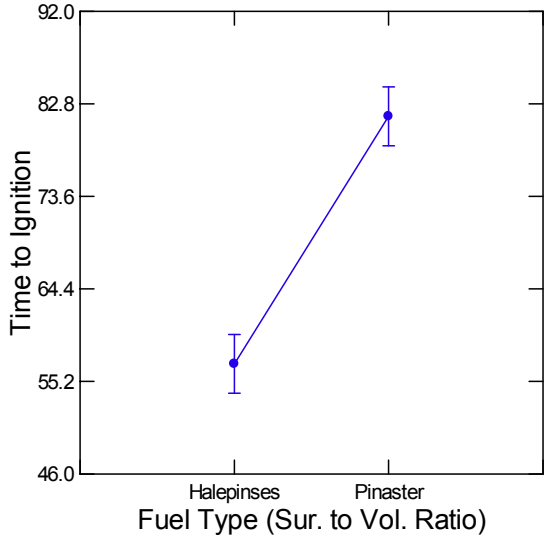

Figure 4. 17. Time to Ignition with Fuel Type

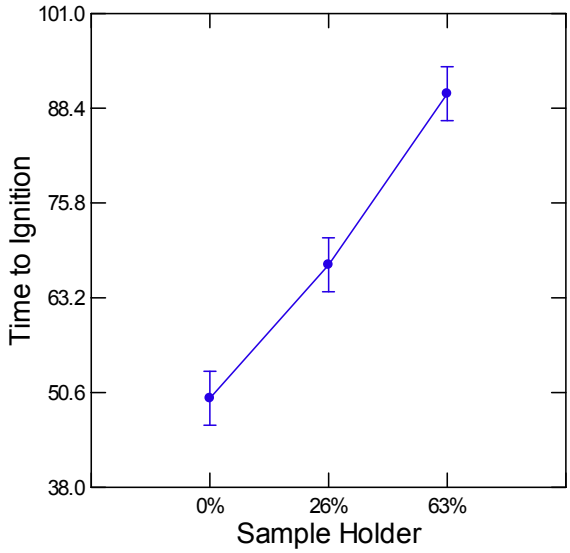

Figure 4. 18. Time to Ignition with Sample Holder

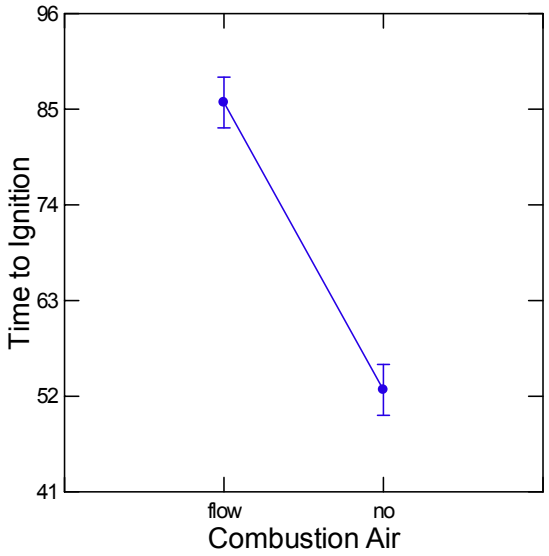

Figure 4. 19. Time to Ignition with Combustion Air

The time to peak HRR variable showed the least dependency on test condition of any of the measured discrete variables. Table 4.12 shows the results of this analysis. As the table indicates, each experimental parameter taken alone had an effect, but the variation in time to reach the peak HRR was too large over all test conditions for any significance to be found. No overall trend could be determined by this measured variable alone because of this. For fuel type, the larger surface to volume ratio reached the peak HRR quickest inferring that flow conditions would have an impact. However, for combustion air the no flow condition reached the Peak HRR more quickly than the flow condition. Additionally, the sample holder that reached Peak HRR quickest was the 26% opening, however, this was only a data trend and not conclusive.

The statistical analysis of the experiments provides interesting insight into the fuel beds burning behavior under various flow conditions. The next section reports the time dependent behavior of the experiments.

Table 4. 12. Effect of Experimental Parameters on Time to Reach Peak HRR

Test Condition Combination	Level	LS Mean, s	Standard Error, sec	N
Fuel	*Pinus halepensis*	12.000	0.568	18
Fuel	*Pinus pinaster*	14.944	0.568	18
Sample Holder	0%	16.750	0.696	12
Sample Holder	26%	11.583	0.696	12
Sample Holder	63%	12.083	0.696	12
Combustion Air	Flow	16.278	0.568	18
Combustion Air	No Flow	10.667	0.568	18

4.3.2 Dynamic Variables

The burning of the pine needles in the fuel beds followed the general behavior of all fire, heating, ignition, flaming combustion and smoldering. The time dependant nature of this behavior was examined to provide further insight into the effects shown to be relevant in the analysis presented above. Much of the data and analysis presented in this section was first presented in reference [42].

HRR can be calculated by several methods. The method presented in Section 2 of this thesis was Oxygen Depletion Calorimetry (ODC) and was extensively used in this study. A second method uses only the mass loss rate during burning and the known heat of combustion for the fuel. An ultimate analysis provided the elemental components of *Pinus halepensis* and allowed calculating the heat of combustion: ΔH_c = 185,000 kJ/kg [40]. The value for *Pinus pinaster* was very close and was assumed equal for this analysis. The HRR using the mass loss method was calculated by equation 4.8. Figure 4.20 shows the HRR estimated by both methods for the no flow test condition.

$$HRR = \Delta H_{comb.} \cdot m(t) \qquad (4.8)$$

The mass loss signals and resulting measurements taken during the tests were noisy; this is a well known problem with calorimetry experiments. The mass loss data was smoothed using the SG method as described Staggs [48].

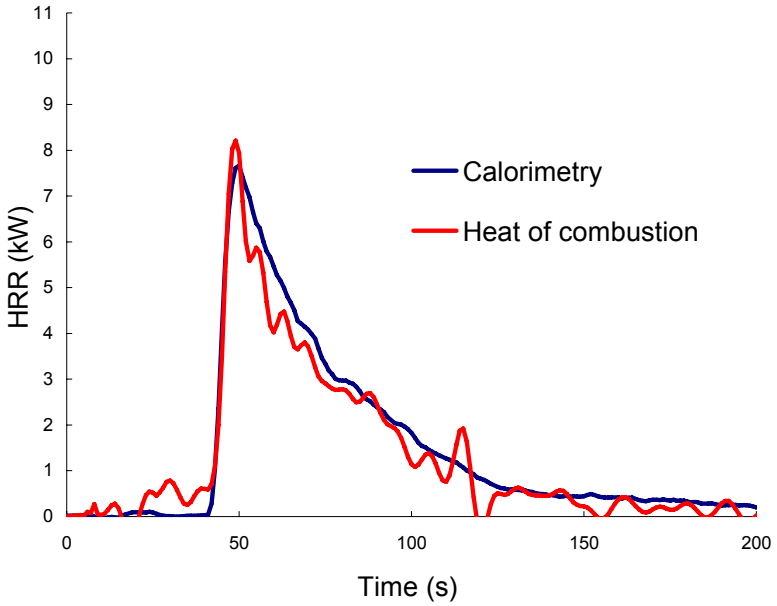

Figure 4. 20. HRR for the Combustion Air No Flow Condition

Figure 4.20 shows a very good match between the two methods of estimation for the entire test run. These results are for a test conducted without forced combustion air flow in the fuel sample.

Figure 4.21 traces the HRR in time for a test with combustion air flow in the fuel sample and shows good agreement between the two methods for HRR calculation. The two methods estimate a different broadness of the peak in the HRR curve. The ODC may be able to account for conditions leading to a sustained steady state on the combustion reaction that the mass loss method can not measure.

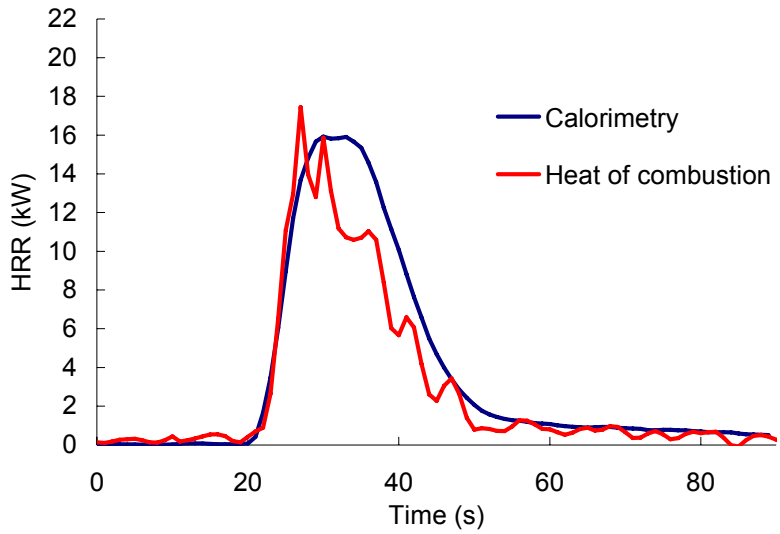

Figure 4. 21. HRR for the Combustion Air Flow Test Condition

The degree of consistency with mass loss demonstrated in Figures 4.20 and 4.21 for the HRR data was found for all runs in the full factorial design tests. The source of most discrepancies between the methods was most probably the mass loss measurements. The load cell did have some uncertainty during the test and the discrepancies in the predicted HRR were assumed to be due mainly to a noisy mass loss signal. The noisy mass loss rate signals have a greater impact on small masses in calorimetry experiments [48].

The differences between the mass loss estimates for HRR and the calorimetry estimates could also have had some roots in the phase of combustion in the fuel beds. The heats of combustion for flaming and smoldering have different values. The heat of combustion for a gas is lower than the combustion of smoldering embers [40]. The mean heat of combustion underestimates during flaming combustion and over estimates during combustion of smoldering embers. Solid fuel in the fuel beds could begin smoldering combustion during a test in the FPA as observed during the cone tests.

The experiments performed in the FPA were well ventilated; only ash remained in the sample basket after test runs (around 0.5 g). This was consistent in the 0% through 63% open sample holders. Under such well ventilated conditions the two methods for HRR measurement presented here should provide equivalent results.

In addition to the HRR estimate methods matching, the experiments in the FPA were very repeatable. Figure 4.22 illustrates the typical combustion behavior for a set of test runs (3 repetitions) for the no flow test condition for *Pinus halepensis* in the 26% sample basket holder. The data had this level of consistency within each set of test conditions for the entire test series. This repeatability of HRR measurements using wildland fuels in calorimetry testing seems unprecedented based on the literature review.

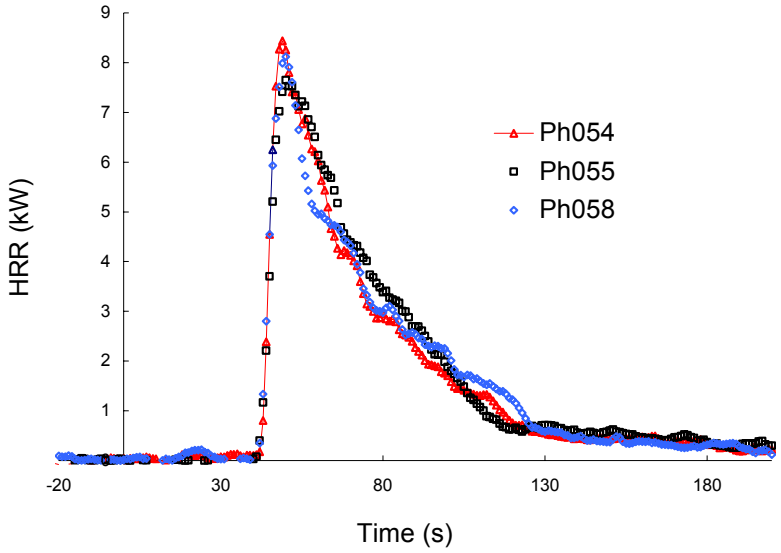

Figure 4. 22. HRR by OCC for the No Combustion Air Flow, 26% Sample Holder, *Pinus halepensis* Test Condition Repeated Three Times

Figure 4.23 shows the oxygen concentration and the HRR for a typical test run. The point of ignition corresponds to the drop in oxygen and flameout is marked by the vertical line. At the point of ignition, the O_2 concentration drops steeply because of the onset of flaming combustion and the reaction of the O_2 with the

pyrolysis gases. The flame grows for approximately 10 seconds before beginning to decrease. The flame extinguishes (flameout) after another ~120 seconds. Glowing or smoldering combustion continues beyond the disappearance of the gas flames. The HRR continues to drop off at a different, but relatively constant rate as the remaining embers smolder.

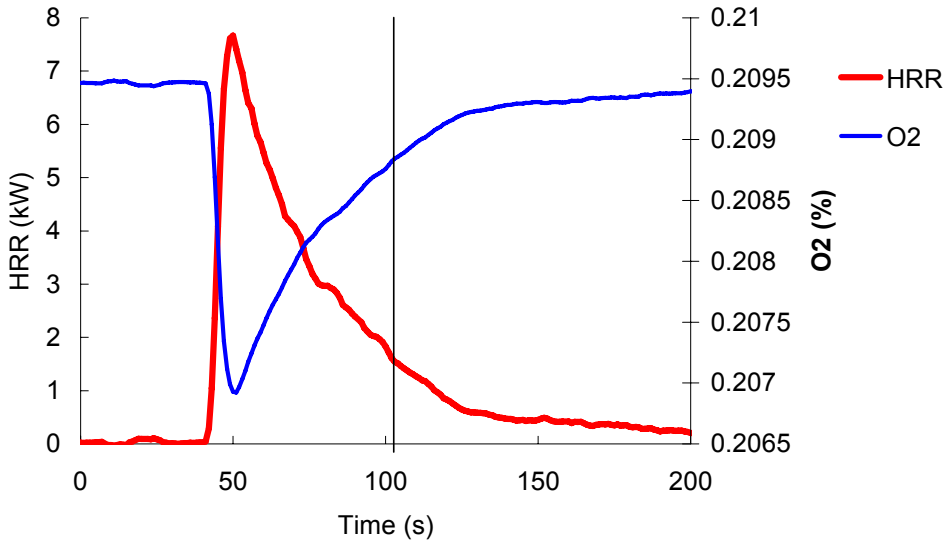

Figure 4. 23. HRR and Oxygen Concentration Behaviour for a Typical No Flow Test Run

Figure 4.24 shows the behavior of CO_2 and CO during a typical test run. At the ignition point (first vertical line) both CO_2 and CO generation rates increase. As the fuel was consumed greater amounts of char and ash were formed. The flame degraded toward extinction and the CO_2 generation rate peaked and then decreased rapidly. CO generation approached the flameout point (vertical line) and became constant at extinction. This general behavior was seen for all test runs with some differences for flow conditions. This aspect of CO behavior is discussed in detail further in this section. As smoldering combustion proceeded, the CO production increased and then fell off until the embers extinguished. At that point the CO generation rate increased.

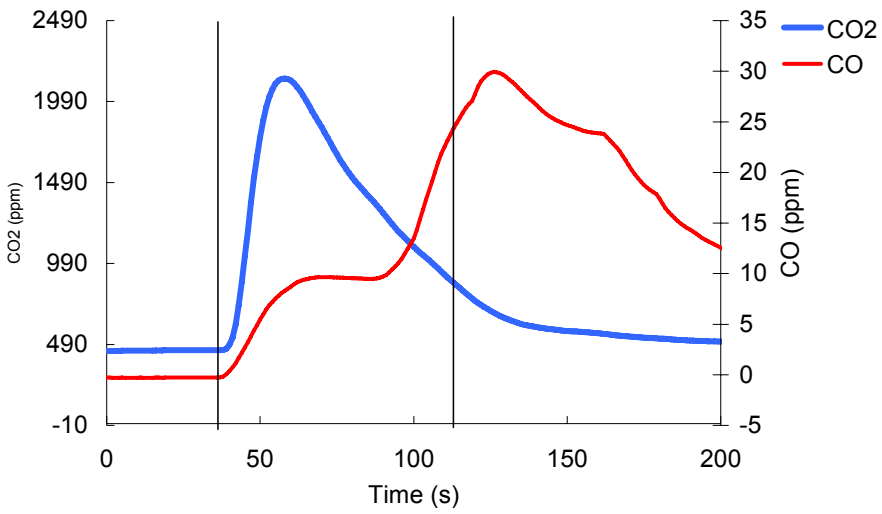

Figure 4. 24. Typical CO_2 and CO Behaviours for Test Run with No Combustion Air Flow Condition

The mass loss rate is illustrated in Figure 4.25 and showed that 80-90% of the mass of a fuel sample was lost prior to flameout. The amount of charring materials in pine needles is estimated at ~40% [49], therefore, this degree of mass loss indicates that the combustion of embers started prior to flameout (again indicated by the vertical line).

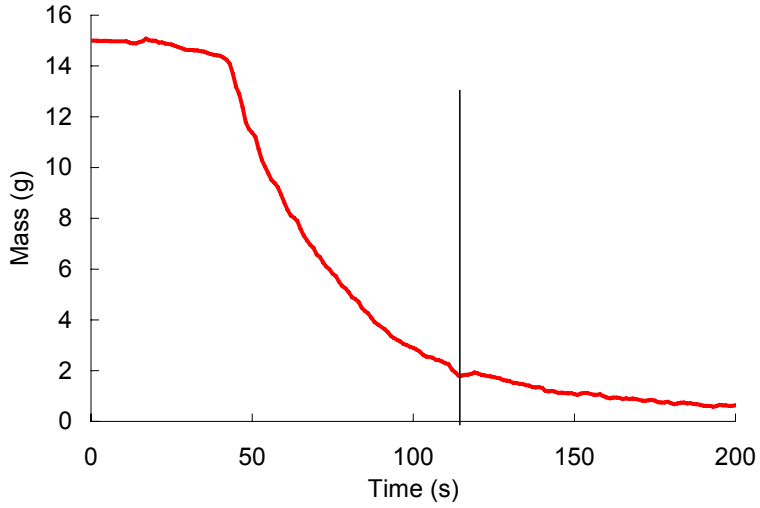

Figure 4. 25. Typical Mass Loss Curve for a No Combustion Air Test

Figures 4.26 and 4.27 contain the HRR curves in time for both types of fuels. Figure 4.26 shows each sample holder and fuel type combination for the no-flow condition. Figure 4.27 shows the sample holders and fuel type for the flow condition.

In Figure 4.26 the peak HRR was reached for all test conditions at approximately the same time, independent of species and the sample holder opening. The magnitude of the HRR was affected by the sample holder opening with the 63% basket having the highest value and the 0% having the lowest HRR. This tendency was stronger with *Pinus halepensis* and attributed to the higher surface-to-volume ratio. As stated, the surface to volume ratio effected the flow internal to the fuel bed and impacted thermal transfers and surface area of the fuel available for contact with oxygen.

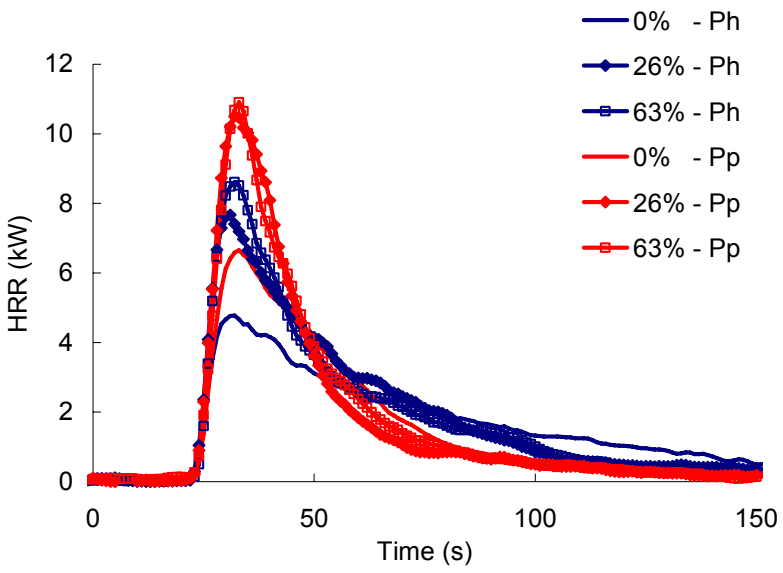

Figure 4. 26. HRR for the No Flow Test Condition for All Sample Holders and Both Fuels

Figure 4.27 shows the HRR in time for the flow condition in the fuel sample baskets. The curves indicate that the fuel has an effect on both the time to reach the peak HRR and the magnitude of the HRR. These results are reversed from the no-flow condition. The Peak HRR for *Pinus pinaster* was lower then that of *Pinus halepensis* when combustion air was flowed through the fuel bed. This result again demonstrates how the transport of air in the fuel bed controls the combustion process.

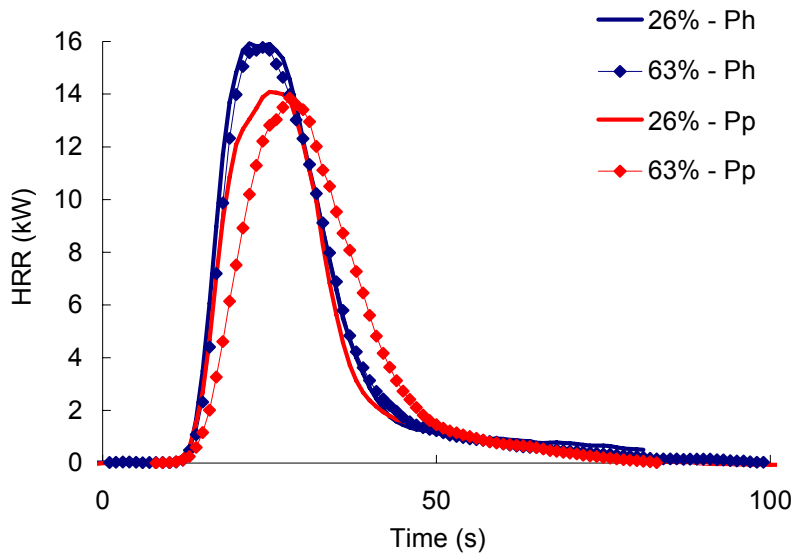

Figure 4. 27. HRR for Combustion Air Flow Condition for All Sample Holders and Both Fuels (Ph = *Pinus halepensis*, Pp = *Pinus pinaster*)

Figure 4.28 illustrates the no-flow and a 0% opening basket. The CO_2 curve reflects a long time of flaming combustion (around 130 s). The CO curve provides insight to the different steps involved in the combustion of the fuel samples when correlated with the observations. The first steep increase was due to the ignition of the sample on the upper surface. A steady production of CO follows. During this step, the burning front spread from the top to the bottom of the basket. When this spreading ended, no more degradation gases were produced and the flame extinguished. Then, oxygen was able to reach the surface of the charred material and combustion of embers within the fuel bed dominated the

combustion. The last decrease in the CO curve corresponded to the extinction of all combustion in the sample.

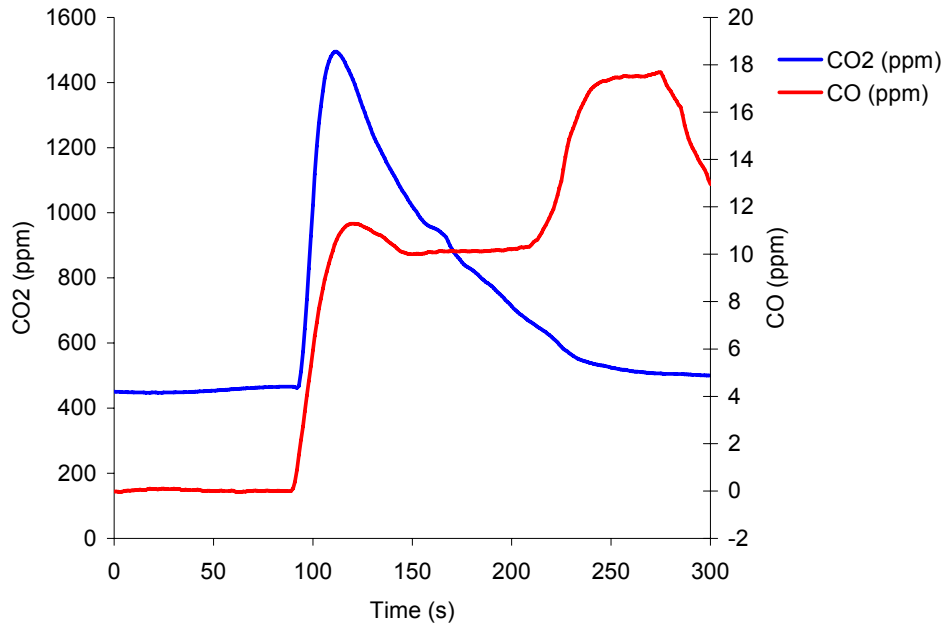

Figure 4. 28. 0% Opening Sample Holder CO_2 and CO Response Curves

In Figure 4.29 the CO response shows the typical one obtained for the flow conditions in the fuel bed. The CO generation was quicker and had no flat portion with a secondary peak. This must be caused by the increase in ventilation of the fuel bed. The magnitudes of the CO production were approximately the same for the flow and no flow conditions.

The CO and CO_2 values can also offer insight into the combustion process by examining the CO/CO_2 Ratio as the test progressed. Figure 4.30 is a plot of the CO/CO_2 Ratio for a combustion air flow test in a 63% open sample basket holder using *Pinus pinaster* needles. The plot starts at ignition of the sample and traces through the rest of the test. Flameout occurred at ~92 seconds. This is reflected by the sharp increase in the ratio at this point. The ratio increases and flattens out somewhat until a sharp decrease as the smouldering combustion rapidly extinguishes.

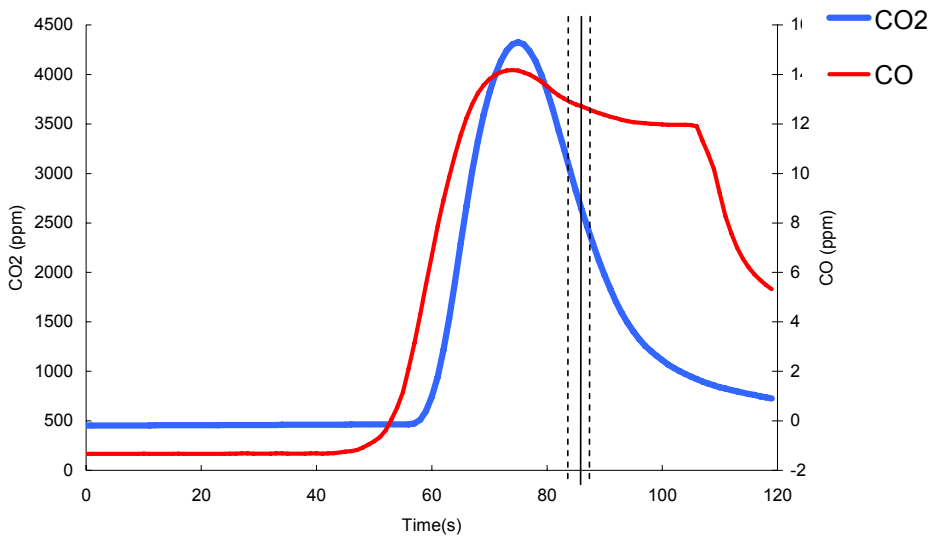

Figure 4. 29. 26% Opening Sample Holder with Combustion Air Flow CO_2 and CO Response Curves

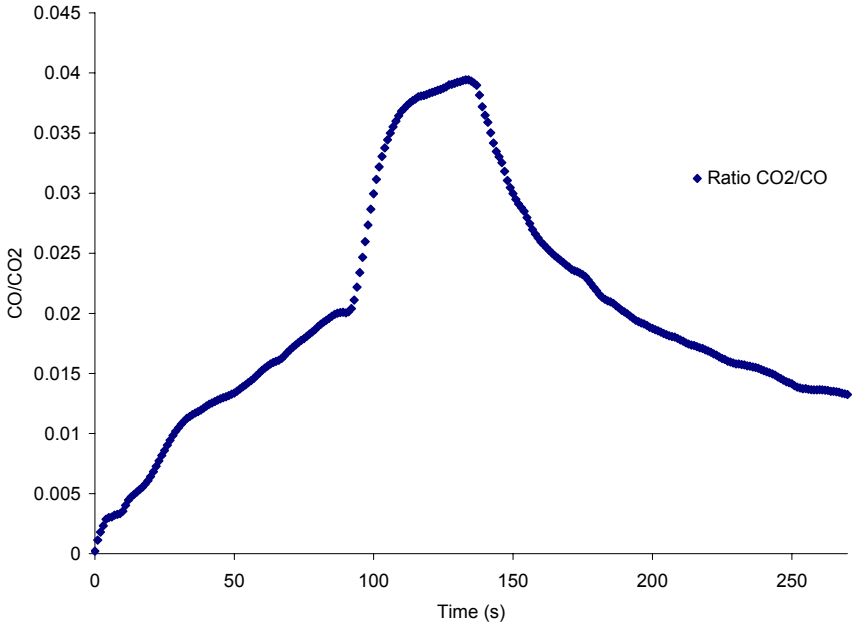

Figure 4. 30. CO/CO_2 Ratio from Ignition for a 63% Open Sample Holder with Combustion Air flow.

The FPA tests were highly repeatable and as a result of this many conclusions about the burning effect of flow through a porous fuel bed were possible. Much of the information gathered in FPA tests was also applied to a flow analysis of the fuel beds presented in the next section of this report.

4.4 Fuel Bed Flow Measurements and Analysis

Analysis of the test data presented so far in this section showed that the combustion air flow in the fuel beds had an effect on the measured HRR. The forced flow conditions in the fuel beds were created by a combustion air flow being introduced to the combustion chamber of the FPA. The velocity of the flows in the fuel samples was attempted to be controlled by the sample baskets surface holes (26% and 63% opening). Once through the sample basket wall, the combustion air was then available to enter the porous fuel bed and establish a flow rate based on the surface to volume ratio of the fuel.

To better understand the flow process in the fuel beds during the tests, an analysis of the combustion air flow and the fuel beds was done. The first step in the analysis was to determine the flow rates in the fuel beds under the different flow conditions. This was done for the 26% and 63% sample basket with each fuel using Partial Image Velocimetry (PIV) measurements.

In addition, some dimensionless analysis was done on the fuel beds for the measured flow rates. The importance of extending bench scale tests to full scale application is a key issue in fire testing in general and wildland fire experimental work in particular. Full scale fire testing is very expensive and often not possible given the scale of fires that present hazards. Therefore, the scalability of test behavior observed in bench scale testing, as in the cone calorimeter and FPA, needs to be understood relative to large scale wildland fire application.

A method is also presented in this section for estimating the effective time constant for the time to reach Peak HRR. This time constant was used as an

effective reaction rate for the portion of the combustion reaction from ignition until Peak HRR. This estimate then allowed a form of the Damköhler number to be calculated and used to examine some of the fuel bed properties. The details of all of these bed flow analysis are presented in this section.

4.4.1 Flow Measurement

To develop a better understanding of the flow phenomena, PIV measurements were taken of the fuel bed in the FPA under the combustion air flow condition. The PIV provided a velocity for the combustion air flow at two levels above the bed. The PIV system measured the air velocity profile above the surface of the needle filled baskets as positioned within the FPA combustion chamber. The section measured was across the diameter of the basket through the center.

Titanium Dioxide particles were used for seeding the flow. The particles have a nominal diameter in the 0.5 - 1 μm range and were introduced through a solid particle seeder linked to the airflow system already present in the FPA. The various PIV components were fixed to system of aluminum extrusion to ensure perpendicularity between the cameras and the light sheet.

The measurements were taken as the sample baskets were in position in the FPA combustion chamber with the combustion air flow on. No tests were made under flaming conditions. The average flow measurements with standard errors are presented for each basket and fuel in Table 4.13.

Table 4. 13. Mean Air Flow Velocity for Sample Baskets

Sample Holder/Fuel	Flow Velocity (mm/s) (SEE)
26% Basket *Pinus pinaster*	14 (3.7)
26% Basket *Pinus halepensis*	26 (2.4)
63% Basket *Pinus pinaster*	50 (4.6)
63% Basket *Pinus halepensis*	23 (2.4)

The 14 and 50 mm/s flow rates were measured for the *Pinus pinaster* and the 23 and 26 mm/s flow rates were for the *Pinus halepensis*. The *Pinus pinaster* has a surface to volume ratio about half that of the *Pinus halepensis*. The surface to volume ratio had the effect of making the fuel bed less sensitive to the sample holder opening. This can be seen in the *Pinus halepensis* flow rates in that they were effectively equal, given the distribution of the measurements as indicated by the standard errors. The confidence intervals for 23 +/- 4.8 mm/s and 26 +/- 4.8 mm/s overlap meaning that the uncertainty in the PIV measurement at these values can not distinguish between them.

The *Pinus pinaster* surface to volume ratio is approximately half that of the *Pinus halepensis*. The smaller surface to volume ratio created a larger void space in the fuel bed. The large void space allowed different flow rates through the fuel samples to be established for the different boundary conditions. The *Pinus halepensis* needles however, have a small void fraction in the bed and seem to have created a resistance to flow that was greater then the basket openings.

4.4.2 Flow and Peak Heat Release Rate

The analysis presented in this section has demonstrated that establishing a forced combustion air flow in a porous fuel bed has an effect, increases the magnitude, on the peak HRR. An ANOVA was run to examine the effect of the magnitude of that air flow as established during these tests on the Peak HRR. The results of the analysis are presented in Tables 4.14 and graphically in Figures 4.31 – 4.33. The results of the ANOVA help to describe how the specific flows in the fuel bed effected Peak HRR.

The Peak HRR achieved for both fuels independently were effectively independent of air flow, once an air flow was established in the fuel bed. The plots show that *Pinus halepensis* and *Pinus pinaster* had different Peak HRR's under combustion air flow conditions.

Table 4. 14. ANOVA for Peak HRR with Flow Magnitude
a) ANOVA Calculation Results, b) Mean Peak HRR

(a) Analysis of Variance

Source	Type III SS	df	Mean Squares	F-ratio	p-value
BED_FLOW	13.943	3	4.648	5.423	0.025
Error	6.857	8	0.857		

(b) Means for the Average Air Velocities in the Fuel Beds

n=3, Standard Error=0.535

Velocity (mm/s)	Mean Peak HRR (kW)
14	15.176
23	16.921
26	17.298
50	14.798

The results taken together are presented in Figure 4.31 and show how the different magnitude for flow that was established in the fuel beds affected the measured Peak HRR only when different fuels were in the beds. Figure 4.29 shows that the values for Peak HRR are only significantly different for the different fuels. *Pinus pinaster* had velocities of ~14 and 50 mm/s and *Pinus halepensis* had the velocities of 23 and 26 mm/s.

The combustion air flows effect on the measured Peak HRR for each fuel is illustrated in Figures 4.32 and 4.33, *Pinus halepensis* and *Pinus pinaster*, respectively. This analysis shows, as the ANOVA presented earlier in this section did, that for the flow magnitudes used in this experimental series, establishing air flow in the bed was the important parameter, not the flow magnitude.

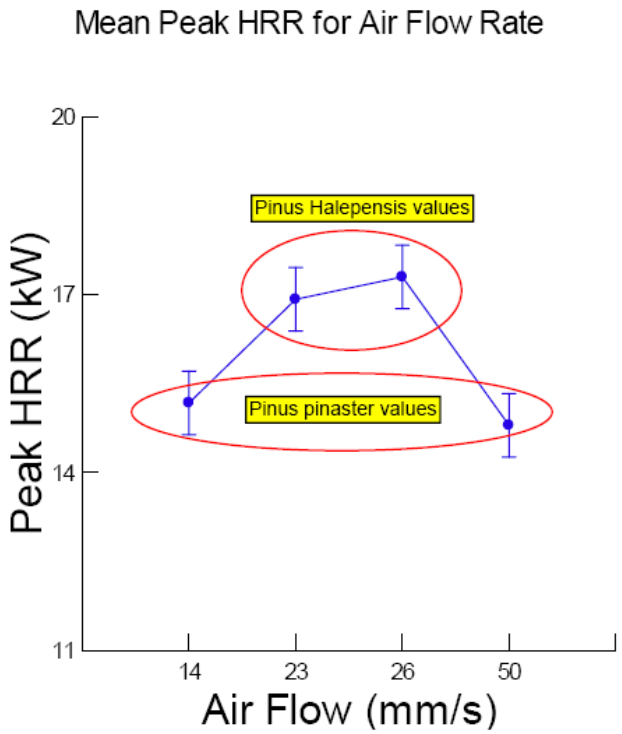

Figure 4. 31. Mean HRR for Samples Baskets at Each Air Flow

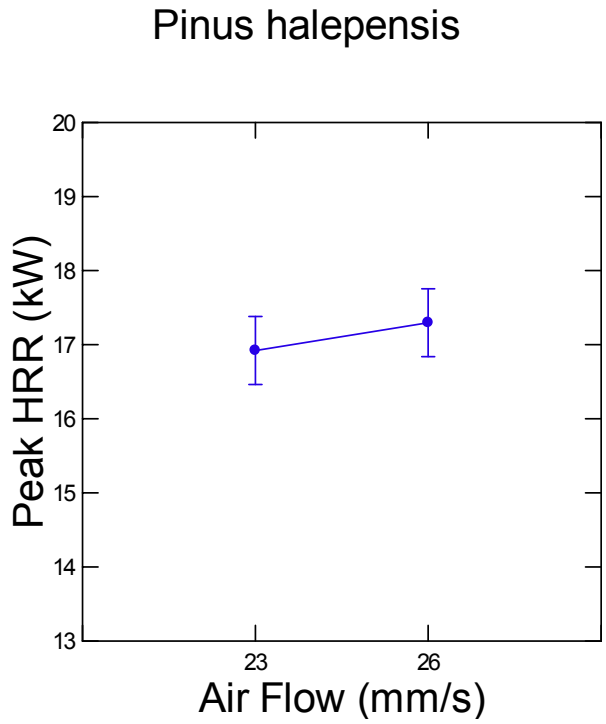

Figure 4. 32. Mean Peak HRR for *Pinus halepensis* with Combustion Air

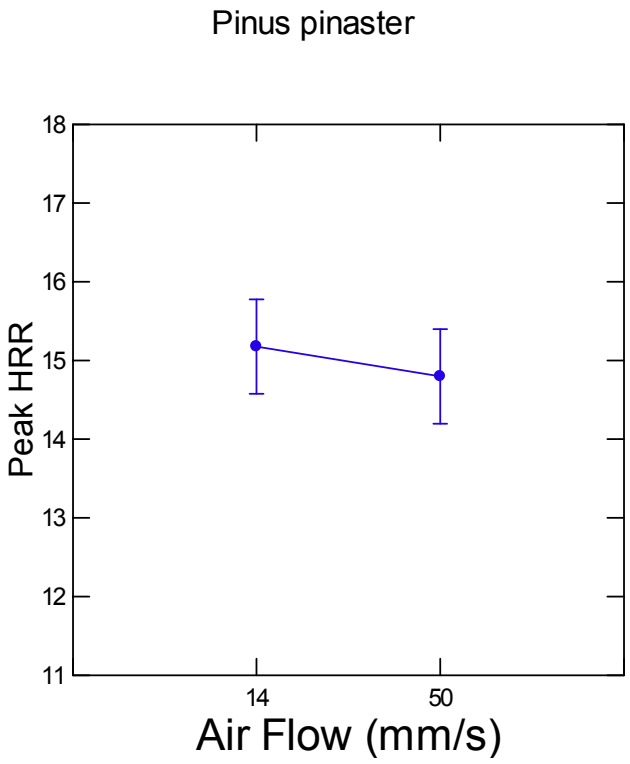

Figure 4. 33. Mean Peak HRR for *Pinus pinaster* with Combustion Air

The results illustrated in this ANOVA for the flow and data analysis helps to address Figures 4.26 and 4.27. Figure 4.26 shows the HRR for all of the no flow tests. Under these conditions the surface to volume ratio of the *Pinus pinaster* has an important effect on HRR. The smaller surface to volume ratio of the fuel translates to a larger void fraction in the fuel bed. With a greater void fraction less resistance was created by the fuel bed to natural convection during flaming. In Figure 4.27 the HRR peak values are reversed and the *Pinus halepensis* has a higher peak HRR under all combustion air flow conditions. This shows that when the fuel bed does not depend on an induced draft for ventilation, then the surface area of the fuel available to combust becomes the limiting factor.

4.4.3 Dimensionless Group and Reaction Rate Analysis

The fuel bed was also analyzed for consistency with some fundamental packed bed relationships to help determine scalability to larger samples of pine needles.

Dimensionless numbers, the Reynolds (Re) and Damköhler numbers (Da), were calculated for the test conditions where flow was measured. When two test conditions have the same or relatively equal dimensionless numbers, the flow dynamics can be considered similar allowing better comparison of the results. This type of analysis allows the values obtained for smaller experimental conditions to be extended to larger geometries when similar dimensionless values are used.

The form of the Reynolds number that applied to the conditions used in this test is presented in equation 4.6 [50].

$$\mathrm{Re}'' = \frac{d_p u \rho}{\mu} \qquad (4.6)$$

The Reynolds number is a ratio of the total momentum transfer to the molecular momentum transfer, or in effect the internal forces/viscous forces. The particle diameter (d_p) for the two fuels was estimated using a bed packing factor relationship for cylindrical packing also found in Treybal [50]. The PIV measured values were used for the flow velocity (u). The density (ρ) and viscosity (μ) of air was taken at the estimated fuel bed temperature.

Table 4.15 list the values of the dimensionless numbers calculated for the experimental conditions. The Reynolds number values for the *Pinus halepensis* were the same for both the 26% and 63% baskets with both being 1. The value for *Pinus pinaster* doubled from 14 for the 26% basket to 27 for the 63% basket. Both of these values were well within the laminar flow regime.

The Damköhler number was calculated using equation 4.11:

$$Da = \theta k \qquad (4.11)$$

The Damköhler number has several forms; however, the general relationship provides perspective on the chemical reaction rate to other processes in the system. The form used in this analysis relates the space volume (θ) to the reaction rate constant (k). The space volume is the inverse of the reaction zones residence time and was estimated based on the PIV velocity measurements and the sample holder dimensions. The reaction rate constant estimation method is described below. These two values provide a quantitative assessment of the reaction process that controls the HRR relative to the flow in the fuel bed.

To calculate the Damköhler number the reaction rate had to be estimated. The portion of the reaction considered for this was the time to reach Peak HRR. This was chosen because experimental observations showed that the fuel bed structure remained largely intact during this stage of burning, so the dimensionless analysis applies better in this region or the reaction.

A reaction rate constant, k, was estimated by calculating the time constant for the reaction rate from ignition until the Peak HRR value was reached. This approach assumed a second order dynamic response of the HRR to the combustion reaction, consistent with the calculations in Section 4.1.2 of the kinetics of the fuel beds. The time constant, τ, was estimated by Equation 4.12 [52].

$$\tau = \frac{3}{2}(t_2 - t_1) \qquad (4.12)$$

The t_1 and t_2 values were taken as 0.283 s and 0.632 s respectfully, of the fraction of time to reach the Peak HRR. This reaction rate was calculated for each flow condition.

Table 4.15 lists the Re and Da numbers along with the reaction rate (k) calculated for each flow condition. The values for all dimensionless numbers for the *Pinus halepensis* fuel beds under all flow conditions are equal. The values for the *Pinus pinaster* differ, indicating that the void fraction of the fuel sample dominated the

flow conditions. The test conditions did not allow for many data points to be measured for flow in the fuel beds. Establishing a larger range of flow velocities and more measured levels of flow velocity is an area that future experiments should explore.

Table 4. 15. Dimensionless Numbers and Estimated Reaction Rate for the Fuel Type, Sample Holder and Measured Flow Velocities (ph=*Pinus halepensis*, pp=*Pinus pinaster*)

	Ph 26% Sample Holder (23 mm/s)	Pp 26% Sample Holder (14 mm/s)	Ph 63% Sample Holder (26 mm/s)	Pp 63% Sample Holder (50 mm/s)
Re	1	6	1	20
Da	5	2	5	13
k (s)	3	1.5	3	5.25

Figure 4.34 shows how the Peak HRR changed with Re. As the Reynolds Number increases the Peak HRR may decrease. Figure 4.35 shows the Damköhler and Peak HRR. No conclusions can be made about this relationship form this data.

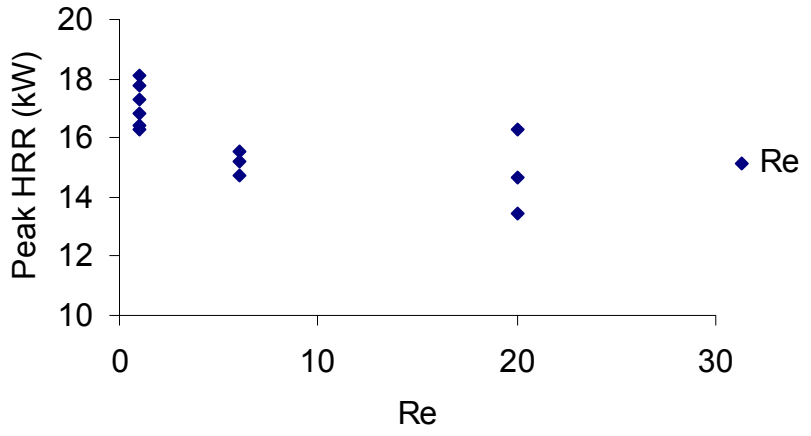

Figure 4. 34. Re and Peak HRR for all Fuel Baskets

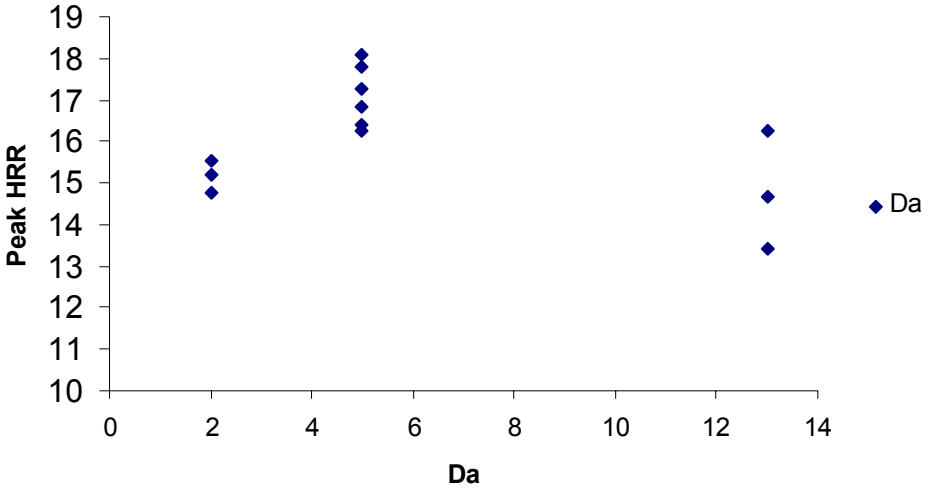

Figure 4. 35. Da and Peak HRR for all Sample Baskets

5.0 CONCLUSIONS

The relevance of the work and the novel contribution to the field of engineering was that by conducting an experimental test series and analyzing the data and examining the scalability of the test conditions, the effect of transport processes on the HRR of porous wildland fuels was determined. Several conclusions can be made based on the test program and the data analysis that have an impact on calorimetry testing of porous fuels. In addition, several of the findings are highly relevant to how fire modeling needs to address porous fuels.

The goal of this research project was to use existing fire test methods and apparatuses to develop an understanding of how transport processes affected combustion of porous wildland fuels. To this end, a series of tests were developed using a test method that allowed air to flow into a porous fuel bed from all directions during combustion. The test series was designed and carried out using standard fire testing equipment, specifically the cone calorimeter and the FPA. Two porous wildland fuels, *Pinus halepensis* and *Pinus pinaster* needles were used as fuel.

A series of cone calorimeter tests examined transport effects by using both the standard sample holder for the cone and an open mesh sample holder. The transport process effects were based on the combustion performance of the fuels in the two types of sample holders. During the tests, the cone allowed the induced draft driven by the flame to flow though the fuel sample in the open mesh sample holder. This was in contrast to the standard Cone sample holder that had solid sides and allowed air to enter the fuel bed only from the top. The cone tests clearly showed that the HRR increased with the use of the open mesh sample holder from an average of ~256 kW/m^2 (2.56 kW) for the standard sample holder to ~617 kW/m^2 (7.72 kW) for the open mesh sample holder.

The test results in the cone for the two types of sample holders also showed that the burning process was much faster for the open mesh holder in both HRR and mass loss. These results are clearly shown in Figures 4.1 – 4.3. However, even though the reaction process was faster, the order of the conversion of fuel to combustion products was found to remain the same for the open mesh sample holder. An analysis of the conversion for the fuel kinetics showed the process to be second order for both the standard sample holder and the open mesh sample holder. This was illustrated in Figures 4.4 – 4.7.

Tests were also conducted in the FPA and designed with parameters that created three methods of regulating transport in the fuel bed. First was the use of a forced combustion air flow in the combustion chamber. The combustion air had two distinct levels of either being on or off. When the forced air flow was on, the sample basket was exposed to a significant flow across the outside surface and around the top of the basket. The openings on the sample holder walls had three levels, 0, 26 and 63 percent open. This parameter regulated flow into the fuel bed at the outside boundary. The third parameter was the fuel type. The two fuels had chemical compositions and heats of combustion that were similar, however, the two fuels had different surface to volume ratios. The different surface to volume ratios created a difference in the void fraction of the fuel beds. The void fraction difference created different internal flow characteristics.

Tests were run that examined these test parameters in all 12 test combinations. Four of these test combinations used the 0% open sample holder, two with a combustion air flow and two without flow. The cone tests were run under similar conditions with the *Pinus halepensis* fuel. The FPA result for similar test parameters (Pinus halepensis, 0% sample holder, no flow) had a HRR of 421 kW/m2 (5.27 kW) and for the combustion air flow condition the HRR was 223 kW/m^2 (2.78kW). The FPA has a fundamentally different combustion chamber that restricts the natural draft that could be established by the porous fuel bed. It appears that the combustion air flow around the 0% sample holder cooled the sample during burning and reduces the HRR.

In the FPA tests with *Pinus halepensis* the HRR (~17 kW) was not significantly different between the 26% and 63% open sample baskets (the two sample baskets capable of allowing combustion air into the fuel sample). This indicated that the sample basket opening was on a different scale then the void space inside the fuel matrix. The PIV measurements also showed that the velocity of the flow inside the fuel bed was approximately the same (between 23-26 mm/s) for both sample holders.

The *Pinus pinaster* fuel also had no significant HRR change between the 26% and 63% sample baskets (~15 kW for both). However, the air flow measured by the PIV showed that the 26% open holder resulted in a 14 mm/s air velocity and the 63% open basket had a 50 mm/s air velocity.

The difference between flow and no flow test conditions in the FPA showed some other interesting effects. The fuel beds surface to volume ratio was a significant predictor of HRR in two ways. Under natural draft conditions inside the fuel bed the surface to volume ratio of the fuel controls HRR. The larger the void fraction of the bed (lower surface to volume ratio) resulted in a higher HRR.

When a forced draft was present, like a wind in a natural setting, the opposite was true. The increase in void fraction for a porous fuel decreases the peak HRR. This relationship was not found anywhere in the literature and has an important impact on how porous fuel beds should be modeled. This effect was best illustrated in Figures 4.14 for peak HRR and Figures 4.26 and 4.27 for the dynamic HRR curves. This proves that when a porous fuel bed does not depend on a flame induced draft for ventilation then the surface area of the fuel bed becomes the limiting factor in the combustion process.

The effect of air flow in the fuel beds was examined using the Reynolds and Damköhler numbers along with an estimate of the reaction rate for the HRR reaction. Theses numbers were consistent for the different sample holders for the

Pinus halepensis fuel beds. For the 26% and 63% open sample holders the values changed by a factor of three for Re, six for Da and three for reaction rate only for the *Pinus pinaster* fuel bed. Table 4.15 shows these values.

For a given fuel the HRR was always significantly higher when the fuel bed was able to establish flow in the entire depth of the layer. The air flow in the fuel layer increased HRR, either induced by the flame or forced by test conditions. However, the forced flow condition resulted in a higher HRR as a function of the fuels surface to volume ratio.

The key finding for wildland fuel testing and modeling was that transport in the depth fuel bed layer was the limiting process on HRR. This test condition was similar to a no wind condition in a wildland fire. With a forced flow like wind an increase in a fuels surface to volume ratio increases the HRR. This phenomenon was not found in the literature as an important test parameter or modeling factor.

The goal of the test series was to test the hypothesis that transport processes were the dominant factor in determining the rate of burning in this type of porous wildland fuel configuration. The conclusion, based on all of the tests reported here, was that the major factor in controlling HRR was the ability of the porous fuel bed to use its internal transport properties during combustion. Once this was established by natural convection in the Cone and forced combustion air in the FPA, the HRR increased significantly.

6.0 REFERENCES

1 Pappa, A.A., Tzamtzis, N.E., Statheropoulos, M.K., Liodakis, S.E., Parissakis, G.K., A Comparative study of the effects of fire retardants on the pyrolysis of cellulose and *Pinus Halepensis* pine-needles, Journal of Analytical and Applied Pyrolysis, 31 (1995) 85 100.

2 Statheropoulos, M.K., Liodakis, Pappa, A.A., Kyriakou, S., Thermal degradation of Pinus Halepensis pine-needles using various analytical methods, Journal of Applied Pyrolysis, 43 (1997) 115-123.

3 Zhou, X., Weise, D., Mahalingam, S., Experimental measurements and numerical modeling of marginal burning in live chaparral fuel beds, Proceedings of the Combustion Institute 30, 2005, 2287-2294. 2004.

4 Babrauskas, V. and Grayson, S. *Heat Release in Fires,* 1992, Elsevier Science Publishing Co., Inc.

5 Rothermal, R.C., A Mathematical Model for Predicting Fire Spread in Wildland Fuels, USDA Forest Service Research Paper INT-115. January 1972.

6 Frandsen, W.H., Fire Spread through Porous Fuels from the Conservation of Energy, Combustion & Flame, 16,9-16, 1971. The Combustion Institute.

7 Rivera, S., Personal Communication, Director of Wildland Fire Loss Prevention, AIG Insurance, August 2007.

8 Drysdale, D., An Introduction to Fire Dynamics, 2nd Edition, 2000, John Wiley and Sons.

9 Keane, R.E., Cary, G.J., Parsons, R. Using simulation to map fire regimes: an evaluation of approaches, strategies, and limitations, International Journal of Wildland Fire, 2003, 12, 309-322.

10 Zhou, X,, Pereira, C.F., A Multidimensional Model for Simulation Vegetation Fire Spread using a Porous Media Sub-model, Fire and Materials, 24, 37-43 (2000).

11 Finney, M.A., FARSITE: Fire Area Simulator-Model Development and Evaluation, USDA, Forest Service, RMRS. Research Paper RMRS-RP-4 Revised March 1998.

12 Scott, J., Burgan, R., Standard Fire Behavior Fuel Models: A Comprehensive Set for Use with Rothermel's Surface Fire Spread Model. USDA Forest Service, RMRS. General Technical Report RMRS-GTR-153, June 2005.

13 Bachmann, A., Allgower, B., Uncertainty propagation in wildland fire behavior modelling, International Journal of Geographical Information Science, 2002, Volume 16, no. 2, 115-127.

14 Andrews, P.L., Queen, L.P., Fire modeling and information system technology, International Journal of Wildland Fire, 2001, 10, 343-355.

15 Catchpole, E.A., Catchpole, W.R., Modelling Moisture Damping for Fire Spread in a Mixture of Live and Dead Fuel, International Journal of Wildland Fire, 1(2): 101-106, 1991.

16 Solomon, P., et.al., General Model for Coal Devolatilization, Energy & Fuels, 1988, 2, 405-422.

17 Rogaume, T., et.al., The effects of different airflows on the formation of pollutants during waste incineration, Fuel, 81, 2002, 2277-2288.

18 Dasappa, S., Paul, P., Gasification of char particles in packed beds: analysis and results, International Journal of Energy Research, 2001: 25: 1053-1072.

19 Morvan, D., Dupuy, J.L., Modeling of Fire Spread Through a Forest Fuel Bed Using a Multiphase Formulation, Combustion and Flame 127: 1982-1984 (2001).

20 Zhou, X., Weise, D., Mahalingam, S., Experimental measurements and numerical modeling of marginal burning in live chaparral fuel beds, Proceedings of the Combustion Institute 30, 2005, 2287-2294. 2004.

21 Morvan, D., Larini, M. Modeling of One Dimensional Fire Spread in Pine Needles with Opposing Air Flow, Combustion and Science Technology, Volume 363, pp 1-28.

22 Dupuy, J.L., Marechal, J., Morvan, D., Fires from a cylindrical forest fuel burner: combustion dynamics and flame properties, Combustion and Flame 135 (2003) 65-76.

23 Mendes-Lopes, J.M., Ventura, J.M., Amaral, J.M., Flame characteristics, temperature-time curves, and rate of spread in fires propagating in a bed of Pinus pinaster needles, International Journal of Wildland Fire, 2003, 12, 67-84.

24 Marcelle, T., Santoni, P., Simeoni, A., Porterie, B., Fire spread across pine needle fuel beds: characterization of temperature and velocity distributions within the fire plume, International Journal of Wildland Fire, 2004, 13, 37-48.

25 Porterie, B., et.al., Firespread through fuel beds: Modeling of wind-aided fires and induced hydrodynamics, Physics of Fluids, Volume 12, Number 7, July 2000.

26 Fatehi, M., Kaviany, M., Adiabatic Reverse Combustion in a Packed Bed, Combustion and Flame 99: 1-17 (1994).

27 Nelson, R., An effective wind speed for models of fire spread, International Journal of Wildland Fire, 2002, 11, 153-161.

28 Weise, D.R., White, R.H., Beall, F.C., Etlinger, M., Use of the cone calorimeter to detect seasonal differences in selected combustion characteristics of ornamental vegetation, International Journal of Wildland Fire, 2005, 14, 321-338.

29 Blank, R.R., White, R.H., Ziska, L.H., Combustion properties of *Bromus tectorum* L: influence of ecotype and growth under four CO_2 concentrations, International Journal of Wildland Fire, 2006, 15, 227-236.

30 Sparks, J. et.al, Season of Burn Influences Fire Behavior and Fuel Consumption in Restored Shortleaf Pine-Grassland Communities, Restoration Ecology, Volume 10, Number 4, 714-722.

31 Benkoussas, B., et.al., Modelling thermal degradation of woody fuel particles, International Journal of Thermal Sciences, 46, 2007, 319-327.

32 Janssens, M. L. and Babrauskas, V., Oxygen Consumption Calorimetry, Heat Release in Fires, Elsevier Applied Science, 1992, pp31-59.

33 Thornton, W.M., The Relation of Oxygen to the Heat of Combustion of Organic Compounds, Philosophical Magazine and Journal of Science, 6(33), 196-203, (1917).

34 Huggett, C., Estimation of Rate of Heat Release by means of Oxygen Consumption Calorimetry, Fire and Materials. 4(2), 61-65, (1980).

35 Tewarson, A., Generation of Heat and Chemical Compounds in Fires, in: P.J. DiNenno (Ed.), SFPE Handbook of Fire Protection Engineering, The National Fire Protection Association Press, 2002, pp. 3-82 - 3-161.

36 Parker, W.J., Calculation of the Heat Release Rate by Oxygen Consumption for Various Applications, Journal of Fire Sciences. 2, 380-395, (1985).

37 BS 476-15: 1993. *Fire Tests on Building Materials and Structures- Part 15: Method for measuring the rate of heat release of products.*

38 Users' Guide for the Fire Propagation Apparatus (FPA) ASTM E-2058. Fire Testing Technology Limited, Issue 2.0: August, 2003.

39 Babrauuskas, V., Ten Years of Heat Release Research with the Cone Calorimeter, Heat Release and Fire Hazard, Volume I, editor Hasemi, Y., Building Research Institute, Tsukuba, Japan, 1993. (Website: www.doctorfire.com/cone).

40 Leroy, V., Cancellieri, D., Leoni, E., Thermal degradation of lingo-cellulosic fuels: DSC and TGA studies, Thermochimica Acta 451 (2006) 131-138.

41 Fernandes, P.M., Rego, F.C., A New Method to Estimate Fuel Surface Area-to-Volume Ratio Using Water Immersion, International Journal of Wildland Fire, 8(3): 121-128, 1998.

42 Schemel, C.F., Simeoni, A., Biteau, H., Rivera, J.D., Torero, J.L. A Calorimetric Study of Wildland Fuels, Experimental Thermal and Fluid Science (2007).

43 SYSTAT 12, SYSTAT Softwae, Inc., 2007.

44 Johnson, R., Miller & Freund's Probability and Statistics for Engineers, Prentice Hall, 1993.

45 Schemel, C.F., Rivera, J.D., Torero, J.L., Calorimetric Study of Wildland Fuel Considering Proous Bed Effects, 5th International Seminar on Fire and Explosion Hazards, April 23-27, 2007, Edinburgh, UK.

46 Brohez, S., Uncertainty analyais of heat release rate measument form oxygen consumption calorimety, Fire and Materials, 2005, 29, 383-394, Wiley InterScience.

47 Taylor, J., An Introduction to Error Analysis, 2nd Edition, University Science Books, 1997.

48 Staggs, J.E.J., Savitzky-Golay smoothing and numerical differentiation of cone calorimeter mass data, Fire Safety Journal, 40, 493-205 (2005).

49 Grishin, A.M., In Albini (Ed.). Mathematical modeling of forest fires and new methods of fighting them. Publishing house of the Tomsk State University, 210 p (1996).

50 Treybal, R. *Mass-Transfer Operations,* 1987, McGraw-Hill Classic Textbook Reissue Series, McGraw-Hill Book Company, Inc.

52 Smith, C., Corripio, A., Principles and Practices of Automatic Process Control, John Wiley and Sons, 2000.

Appendix A

SYSTAT Output: ANOVA for Peak HRR with Fuel Type, Basket Type and Flow Condition

▼Analysis of Variance for Peak HRR with Fuel, Basket and Flow

Effects coding used for categorical variables in model.
The categorical values encountered during processing are

Variables	Levels		
FUEL$ (2 levels)	Halepinses	Pinaster	
BASKET$ (3 levels)	0%	26%	63%
FLOW$ (2 levels)	flow	no	

Dependent Variable	Peak HRR
N	36
Multiple R	0.993
Squared Multiple R	0.985

Estimates of Effects B = $(X'X)^{-1}X'Y$

Factor	Level	Peak HRR
CONSTANT		10.309
Fuel Type (Sur. to Vol. Ratio)	Halepinses	-0.335
Sample Holder	0%	-5.560
Sample Holder	26%	2.690
Combustion Air	flow	1.486
Fuel Type (Sur. to Vol. Ratio)*Sample Holder	Halepinses*0%	-0.385
Fuel Type (Sur. to Vol. Ratio)*Sample Holder	Halepinses*26%	0.117
Fuel Type (Sur. to Vol. Ratio)*Combustion Air	Halepinses*flow	0.874
Sample Holder*Combustion Air	0%*flow	-2.947
Sample Holder*Combustion Air	26%*flow	1.753
Fuel Type (Sur. to Vol. Ratio)*Sample Holder*Combustion Air	Halepinses*0%*flow	-0.658
Fuel Type (Sur. to Vol. Ratio)*Sample Holder*Combustion Air	Halepinses*26%*flow	-0.404

Analysis of Variance

Source	Type III SS	df	Mean Squares	F-ratio	p-value
Fuel Type (Sur. to Vol. Ratio)	4.041	1	4.041	7.715	0.010
Sample Holder	556.658	2	278.329	531.420	0.000
Combustion Air	79.480	1	79.480	151.753	0.000
Fuel Type (Sur. to Vol. Ratio)*Sample Holder	2.812	2	1.406	2.684	0.089
Fuel Type (Sur. to Vol. Ratio)*Combustion Air	27.519	1	27.519	52.542	0.000
Sample Holder*Combustion Air	158.218	2	79.109	151.040	0.000

Analysis of Variance

Source	Type III SS	df	Mean Squares	F-ratio	p-value
Fuel Type (Sur. to Vol. Ratio)*Sample Holder*Combustion Air	7.939	2	3.970	7.579	0.003
Error	12.570	24	0.524		

Least Squares Means

Factor	Level	LS Mean	Standard Error	N
Fuel Type (Sur. to Vol. Ratio)	Halepinses	9.974	0.171	18.000
Fuel Type (Sur. to Vol. Ratio)	Pinaster	10.644	0.171	18.000

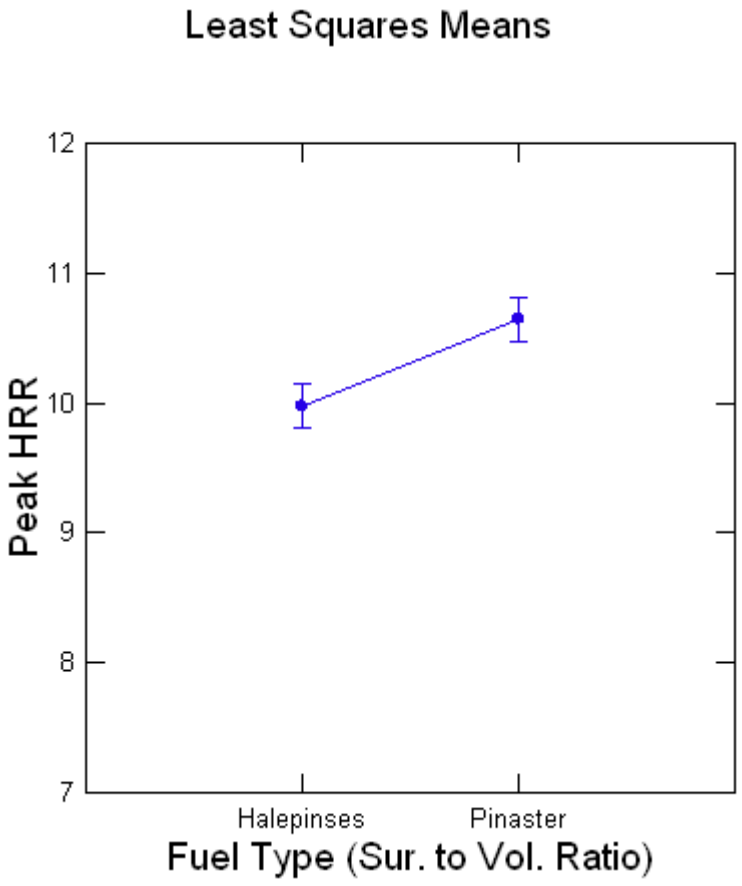

Least Squares Means

Factor	Level	LS Mean	Standard Error	N
Sample Holder	0%	4.749	0.209	12.000
Sample Holder	26%	12.998	0.209	12.000
Sample Holder	63%	13.179	0.209	12.000

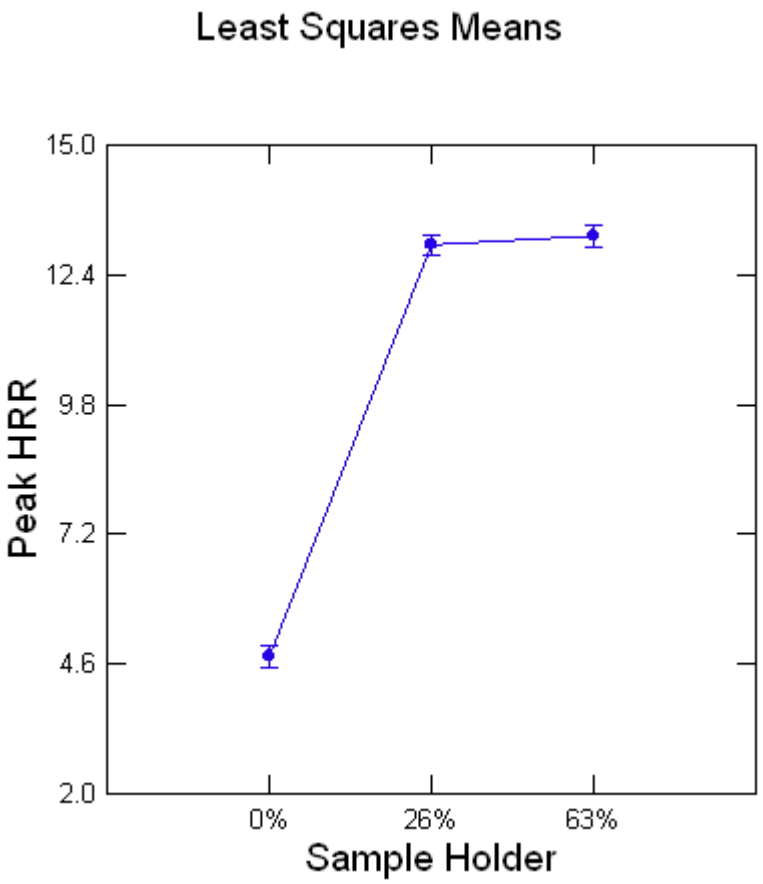

Least Squares Means

Factor	Level	LS Mean	Standard Error	N
Combustion Airflow		11.795	0.171	18.000
Combustion Airno		8.823	0.171	18.000

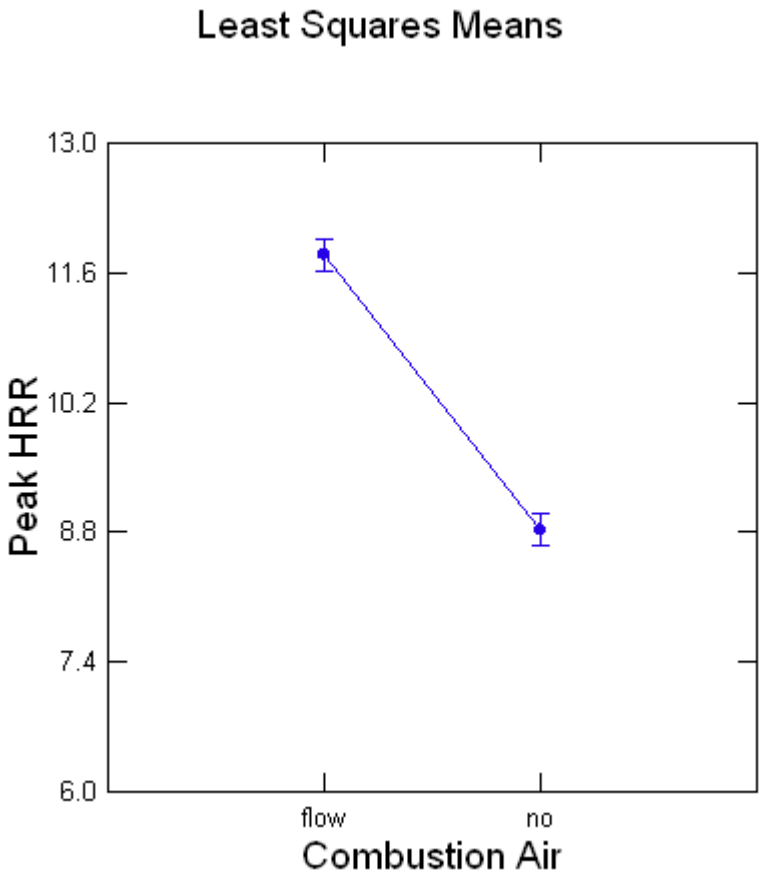

Least Squares Means

Factor	Level	LS Mean	Standard Error	N
Fuel Type (Sur. to Vol. Ratio)*Sample Holder	Halepinses*0%	4.028	0.295	6.000
Fuel Type (Sur. to Vol. Ratio)*Sample Holder	Halepinses*26%	12.781	0.295	6.000
Fuel Type (Sur. to Vol. Ratio)*Sample Holder	Halepinses*63%	13.113	0.295	6.000
Fuel Type (Sur. to Vol. Ratio)*Sample Holder	Pinaster*0%	5.469	0.295	6.000
Fuel Type (Sur. to Vol. Ratio)*Sample Holder	Pinaster*26%	13.216	0.295	6.000
Fuel Type (Sur. to Vol. Ratio)*Sample Holder	Pinaster*63%	13.246	0.295	6.000

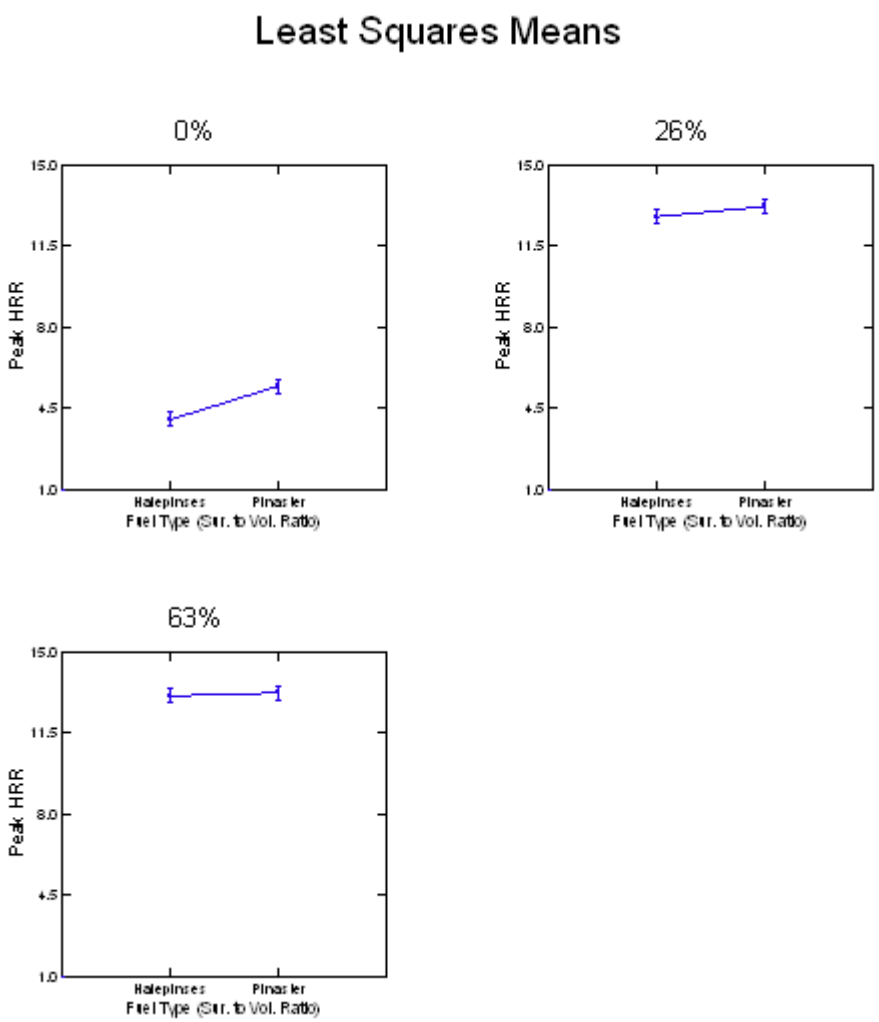

Least Squares Means

Factor	Level	LS Mean	Standard Error	N
Fuel Type (Sur. to Vol. Ratio)*Combustion Air	Halepinses*flow	12.334	0.241	9.000
Fuel Type (Sur. to Vol. Ratio)*Combustion Air	Halepinses*no	7.614	0.241	9.000
Fuel Type (Sur. to Vol. Ratio)*Combustion Air	Pinaster*flow	11.255	0.241	9.000
Fuel Type (Sur. to Vol. Ratio)*Combustion Air	Pinaster*no	10.032	0.241	9.000

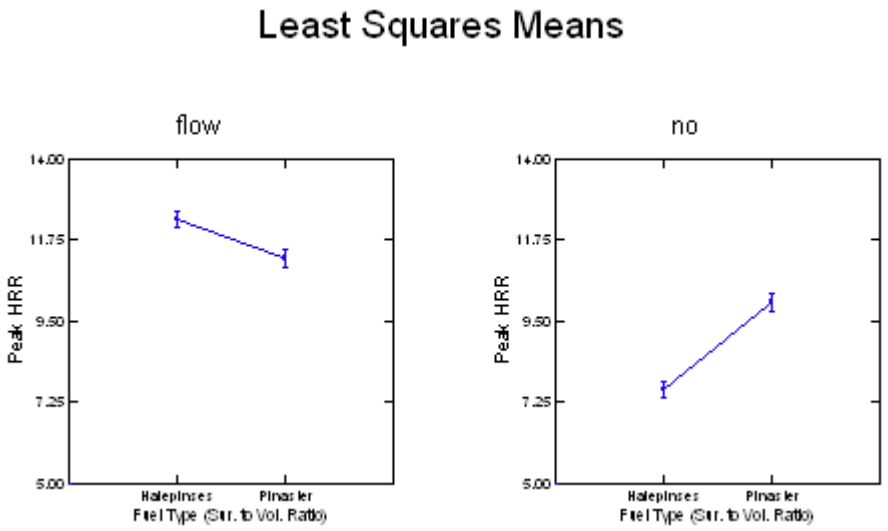

Least Squares Means

Factor	Level	LS Mean	Standard Error	N
Sample Holder*Combustion Air	0%*flow	3.287	0.295	6.000
Sample Holder*Combustion Air	0%*no	6.210	0.295	6.000
Sample Holder*Combustion Air	26%*flow	16.237	0.295	6.000
Sample Holder*Combustion Air	26%*no	9.760	0.295	6.000
Sample Holder*Combustion Air	63%*flow	15.860	0.295	6.000
Sample Holder*Combustion Air	63%*no	10.499	0.295	6.000

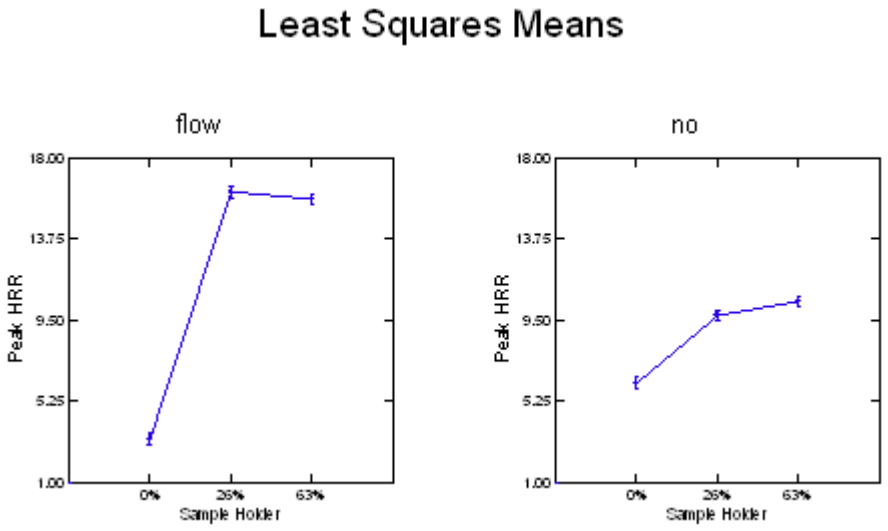

Least Squares Means

Factor	Level	LS Mean	Standard Error	N
Fuel Type (Sur. to Vol. Ratio)*Sample Holder*Combustion Air	Halepinses*0%*f-low	2.783	0.418	3.000
Fuel Type (Sur. to Vol. Ratio)*Sample Holder*Combustion Air	Halepinses*0%*n-o	5.274	0.418	3.000
Fuel Type (Sur. to Vol. Ratio)*Sample Holder*Combustion Air	Halepinses*26%*-flow	17.298	0.418	3.000
Fuel Type (Sur. to Vol. Ratio)*Sample Holder*Combustion Air	Halepinses*26%*-no	8.263	0.418	3.000
Fuel Type (Sur. to Vol. Ratio)*Sample Holder*Combustion Air	Halepinses*63%*-flow	16.921	0.418	3.000
Fuel Type (Sur. to Vol. Ratio)*Sample Holder*Combustion Air	Halepinses*63%*-no	9.304	0.418	3.000
Fuel Type (Sur. to Vol. Ratio)*Sample Holder*Combustion Air	Pinaster*0%*flo-w	3.792	0.418	3.000
Fuel Type (Sur. to Vol. Ratio)*Sample Holder*Combustion Air	Pinaster*0%*no	7.146	0.418	3.000
Fuel Type (Sur. to Vol. Ratio)*Sample Holder*Combustion Air	Pinaster*26%*flow	15.176	0.418	3.000
Fuel Type (Sur. to Vol. Ratio)*Sample Holder*Combustion Air	Pinaster*26%*no	11.256	0.418	3.000
Fuel Type (Sur. to Vol. Ratio)*Sample Holder*Combustion Air	Pinaster*63%*flow	14.798	0.418	3.000
Fuel Type (Sur. to Vol. Ratio)*Sample Holder*Combustion Air	Pinaster*63%*no	11.694	0.418	3.000

Least Squares Means

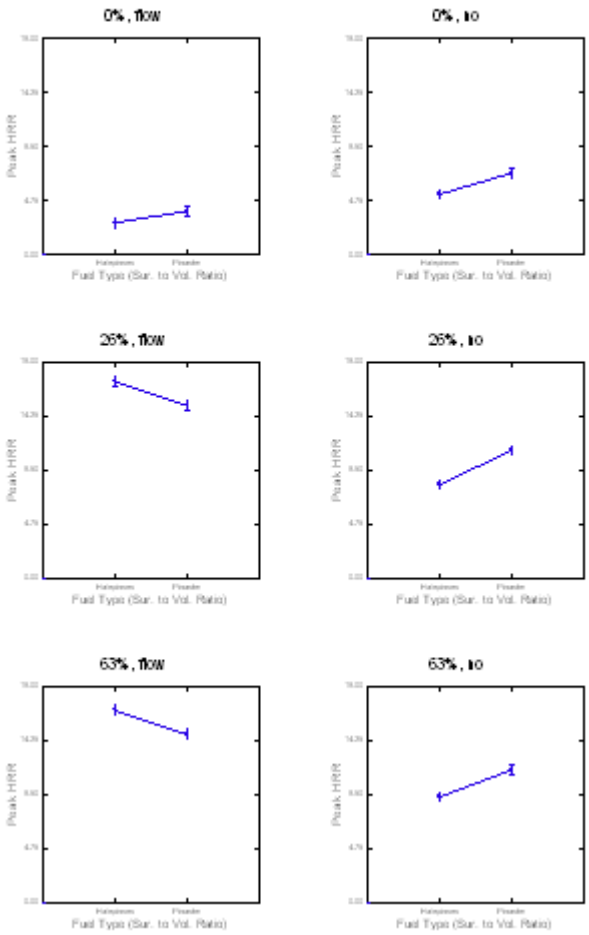

Durbin-Watson D Statistic	2.492
First Order Autocorrelation	-0.261

Information Criteria

AIC	90.284
AIC (Corrected)	106.829
Schwarz's BIC	110.870

Appendix B

CALIMETRIC STUDY OF VARIOUS WILDLAND FUELS CONSIDERING POROUS BED EFFECTS

CALORIMETRIC STUDY OF WILDLAND FUEL CONSIDERING POROUS BED EFFECTS

C. F. Schemel[1,2], J. D.Rivera[3],
J. L. Torero[1]
University of Edinburgh, Edinburgh, UK
Pontificia Universidad Catolica de Chile, Santiago, Chile
Packer Engineering Inc., USA

5th International Seminar on Fire and Explosion Hazards
April 23 – 27, 2007
Edinburgh, United Kingdom

Abstract:

The application of transport processes, pyrolysis, combustion and fluid dynamics to predict large scale wildland fire behavior is a complex engineering problem. Many aspects of wildland fire spread modeling are still in the very early stages of development. The testing program presented in this paper examines the combustion of pine needles (*Pinus Halepensis*) as a porous fuel bed. The pine needles were burned using a cone calorimeter and fuel sample holders that established distinctly different levels of permeability for the fuel bed. One sample holder maximized the fuel bed permeability and the other minimized the permeability effects. This allowed for a level effect analysis on fuel bed permeability and its effect on key combustion parameters. Measured cone parameters involving energy release; total energy and Rate of Heat Release, in addition to mass loss were shown to be significantly affected by the permeability of the fuel sample holder. The test results also showed that the non- permeable samples fuel decomposition rate was described by first order kinetics and the permeable sample fuel beds decomposition rate was described by second order kinetics. The influence of sample permeability on energy release on a mass loss basis was also identified in the data.

INTRODUCTION

The physical process of wildland fire spread has been researched for many years. There is significant understanding of the underlying phenomena including heat and mass transfer, pyrolysis, combustion and fluid dynamics. However, the application of these basic principles to predict large scale wildland fire behavior, to the degree necessary for reliable engineering applications, is still in its infancy. Therefore, the need exists to continue research in this area and further develop wildland fire modeling tools.

The testing program presented here has identified six forest floor fuels, relevant to Mediterranean and Scandinavian regions, to be analyzed to better understand their combustion characteristics. These fuels are *Pinus Halepensis* (alive/dead), *Pinus Pinaster* (alive/dead), *Quercus coccifera* foliage and *Feather moss*. The goal is to help advance wildland fire spread modeling by developing a detailed understanding of the combustion process in these selected fuels.

This paper offers a brief background on the development of wildland fire spread modeling. An emphasis is placed on developments in understanding forest floor fuels and how they behave as permeable fuel beds during heating, ignition, and burning. Additionally, the general trend in forest fuel calorimetry research is presented. These reviews are intended to provide a perspective and add relevance to the current research.

The test results presented and analyzed here are intended to develop a testing methodology and involve only characterizing the behavior of dead *Pinus Halepensis* in the cone calorimeter. The fuel was burned under two distinct test conditions, one maximized fuel bed permeability and the other minimized permeability effects. Differences in the bulk burning characteristics of the fuel beds and the kinetics of the burning process under the two test conditions were demonstrated for several relevant parameters.

BACKGROUND

Spatial depiction of wildland fire characteristics, such as severity, intensity and pattern, are indispensable in fire management [1]. To provide useful and timely wildland fire

behavior information, computer codes have been applied to the problem of modeling wildland fire spread in a practical way since 1972 [2]. Rothermel developed the first widely accepted complete spread model for wildland fires for the U.S. Forestry Service. At the core of the model, Rothermel used an equation that described fire spread in a porous fuel bed as a function of the fuel heat release rate, fuel bed depth, effective heat of combustion of the fuel and the mass of the fuel burned [3]. Rothermel's method for predicting fire spread, although complete for a set of underling assumptions, was restricted to a homogenous fuel bed and a quasi-steady state, fully developed line fire. The method did not include the chemical kinetics of the combustion process, and transport processes were empirically derived for specific fuel geometries. Wind effects are a derived multiplier to an already spreading fire and the model will not predict the rate of spread when wind is required for successful spread [4].

The foundation laid by Rothermel was the basis for the FARSITE and BEHAVE fire model packages in use by the U.S. Forest Service today [5,6]. Rothermel's model is the most widely used fire behavior model in wildland fire research and management [7].

The FARSITE and BEHAVE packages have limitations with respect to predicting fire spread and require further development with respect to the transfer of energy from the fire to the surroundings and flame structure, in addition to other predictive capabilities [8]. Rothermel's model is sensitive to input parameters, and natural fuel variations can lead to a big error in the results [7]. In addition, the model requires continued improvement in order to model behavior of fire in mixed fuels [9].

As part of the effort to improve the state of wildland fire modeling, new, more complete wildland fire models are being developed within the European Community. Many scientific disciplines have contributed and continue to study many aspects of porous media combustion with a wide range of goals. Many of these efforts come from research into alternative fuels and provide some very detailed work on modeling of char particles in packed beds [10].

The latest generation of wildland fire models can take advantage of ongoing related research and more advanced computer power to solve more complex evaluation schemes. Complete model frameworks use an approach consisting of heat, mass and momentum

conservation equations along with chemical kinetics models of the combustion process. Solutions for sets of these equations are done in control volumes containing both solid and gas and are incorporated into Computational Fluid Dynamics (CFD) models [11].

Fuels found on the forest floor are generally arranged to form a porous media and have different burning characteristics collectively than they do as individual solid fuel elements. A porous fuel bed is a hybrid arrangement of a solid fuel with relatively large open gas spaces and will undergo significant internal flows during combustion. Characterizing combustion in this complex environment is one of the most difficult problems in predicting wildland fires [12].

Pinus halepensis thermal degradation pathways have been studied under analytical methods such as differential scanning calorimetry, mass spectrometry, and thermal galvanometric analysis. *Pinus halepensis* are of special interest in forest fire research because of their high flammability, their contribution to the spread of fire, and for environmental reasons as well [13,14].

One-dimensional fire spread in pine needles for different airflow conditions have been studied [15]. Many studies have examined the open burning of pine needles in bulk and measured various parameters of the combustion process [16,17,18]. These studies all bring out the importance of understanding pine needle fire behavior for advancing fire spread modeling.

The current study desires to better understand how flow conditions effect burning of porous fuel beds. Multiple experimental studies have shown that combustion in porous media can be greatly influenced by the prevailing flow through the media. In a porous media at high oxidant flow rates surface reactions and gas-phase reactions compete for the available oxidant [19]. Empirical evidence and analytical evidence indicate that with higher rates of fluid flow, fire spread through a porous fuel will be enhanced. Developing and validating improved CFD sub-grid models for fire spread in forest floor fuels requires a detailed understanding of the physical phenomenon which dominate combustion processes under fire conditions.

The cone calorimeter has been used for a long time to help understand how particular fuels burn. The cone calorimeter has been applied to define forest fuel combustibility by several researchers. Some of these studies take into account several aspects of the fuel's physical configuration, but mainly examine heat release effects by vegetation type [20] and growth conditions [21].

Much work in the past has developed how the physical arrangement of wildland fuel affects fire spread on a global level. The understanding of how solid fuels make up the forest floor and form porous fuel beds is still developing within wildland fire research. A great deal of research effort is based on understanding the breakdown of porous fuel beds and how they form flammable mixtures. However, relatively little work could be found that details the relationship between transport processes and chemical kinetics in forest floor fuels.

Models under development will require a more complete understanding of how porous fuel beds decompose under fire conditions, ignite and spread fire. The flow effects of heat and mass transfer during combustion are the subject of interest for the current study. The research hopes to define flow regimes where fluid transport through the fuel bed and fluid composition within the fuel bed control combustion. The first step in this process involves the tests described in the following section.

EXPERIMENTAL METHODOLOGY

Tests were performed in a standard cone calorimeter, made by Stanton Redcroft, with oxygen, carbon monoxide and carbon dioxide analyzers, and spark ignition [22]. Two types of sample holders were used, the standard for a cone and a permeable basket that allowed air flow through the fuel bed. Other than permeability, the baskets differed from the standard sample holder in the cross section and in being circular instead of square.

Permeability of the open mesh basket was expressed as the percent open, which was the open area as a percentage of the total area of the basket walls. The open basket was made of steel wire mesh and 76% of the basket was open. The standard cone sample holder was considered to have 0% permeability. The sample holder dimensions for the basket and the standard are presented in Table 1.

Table 1

Main dimensions of sample holders

Type	Horizontal dimension, cm	Area, cm^2	Depth, cm
Permeable, 76% open	12.6 diameter	125	3.1
Standard, non-permeable	10.0 by 10.0	100	5.0

Dead needles of *Pinus halepensis,* collected in the south of France, were the fuel used in all tests presented here. This fuel was provided by Institute National de Recherché Agronomique and its moisture was at equilibrium with the ambient air. No adjustment by conditioning was done to the fuel prior to testing. The moisture remained fairly constant during the testing period, between 8 and 9 percent. This was checked by measuring the moisture by weighing a sample before and after drying in an oven at 105°C until constant weight.

The bed thickness was between 3 and 4 cm, resulting in bulk densities of 17 to 38 kg of dry fuel per cubic meter, which was on the order of the values found in *Pinus halepensis* forests [23]. However, it is important to point out that it is difficult to assess the exact position of the fuel bed, since it is not regular, and, therefore, the bed thickness values are approximate.

The surface area to volume ratio was 8100 ± 700 m^{-1}, calculated measuring the thickness and width of the needles and neglecting the ends. Sample mass was between 8 and 13 grams for the open mesh sample holder and 10 to 15 grams for the standard holder.

The external heat flux used in the cone was 25 kW/ m^2 for all tests. The small heat flux was used because with larger ones sample ignition was too fast, making tests more difficult to perform. After a preheating period, which fluctuated between 11 s and 40 s, pyrolysis gases are ignited by the spark.

Data reduction presented some difficulties because of the small sample masses used. Indeed, the rate of mass loss, obtained by differentiation of the mass versus time plot, resulted in a very noisy curve. An eight point polynomial curve fit was performed and then differentiated to obtain mass loss rates. To make a valid comparison of the

experimental curves, for example, RHR or mass loss, every plot was started at the ignition time.

RESULTS AND ANALYSIS

In this section, the results of the cone calorimeter tests are summarized and some analysis is provided. A set of statistical tests (t-tests) were performed to determine the effect of the sample holder type on the bulk burning properties of fuel bed. Another analysis was done to examine the effect of the sample holder type on the dynamics of the combustion process by determining the order of the combustion kinetics. The production of CO and CO_2 were normalized to mass loss and these plots presented. A description of the combustion process during the tests provides some significance to the normalized CO and CO_2 curves.

Bulk Fuel Bed Properties

Table 2 (A-D) shows the results of several t-tests. This analysis determines if the mean value of a measured parameter was significantly affected by the sample holder type. A t-test does this by calculating the probability (p) that the mean value for each sample holder type came from a similar population of reported values. If the p value reported by the t-test is less than or equal to a chosen level of significance, then the means are said to be significantly different for each test condition. If the mean values are significantly different then the sample holder type had a measurable effect on the tested parameter. The level of significance for these tests was set at 95% ($p \leq 0.05$).

This first set of tests presented in Table 2 examined the bulk fuel bed properties because it examined the average value of a given parameter over the entire time of the cone test run. The parameters tested were: (A) total energy released during test; (B) maximum rate of Heat Release (RHR); (C) percent of mass loss; and, (D) time to ignition. This analysis provides a general description of the overall fuel bed performance for the two test conditions.

The t-tests results indicate that the sample holder type had a significant effect on the mean differences for; total heat released, RHR and the percent mass loss during the burn. The

means of time to ignition for the two sample holders differed by ~9 seconds. However, the distribution of values for each sample holder indicates that these means are not significantly different.

Table 2. t-Test results for parameters A-D

A. Total energy released, kW

Group	N	Mean	SD
Basket.	8	7.724	0.713
Standard.	9	2.559	0.305

t-test results:

p = 0.000

Difference in Means = 5.165

B. Maximum RHR, kW/m^2

Group	N	Mean	SD
basket	8	617.316	56.986
standard	9	255.878	30.498

t-test results:

p = 0.000

Difference in Means = 361.438

C. Percent mass loss, m(t)/m$_i$

Group	N	Mean	SD
basket	8	85.987	4.125
standard	9	68.811	11.771

t-test results:

p = 0.002

Difference in Means = 17.176

D. Time to Ignition, seconds

Group	N	Mean	SD
basket	8	24.750	17.903
standard	9	15.889	1.833

t-test results:

p = 0.205

Difference in Means = 8.861

Fuel Bed Dynamics

The next step in the analysis was to determine the sample holder effect in time on the burning process. Figure 1 shows a plot of the average RHR in time for both the standard and open mesh baskets over all test runs. As the plots indicate, the effect of the sample holder appears to be significant on RHR for the entire duration of the combustion of the fuel bed. This includes both flaming and smoldering combustion for the open sample holder. For the standard sample holders flaming was maintained over most of the test runs.

Figure 1

RHR vs. time for standard and open mesh sample holders

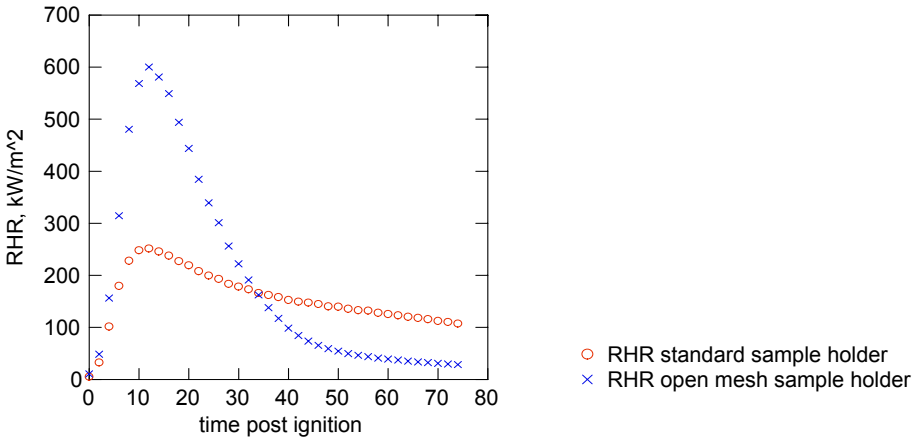

To better understand the process, the mass loss for each test was normalized to a percent mass loss of the sample. This variable was named alpha and was defined as:

$$alpha = \frac{mass(t)}{mass_i}$$

This was done because several different starting sample masses were used during the test runs. The relationship of alpha in time for each sample holder (standard: alpha S and open mesh basket: alpha M) is presented in Figure 2.

Figure 2

Alpha S and Alpha M holders vs. time post ignition

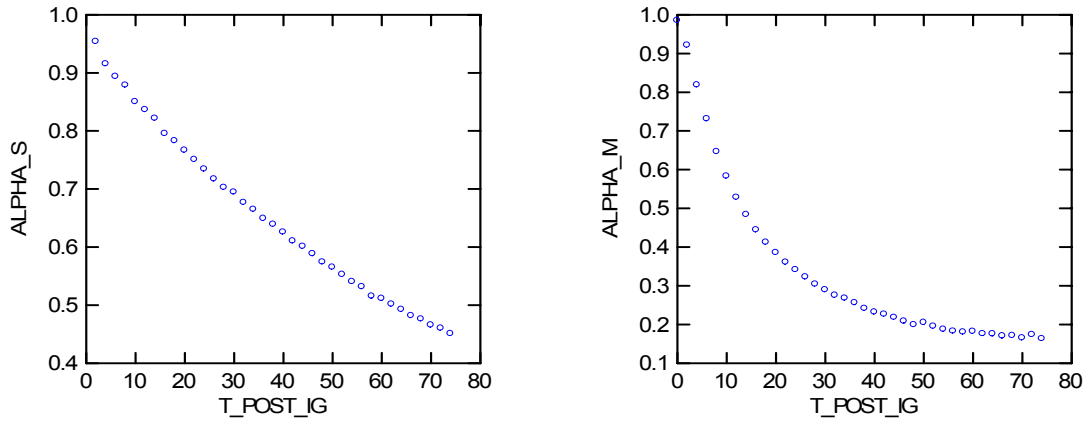

Alpha's response during combustion can be used to show several effects on the fuel bed. A plot of $\frac{RHR}{\frac{d(alpha)}{dt}}$ vs. time is presented in Figure 3. This plot emphasizes the role of ventilation in the porous fuel bed during both flaming and smoldering combustion.

Alpha can also be used to define the kinetics for the decomposition reaction of the fuel bed. First order reaction kinetics for this application can be described by the equation:

$$\ln(alpha) = -kt$$

Where:

k = reaction rate constant, sec^{-1}

t = time, sec

The experimental reaction data can be plotted as ln(alpha) vs. time. If the data forms a line then the reaction can be considered first order with the slope being equal to k.

Figure 3

Mass normalized Effective Heat of Combustion in time for both the standard and open mesh sample holders

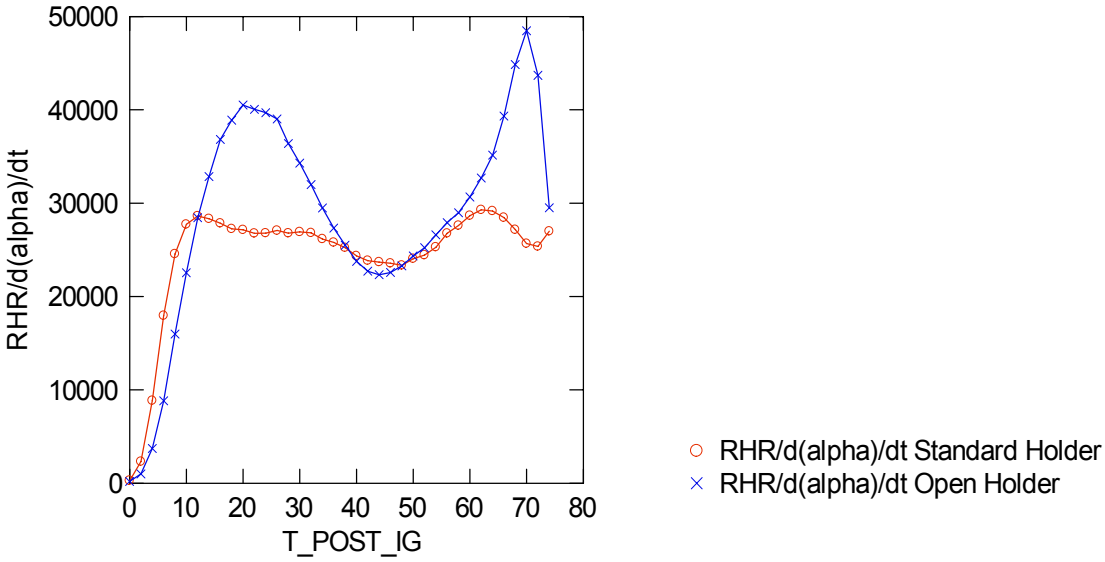

Second order reaction kinetics can be described as:

$$\frac{1}{alpha_O} - \frac{1}{alpha_t} = kt$$

The experimental data for the open mesh basket was plotted as 1/alpha vs. t. If the plot of the experimental data forms a line then the reaction can be considered second order with the slope being equal to –k and the intercept being $1/alpha_o$.

The data from both sample holders during flaming combustion was plotted using both methods. The data from the standard sample holder was found to be first order and the data from the open mesh holder was found to be second order. These plots are presented in Figures 4 and 5 along with the linear regression analysis.

The production rates of CO and CO_2 were normalized with alpha to give a mass loss perspective to their generation rates. The normalized generation of both CO and CO_2 in the standard holder had the same trend. However, the normalized rate of CO production

was quite different from the CO_2 production rate in the open mesh basket. These plots are presented in Figure 6.

Figure 4

Standard holder data analyzed for first order kinetics

Dependent Variable = ln(alpha) standard holder

N = 38 Multiple R: 0.998 Squared multiple R: 0.997

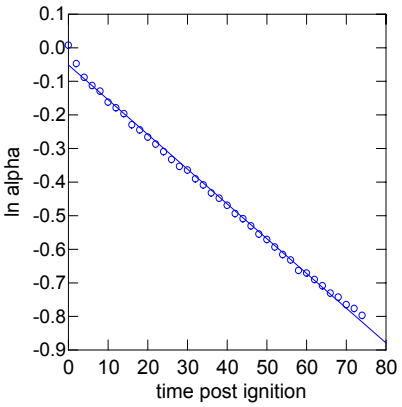

Effect	Coefficient	Std Error
CONSTANT	-0.051	0.004
Time	-0.010	0.000

Figure 5

Open mesh holder analyzed for second order kinetics

Dependent Variable: 1/alpha (open mess holder)

N = 16 Multiple R = 0.999 Squared multiple R = 0.998

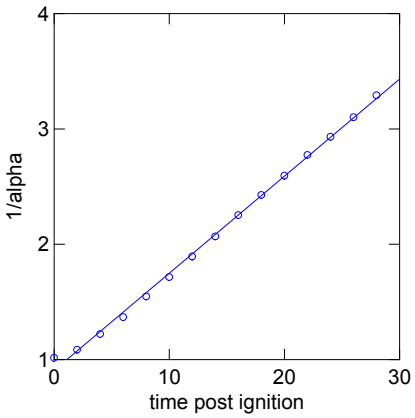

Effect	Coefficient	Std Error
CONSTANT	0.905	0.018
Time	0.084	0.001

Figure 6

CO and CO_2 normalized with rate of mass loss vs. time

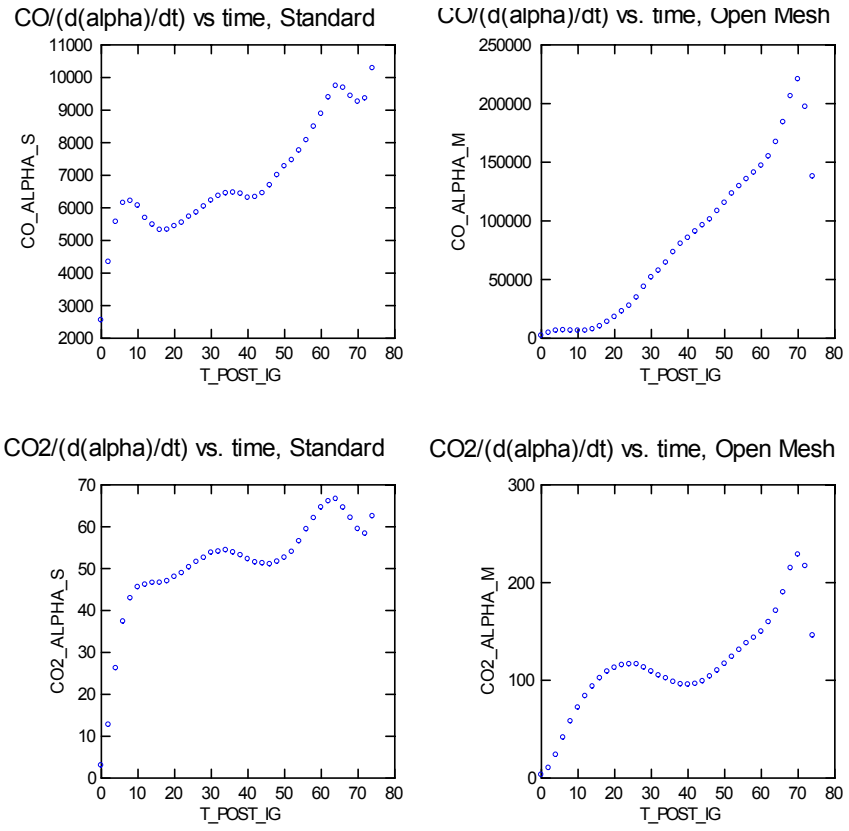

A description of the progression of the open mesh basket tests provides some perspective on the plots for the open mesh holder. After ignition, the subsequent burning was very intense in the open baskets during flaming combustion. During all tests the open mesh basket became ignited and spread fire across the top of the fuel bed in less then 5 seconds. The downward spread in the basket was done in less than 7 seconds after the top spread was completed. The open mesh bed was fully involved in flame (fire supported from the top to the bottom of the fuel bed) for no more then 30 seconds in any test.

In some cases there was a flash of flame supported for ~1 second shortly after the initial extinction. At the current level of resolution, the normalized CO_2 curve for the open mesh holder seems to have distinct responses at each point in the fuel beds evolution in time with respect to the combustion process.

The standard holder supported flaming combustion that started somewhat rigorous and then steadily dropped off during the test. Spread across the top and downward in the fuel bed for the standard sample holder was difficult to determine with any precision. Therefore, no similar description of the bed burning behavior could be provided.

CONCLUSIONS

The test series presented here was the first step in a larger program with the hope of developing a detailed understanding of how fluid flow in porous wildland fuels affect fire spread rate. The research hopes to define a relationship between flow regimes and fuel bed porosities that affect the combustion process in a porous fuel bed. A good deal of wildland fire research shows that fuel type and configuration have a significant impact on wildland fire spread rates. This understanding and study of specific fuel packages has led to many empirical formulations being developed to address each case of relevant fuel configuration.

The work presented here is a first step in developing a physically based model for how wildland porous fuel beds burn. In the tests presented and analyzed above, the general parameters of energy release during combustion (total energy and RHR) in addition to mass loss were shown to be significantly affected by the permeability of the fuel sample holder. The sample holder controlled the flow conditions in the fuel bed during these tests. The result provides a basis to examine fuel bed permeability over a broader range. This further study should help to establish what physical parameters are involved in limiting the combustion process in these types of fuels.

The test results also showed that the standard sample holder was described by first order kinetics and the open mesh holder by second order kinetics. When this is viewed with the perspective that the open mesh combustion was much faster then the standard combustion process, it indicates that whatever is causing the second order effect in the kinetics is also allowing the combustion process to be faster.

This is a strong indication that if the higher permeability of the open mesh sample holder did allow more flow through the fuel bed during combustion, then that flow was controlling the rate of the process. From this idea that the transport process through the

bed controls the kinetics of porous fuel bed combustion, the next series of tests for this project will be designed.

The goal of the next step is to perform tests using several fuel sample holders with a wide range of permeabilities. The next set of tests will be done in a Factory Mutual Fire Propagation Apparatus (FPA). The FPA will allow for direct control of the prevailing flow rate around the sample holder, in addition to control of the composition of the flow stream. Tests under these conditions should be able to indicate under what test conditions the oxidant level in the flow begins to limit the combustion process, rather than the flow in the fuel bed limiting the combustion process.

Once these regimes of flow rate and oxidant concentration are understood, models can be developed and tested that use the physical phenomenon that are driving fire spread under wildland fire conditions in porous fuel beds. This should greatly aid in developing more accurate sub-grid level models for use in complete wildland fire CFD model applications.

REFERENCES

1. Keane, R.E., Cary, G.J., Parsons, R. Using simulation to map fire regimes: an evaluation of approaches, strategies, and limitations, International Journal of Wildland Fire, 2003, 12, 309-322.

2. Rothermal, R.C., A Mathematical Model for Predicting Fire Spread in Wildland Fuels, USDA Forest Service Research Paper INT-115. January 1972.

3. Frandsen, W.H., Fire Spread through Porous Fuels from the Conservation of Energy, Combustion & Flame, 16,9-16, 1971. The Combustion Institute.

4. Zhou, X,, Pereira, C.F., A Multidimensional Model for Simulation Vegetation Fire Spread using a Porous Media Sub-model, Fire and Materials, 24, 37-43 (2000).

5. Finney, M.A., FARSITE: Fire Area Simulator-Model Development and Evaluation, USDA, Forest Service, RMRS. Research Paper RMRS-RP-4 Revised March 1998.

6. Scott, J., Burgan, R., Standard Fire Behavior Fuel Models: A Comprehensive Set for Use with Rothermel's Surface Fire Spread Model. USDA Forest Service, RMRS. General Technical Report RMRS-GTR-153, June 2005.

7. Bachmann, A., Allgower, B., Uncertainty propagation in wildland fire behavior modelling, International Journal of Geographical Information Science, 2002, Volume 16, no. 2, 115-127.

8. Andrews, P.L., Queen, L.P., Fire modeling and information system technology, International Journal of Wildland Fire, 2001, 10, 343-355.

9. Catchpole, E.A., Catchpole, W.R., Modelling Moisture Damping for Fire Spread in a Mixture of Live and Dead Fuel, International Journal of Wildland Fire, 1(2): 101-106, 1991.

10. Dasappa, S., Paul, P., Gasification of char particles in packed beds: analysis and results, International Journal of Energy Research, 2001: 25: 1053-1072.

11. Morvan, D., Dupuy, J.L., Modeling of Fire Spread Through a Forest Fuel Bed Using a Multiphase Formulation, Combustion and Flame 127: 1982-1984 (2001).

12. Zhou, X., Weise, D., Mahalingam, S., Experimental measurements and numerical modeling of marginal burning in live chaparral fuel beds, Proceedings of the Combustion Institute 30, 2005, 2287-2294. 2004.

13. Pappa, A.A., Tzamtzis, N.E., Statheropoulos, M.K., Liodakis, S.E., Parissakis, G.K., A Comparative study of the effects of fire retardants on the pyrolysis of cellulose and *Pinus Halepensis* pine-needles, Journal of Analytical and Applied Pyrolysis, 31 (1995) 85 100.

14. Statheropoulos, M.K., Liodakis, Pappa, A.A., Kyriakou, S., Thermal degradation of Pinus Halepensis pine-needles using various analytical methods, Journal of Applied Pyrolysis, 43 (1997) 115-123.

15. Morvan, D., Larini, M. Modeling of One Dimensional Fire Spread in Pine Needles with Opposing Air Flow, Combustion and Science Technology, Volume 363, pp 1-28.

16. Dupuy, J.L., Marechal, J., Morvan, D., Fires from a cylindrical forest fuel burner: combustion dynamics and flame properties, Combustion and Flame 135 (2003) 65-76.

17. Mendes-Lopes, J.M., Ventura, J.M., Amaral, J.M., Flame characteristics, temperature-time curves, and rate of spread in fires propagating in a bed of Pinus pinaster needles, International Journal of Wildland Fire, 2003, 12, 67-84.

18. Marcelle, T., Santoni, P., Simeoni, A., Porterie, B., Fire spread across pine needle fuel beds: characterization of temperature and velocity distributions within the fire plume, International Journal of Wildland Fire, 2004, 13, 37-48.

19. Fatehi, M., Kaviany, M., Adiabatic Reverse Combustion in a Packed Bed, Combustion and Flame 99: 1-17 (1994).

20. Weise, D.R., White, R.H., Beall, F.C., Etlinger, M., Use of the cone calorimeter to detect seasonal differences in selected combustion characteristics of ornamental vegetation, International Journal of Wildland Fire, 2005, 14, 321-338.

21. Blank, R.R., White, R.H., Ziska, L.H., Combustion properties of *Bromus tectorum* L: influence of ecotype and growth under four CO_2 concentrations, International Journal of Wildland Fire, 2006, 15, 227-236.

22. Tewarson A (2002) Generation of Heat and Chemical Compounds in Fires. In 'The SFPE Handbook of Fire Protection Engineering' 3rd Edition (Society of Fire Protection Engineers) pp 3-82, 3-160, The National Fire Protection Association Press, Quincy M

23. Albert Simeoni, 2007, personal communication.

Appendix C

A CALORIMETRIC STUDY OF WILDLAND FUELS

A CALORIMETRIC STUDY OF WILDLAND FUELS

C. F. Schemel[*,], A. Simeoni[***], H. Biteau[*], J. D. Rivera[****] and J.L. Torero[*]**

Corresponding Author: C. F. Schemel: cschemel@packereng.com
Phone: +1-301-512-8317 fax: +1-240-554-1420
Post: c/o Packer Engineering, Inc.
6700 Alexander Bell Drive, Suite 100
Columbia, Maryland 21046
USA

[*]BRE Centre for Fire Safety Engineering, University of Edinburgh, Edinburgh, Scotland, UK
[**]Packer Engineering, Inc., Columbia, Maryland, USA
[***]CNRS-SPE, UMR 6134, University of Corsica, Corte, France
[****]Pontificia Universidad Catolica de Chile, Santiago, Chile

Abstract

The burning of two species of pine needles: *Pinus halepensis* and *Pinus pinaster*, was studied to characterize the behavior of the forest floor in wildland fires. These fuels are representative of the Mediterranean ecosystem and have very different shapes and surface-to-volume ratios. Calorimetry was performed using the FM Global Fire Propagation Apparatus (FPA). To better understand the effects of transport in the fuel beds, the standard sample holder was replaced by a holder that allowed for the porous properties of the fuel to be studied in a systematic manner. These holders were designed with holes on the surface to allow for different air flow rates to pass through the holder and into the fuel sample. These characteristics created different internal fuel bed conditions and were the first such tests that could be identified that examined transport on this level in these types of wildland fuels. Tests were conducted under natural convection and forced flow. The test series results were analyzed with respect to the direct values of the measured variables and calculated values of Heat Release

Rate. Discrete variables of time to ignition, duration of flaming combustion and peak Heat Release Rate were compared using an Analysis of Variance method. As the experiments were conducted under well-ventilated conditions, the Heat Release Rate calculated by calorimetry was compared to mass loss rate and heat of combustion. CO concentration in time proved to be a good indicator of the combustion dynamics in the fuel bed. Heat Release Rate, time to ignition and time to reach peak Heat Release Rate indicated a strong dependence on flow conditions and on fuel specie. It was shown that the transport processes in the fuel beds had a significant effect on the burning characteristics.

Keywords: wildland fuels, calorimetry, porous fuels, heat release rate

Introduction

The need to understand the combustion characteristics of wildland fuels is currently a matter of great urgency to wildland fire professionals. As buildings and other human activities increasingly encroach into wildland areas, the impact of wildland fires on human endeavors is acquiring greater importance. This impact usually manifests as loss of life, loss of property and the use of resources in fire mitigation efforts. To help manage these increasing risks and better understand wildland management issues, improved assessment tools need to be developed. The precision of wildland fire assessment tools is limited by the understanding of many key variables.

The understanding of the fuel dependent behavior and other parameters affecting combustion are of great importance. Heat Release Rate (HRR) of a fuel

is among the most important parameters for understanding combustion process, fire characteristics and propagation rates. It serves to define parameters such as flame geometry and temperature fields.

Many difficulties exist when analyzing wildland fuels. Obtaining repeatable calorimetry data for wildland fuels is difficult because of the number of parameters that significantly affect uncertainty associated with the HRR [1]. Weise et al. [2] compared methods of oxygen consumption calorimetry to measure the flammability characteristics of several types of vegetation in two calorimeters; a cone calorimeter and an intermediate scale bio-mass calorimeter. The work of Weise et al. illustrates many of the complications involving consistency of HRR results when using cone calorimetry to characterize wildland fuels.

The parameters of concern are not only associated with testing issues, such as experimental methodology and fuel configuration, but also to fuel origin, (i.e. moisture content or chemical composition). Although wildland fuels are largely living or dead bio-mass where the general chemical composition is well defined [3], they also include a number of specific components that have not been properly identified or characterized for each individual material. These minor components and other environmental variables can have a significant impact on a fuel's burning characteristics. Furthermore, most test conditions do not map well to real fire scenarios and, therefore, gaps exist between HRR data and useful applications for that data in real problem solving. Many of the problems associated with the definition of the HRR data for wildland fuels are the same as

those appearing when assessing standard fuels and the extrapolation of test data to the modeling of real fires.

A study involving two Mediterranean pine needles is presented in this paper. Pine needles present a clear fire hazard in the Mediterranean region by providing a continuous fuel matrix across the forest floor. Whilst other shrubs and crown fires contribute to wildland fire intensity, forest floor fuels, like pine needle beds, sustain wildland fires and provide for the greatest extent of fire spread [4]. Detailed research into characterizing fire spread in pine needle beds has taken place over the past years. Porterie et al. [5] described the level of detail required for modeling porous fuel beds accounting for the hydro-dynamic effects inside the fuel bed, prediction of detailed kinetics and products of combustion. Most recent experimental work in this area concentrates on the bulk behavior of the fuel bed for various external conditions, such as, slope [6], plume velocities and temperature profiles [7] but very limited effort has concentrated on the characterization of pine needles as a fuel.

This paper studies several variables associated with the uncertainty of calorimetry when applied to wildland fuel characterization. The test results provide data describing how two types of pine needle varieties behave during combustion under specific, controlled conditions. The test conditions allow the internal porous fuel bed characteristics to be examined. By controlling the fuel sample holder basket opening and combustion air flow rate during the tests, mass transport characteristics were varied systematically. This approach allowed for an analysis of the dynamics of HRR and products of combustion relative to flow conditions in the fuel bed.

Calorimetric Calculations

Oxygen consumption calorimetry is a convenient and widely used method for measuring the amount of heat release for a laboratory scale fire test [8]. The HRR from a fire can be calculated from the amount of O_2 consumed by the combustion process [9]. The HRR is calculated using the following equation:

$$\dot{q} = E_{O_2} \left(\dot{m}^0_{O_2} - \dot{m}_{O_2} \right) \qquad (1)$$

In general, several simplifying assumptions are associated with the calculation of HRR by oxygen consumption and carbon dioxide generation calorimetry. All gases are considered to behave as ideal. The apparatus used for the HRR calculations in the test series presented in this paper were conducted at atmospheric pressure lending validity to this assumption. The amount of energy released by complete combustion of an organic fuel per unit mass of O_2 consumed is constant at [10] 13.1 $kJ.g^{-1}$.

Combustion air contains only O_2, H_2O, CO_2, and N_2. All inert gases were assumed to have the properties of nitrogen. Prior to measurement in the experimental apparatus, the combustion exhaust gases were dried. The mole fraction of O_2 (CO_2, CO, Total Hydrocarbon) in the exhaust flow is different from the one measured in the analyzer.

$$Y_{O_2} = \left(1 - Y_{H_2O}\right) Y^A_{O_2} \qquad (2)$$

The only exhaust gases considered were O_2, H_2O, CO_2, CO and N_2. They were assumed to represent for over 99% of the exhaust gases in almost all fire tests [8].

Nitrogen does not participate in the combustion reaction and assumed to be conserved, allowing the following assumption:

$$\dot{n}_{N_2} = \dot{n}^0_{N_2} \qquad (3)$$

Water vapor production during combustion is not considered in the calorimetry calculation. In the absence of a measure for water vapor in the exhaust gases the molecular weight of the exhaust gases are assumed equal to the molecular weight of the incoming air. The flow rate was measured by a Pitot tube. It is evaluated by the pressure drop across the device:

$$\dot{V}_e = K\,A\sqrt{\frac{2\,\Delta P}{\rho_e}} \qquad (4)$$

The density of the exhaust stream is given by the following expression:

$$\rho_e = \frac{P_{duct}}{RT_e} M_e \qquad (5)$$

The parameter ϕ is defined as the depletion factor. It is the fraction of the incoming air that is fully depleted of its oxygen during the combustion process. It is given by the expression below:

$$\varphi = \frac{\dot{n}^0_{O_2} - \dot{n}_{O_2}}{\dot{n}^0_{O_2}} = \frac{Y^{A^0}_{O_2}\left(1 - Y^A_{CO_2} - Y^A_{CO}\right) - Y^A_{O_2}\left(1 - Y^{A^0}_{CO_2}\right)}{Y^{A^o}_{O_2}\left(1 - Y^A_{O_2} - Y^A_{CO_2} - Y^A_{CO}\right)} \qquad (6)$$

α is the expansion factor. During a combustion reaction, a fraction of the incoming air is depleted of its oxygen and is replaced by an equal or larger number of moles of combustion products. The expansion factor is the ratio of these two molar quantities. It is given by:

$$\alpha = 1 + Y_{O_2}^{A^0}\left(1 - Y_{H_2O}^{0}\right)\left(\beta - 1\right) \qquad (7)$$

$$\beta = \frac{\sum n_{stoichio\ products}}{n_{stoichio\ O_2}} \qquad (8)$$

To simplify the calculation, an average value for the expansion factor α is assumed to be equal to 1.105 with a maximum relative error of 10% [11].

The HRR can also be corrected thanks to CO measurements. The heat of formation per kg of CO present in smoke is subtracted from the heat released by oxygen consumption (1). In the tests presented here, flames were well ventilated and this correction brought no improvement.

Experimental Method

The FM-Global Flame Propagation Apparatus (FPA) was used to conduct the test series presented in this paper [12]. Its basic layout is presented in Fig. 1. The FPA operates on a similar concept to a cone calorimeter. A fuel sample is radiated and an ignition source provided. The mass loss rate of the sample is measured and the exhaust gases are analyzed for composition, temperature, optical obscuration and pressure drop across an orifice plate. One key difference with the FPA in comparison to the cone calorimeter is that the combustion chamber for the sample allows for a controlled environment with respect to gas flow rate and composition.

The combustion chamber and the sample holder for the FPA are cylindrical. The sample holder fits inside the combustion chamber and is positioned on a balance. Specific sample holders were designed for this test series and are pictured in Fig. 2. They were made of stainless steel and had uniform, small holes in all

(side and bottom) of the outside surfaces of each holder. These holes created an open space for inlet combustion gases to pass into the holders and through the fuel samples. Baskets were also lined with aluminum foil to provide for a no internal flow condition for the fuel bed, either natural convection or forced air.

The two fuels studied in this test series, *Pinus pinaster* and *Pinus halepensis,* were collected from Mediterranean wildland areas. The needles were dead and not conditioned prior to testing. The moisture levels of the needles were determined by oven drying of a sample for 24 hours at 60 degrees Celsius. The surface to volume ratio for *Pinus pinaster* was 4,260 m^{-1} and 9,170 m^{-1} for *Pinus halepensis* with an approximate 15% error [11].

The experiment was designed to test each pine needle species in three sample holders allowing different airflows at both natural convection and forced combustion air flow conditions. The baskets were filled to the top and had a constant mass of 15 *g*. The needles provided one experimental factor (fuel) with two levels (*Pinus pinaster* and *Pinus halepensis*). The baskets were a second experimental design factor (porosity) with three levels (0, 26 and 63% opening). A third experimental design factor was flow of air to the combustion chamber. The flow control allowed for two levels to the fuel sample; natural convection (no-flow) and forced combustion air (flow). A single value of 200 l/min for the forced air flow was used and supplied to the combustion chamber. The precise value of the flow through the fuel bed samples was not directly measured. A camera was positioned to observe the behavior of the pine needle bed during combustion. Each test condition was repeated three times for a total of thirty test runs. The test matrix is presented in Table 1.

Results and Discussion

The test series was analyzed with respect to the direct values of the measured variables and calculated values of HRR. In addition to the continuous variables of gas concentrations and fuel mass measured during the test runs, the discrete variables of time to ignition, duration of flaming combustion and peak HRR were also analyzed.

Statistical analysis of the results

The statistical analysis of the discrete data was done using an Analysis of Variance (ANOVA) and based on the experimental design shown in Table 1. In short, ANOVA is a method that compares measured variables for given set of experimental conditions to determine if the mean values are significantly different. The factors and levels for this experiment were: fuel type, *Pinus halepensis* or *Pinus pinaster*, basket opening, 0, 26 or 63%; and combustion air, flow or no flow. The experiments were designed so the factors were repeated three times at each level. Significance of a test result was determined, as in many statistical tests, by selecting a confidence level, e.g. 95%, about the mean. In the ANOVA this confidence level is determined by a calculated probability statistic based on an assumed F-distribution. The probability statistic is analogous to confidence intervals using the tails of a normal distribution.

ANOVA is a valuable analysis method in this type of parametric testing because it allows inferences about test parameters to be examined both individually and in combination. ANOVA is also valuable for evaluating systems that may have a high degree of uncontrolled variation, as in wildland fuels and

porous fuel beds. A well designed experiment allows for conclusions to be made about the effect of controlled parameters by measuring variables of interest at all combinations of test conditions. The tests presented here used a full factorial design with three replications. The analysis of this experiment and the conclusions are valid as a level effect, but not a detailed empirical model. The consistency of the experiments allowed for high confidence (>99%) levels to be used in determining test condition effect on the measured mean values.

In Table 2, some of the calculated results of the ANOVA are presented as an example. The first column shows the test condition of combustion air flow or no-flow. The second column shows the mean value of all tests repeated under the condition indicated in the first column with the standard deviation of the sample means (standard error of the estimate) in parenthesis. The final column reports the number of trials included in the mean, for example the number of tests conducted at the flow or no-flow condition.

A combined ANOVA was run to determine if the test conditions, either alone or in some combination, had an effect on the peak HRR. When all test conditions were analyzed, only the combustion air (flow or no-flow) condition had a significant effect by itself on peak HRR. Taken in combination, however, fuel type and combustion air flow had a significant effect on HRR. The basket percent opening was a significant parameter only when combined with flow condition and fuel type. Fuel type combined with combustion air also had a significant effect on peak HRR.

Table 3 shows the ANOVA results for time to ignition. Each test condition had a significant effect on time to ignition. The basket opening at the 26% level

had the shortest time to ignition. The variance in the time to ignition was believed to be linked to the heterogeneous nature of the porosity of the fuel bed. While radiative heating during the tests was homogeneous across the surface of the samples, the porous matrix structure had significant spatial variations. This condition resulted in non-homogenous absorptivity, as well as variable convective pyrolysis gas flows. The result was thought to be localized heating and non-homogenous gas concentrations generated by the fuel bed degradation during the pre-ignition time. Thus, the relative placement of the pilot flame with respect to the localized heating and gas mixing may have resulted in time to ignition variation. These were parameters that were not controlled during the experiment. It was unclear in some of the tests if the ignition was piloted or unpiloted. Unpiloted ignition would account for some of the variability of ignition times.

The time of burning (flame out) was also analyzed by ANOVA. The flame out time was significantly shorter for both *Pinus pinaster* and the forced flow condition, individually. In combination the fuel type with basket opening had an effect, as did fuel type with flow condition on flame out. The basket opening with flow condition had an effect on flame out time with the 26% opening basket for both the flow and no flow conditions having the shortest flame out times.

The inference from the statistical analysis of the peak HRR, time to ignition and flame out time all indicated a dependence on the flow/no flow condition. The other test parameters of basket opening and fuel type effected the measured variables, but not with the same consistency as the flow/no flow condition. Both basket opening and fuel type have an effect on the beds ability to move air through the fuel sample, but the air moving through the sample was the greatest

predictor of HRR and flame out time. Time to ignition was effected at each test condition. The 26% open basket may have an optimal flow condition for time to ignition and flame out. The transport processes inside the bed had a significant effect on the combustion process.

Analysis of the time dependent results

Figure 3 shows the HRR estimated in two different ways for given conditions with no-flow and flow. The first HRR estimation was done by oxygen depletion from the O_2, CO and CO_2 measurements. The second method was done using the mass loss rate and a value for the heat of combustion obtained independently. Mass loss rate was obtained from mass loss measurements taken during the tests. These measurements were noisy so the mass loss was smoothed to decrease the oscillations. An ultimate analysis provided the elemental components of *Pinus halepensis* and allowed calculating the heat of combustion: $\Delta H_c = 185{,}000\ kJ/kg$ [14]. The value for *Pinus pinaster* was very close and can be assumed equal. The HRR was corrected to take into account incomplete combustion. This was done on the basis of CO measurements.

A comparison between the two methods of analysis indicated accuracy under the test conditions. The same level of repeatability demonstrated in Fig. 2 was found for all test runs with the source of most discrepancies probably being the mass loss measurements. The load cell did show some uncertainty during the test and the discrepancies in the predicted HRR were due mainly to a noisy mass loss signal. Noisy mass loss rate signals are a well known problem in calorimetry experiments especially for small masses as the ones used here [15]. Nevertheless, the “Heat of Combustion” curves overestimate the “Calorimetry” curves at the

first stage of combustion and underestimated them after this point. This behavior could be due to different heats of combustion for flaming and smoldering. The heat of combustion for a gas is lower than the combustion of embers [16]. The mean heat of combustion underestimates during flaming combustion and over estimates during combustion of embers.

The experiments performed in the FPA during this test series were well ventilated; only ash remained in the sample basket after test runs (around 0.5 g). The 0% opening baskets had a very small amount of char residue (< 0.5 g). Under such well ventilated conditions the two methods for HRR measurement provided equivalent results.

Figure 4 illustrates the typical combustion behavior for a set of test runs (3 repetitions). The data was consistent within each set of test conditions for the entire test series. This was reflected in the repeatable estimates for the HRR showed in Fig. 4a. The HRR was calculated using O_2, CO_2 and CO values, therefore, the repeatability of the HRR was also an indication of the repeatability of all the measured gas concentrations. The vertical lines indicate the minimum and maximum time to flameout for the test runs.

In the following section, the results are discussed using the measured results of the time curves and visual observations made during the tests. The tests were videotaped; however, the light from infrared heaters prevented seeing the embers in the fuel bed. The visual observations were completed using cone test observations for the same conditions of natural convective flow [17] that were also taped.

In Fig. 4b, the points of ignition and flameout can be seen relative to the HRR and O_2 concentration. At the point of ignition, the O_2 concentration drops steeply because of the onset of flaming combustion. The flame grows for approximately 10 seconds before beginning to decrease. The flame extinguishes (flameout) after another ~120 seconds. Glowing combustion continues beyond the disappearance of the gas flames. The HRR continues to drop off at a different, but relatively constant rate as the remaining embers burn.

Figure 4c shows the behavior of CO_2 and CO during a typical test run. At the ignition point both CO_2 and CO generation rates increase. As the fuel was consumed greater amounts of char and ash were formed. The flame degraded toward extinction and the CO_2 generation rate peaked and then decreased rapidly. CO generation approached the flameout point and became constant at extinction. This general behavior was seen for all test runs with some differences for flow conditions. This aspect is discussed in detail further in this section. As smoldering combustion proceeded, the CO production increased and then fell off until the embers extinguished. At that point the CO generation rate increased.

The mass loss rate is illustrated in Fig. 4d and showed that 80-90% of the mass was lost before flameout. The amount of charring materials in pine needles is estimated at ~40% [18], therefore, the combustion of embers started prior to flameout. The flame was observed decreasing in height and radius, allowing more O_2 to reach the edge of the fuel bed and facilitated the surface reaction. The last decrease of mass was observed as the ember zone decreased to the centre of the sample holder and extinguished.

Figure 5 contains the HRR curves for all of the tests including both types of needles. Figure 5a shows the no-flow condition and indicates that the peak HRR was reached at approximately the same time, independent of species and the basket opening. The magnitude of the HRR was affected by the basket opening with the 63% basket having the highest value and the 0% having the lowest HRR. This tendency was stronger with *Pinus halepensis* and attributed to the higher surface-to-volume ratio. This parameter affected the internal fuel bed and impacted thermal transfers and surface area for contact with oxygen. *Pinus pinaster* also exhibited a higher HRR for a given flow condition.

Figure 5b shows the HRR estimate for the flow conditions, indicating that the flow has an effect on both the time to reach peak HRR and the magnitude of the HRR. The tendencies are reversed for peak HRR and *Pinus pinaster* exhibited an influence of the basket opening on the time to reach peak HRR. This effect could be due to the changing in the inlet flow through the fuel bed as the needle beds are less dense and cooling by fresh air was allowed. With *Pinus halepensis*, as the flow was driven by the dense fuel bed, the opening of the basket has no effect.

Figure 6 presents CO_2 and CO production for different test conditions. The conditions presented here demonstrate, along with Fig. 4c, changing in behavior of the combustion process. CO concentration was a good indicator of the fuel bed behavior with respect to the dynamics of flaming versus glowing combustion. The following descriptions were made of different behaviors: impermeable basket, natural convection and with flow for figures 6a, 4c and 6b, respectively.

Figure 6a illustrates the no-flow and a 0% opening basket. The CO_2 curve reflects a long time of flaming combustion (around 130 s). The CO curve provides

insight to the different steps involved in the combustion of the fuel samples when correlated with the observations. The first steep increase was due to the ignition of the sample on the upper surface. A steady production of CO follows. During this step, the burning front spread from the top to the bottom of the basket. When this spreading ended, no more degradation gases were produced and the flame extinguished. Then, oxygen was able to reach the surface of the charred material and combustion of embers within the fuel bed started. The last decrease in the CO curve corresponded to the extinction of all combustion in the sample.

In Fig. 4c, the steady step was shorter than the one for no-flow conditions (see Fig. 6a). This was mainly due to an increased spreading of the flame through the fuel bed. The bottom of the bed was ventilated as natural convection through the fuel bed was allowed thanks to the open basket. The short steady step and the two slopes in the consecutive increase of CO (before and after the line representing flame extinction) are mainly due to the overlap between flaming and char combustion. The combustion of embers started on the edges of the fuel sample before flameout, leading to an increase in CO production.

Figure 6b describes the 26% opening basket and flow conditions. The CO_2 curve demonstrates a short time of combustion (around 40 s). The steady state disappeared. We observed a fast phenomenon with embers starting to burn before the end of the flame spreading through the fuel bed. This behavior was mainly due to the additional oxygen supplied inside the fuel bed by the forced flow.

Conclusions

We conducted FPA tests on pine needles samples with sample holders designed to allow the porous nature of the fuel to be studied during the tests. The goal of this test series was to help characterize the pine needle beds with some detail as forest floor fuels. The test series exhibited a high level of repeatability for each test condition. Repeatability is difficult to attain in calorimetry using wildland fuels. The repeatability of these test runs demonstrates the usefulness of the techniques used in this test series. The application of the FPA and the use of sample holders that allow internal fuel bed flow seem to increase reliability of the test data.

The HRR calculated by means of calorimetry was reinforced by the use of mass loss rate and heat of combustion in the well-ventilated test conditions. CO concentration profiles proved to be a good indicator of the dynamics of the combustion process. The transition between flaming combustion and glowing embers was reflected in the measured CO responses. Again, the ability for combustion air to flow into the porous bed allowed the measured CO concentrations to provide good data on internal fuel bed dynamics.

HRR, time to ignition and time to reach peak HRR indicated a strong dependence on flow conditions within the fuel bed. The pine needle species studied behaved differently due to different packed densities and different surface-to-volume ratios.

The test series and the results presented here seem to indicate that the transport processes inside the bed have a significant impact on the combustion process within the porous fuel bed. Further test are necessary with smaller opening baskets

and denser fuel beds to confirm the flow effects and the fuel bed effects, respectively. An important new step to study the role of kinetics, will be to use air with different oxygen concentrations.

Acknowledgments

This research work was funded by the European Union's Fire Paradox research project. The wildland fuels were provided by INRA. Support was also provided for the research program by Packer Engineering, Inc.

The authors would like to particularly thank Factory Mutual Global Corporation for their generous donation of the Fire Propagation Apparatus and continued support of the Fire Safety Engineering program at the University of Edinburgh.

Nomenclature

A	Cross-sectional area of the exhaust duct, m^2
E	Energy release per unit mass, kJ/kg
K	Pitot tube coefficient
M	Molecular weight, $g.mol^{-1}$
$\dot{m}$	Mass flow rate, $kg.s^{-1}$
n	Number of moles
ΔP	Pressure drop in the Pitot tube, Pa
q	Heat Release Rate, kW
T	Temperature, K
Y	Molar fraction

ρ Density, $kg.m^{-3}$

ϕ Oxygen depletion

Subscripts

a Incoming gas

e Exhaust gas

Superscript

A Measured analyzer value

0 Initial conditions

References

[1] Brohez, S., *Fire and Materials*, 29, 383-394, (2005).

[2] Weise, D., White, R., Beall, F., Etlinger, M., *International Journal of Wildland Fire.* 14, 321-338, (2005).

[3] Alén, R., Kuoppala, E., Oesch P., *Journal of Analytical and Applied Pyrolysis*, 36, 137–148, (1996).

[4] Cohen, J.D., Finney, M.A., Yedinak, K.M., *V International Conference on Forest Fire Research*, Figueira da Foz, Portugal (2006).

[5] Porterie, B., Morvan, D., Loraud, J.C., Larini, M., *Physics of Fluids* 12 (7), 1762-1872 (2000).

[6] Dupuy, J., *International Journal of Wildland Fire.* 5(3), 154-164, (1995).

[7] Marcelli,T., Santoni, P.A., Simeoni, A., Leoni, E., Porterie, B., *International Journal of Wildland Fire* (13):11, 37-48 (2004).

[8] Janssens, M. L. and Babrauskas, V., Heat Release in Fires, Elsevier Applied Science, 1992, pp31-59.

[9] Thornton, W.M., *Philosophical Magazine and Journal of Science*, 6(33), 196-203, (1917).

[10] Huggett, C., *Fire and Materials*. 4(2), 61-65, (1980).

[11] Tewarson, A., *Generation of Heat and Chemical Compounds in Fires*, SFPE Handbook of Fire Protection Engineering, The National Fire Protection Association Press, 2002, pp. 3-82 - 3-161.

[12] Parker, W.J., *Journal of Fire Sciences*. 2, 380-395, (1985).

[13] Standard Test Method for Measurement of Synthetic Polymer Material Flammability Using a Fire Propagation Apparatus, ASTM, E2058-03 (2003).

[14] Kathiravale, S., Yunus, M., Samsuddin, K.S.A., Rahman, R., *Fuel* 82 (2003) 1119-1125.

[15] Staggs, J.E.J., *Fire Safety Journal*, 40, 493-205 (2005).

[16] Leroy, V., Cancellieri, D., Leoni, E., *Thermochimica Acta* 451 (2006) 131-138.

[17] Schemel, C.F., Rivera, J.D., Torero J.L., *5th International Seminar on Fire and Explosion Hazards*, Edinburgh, UK, April 2003, CD-Rom.

[18] Grishin, A.M., In Albini (Ed.). *Mathematical modeling of forest fires and new methods of fighting them*. Publishing house of the Tomsk State University, 210 p (1996).

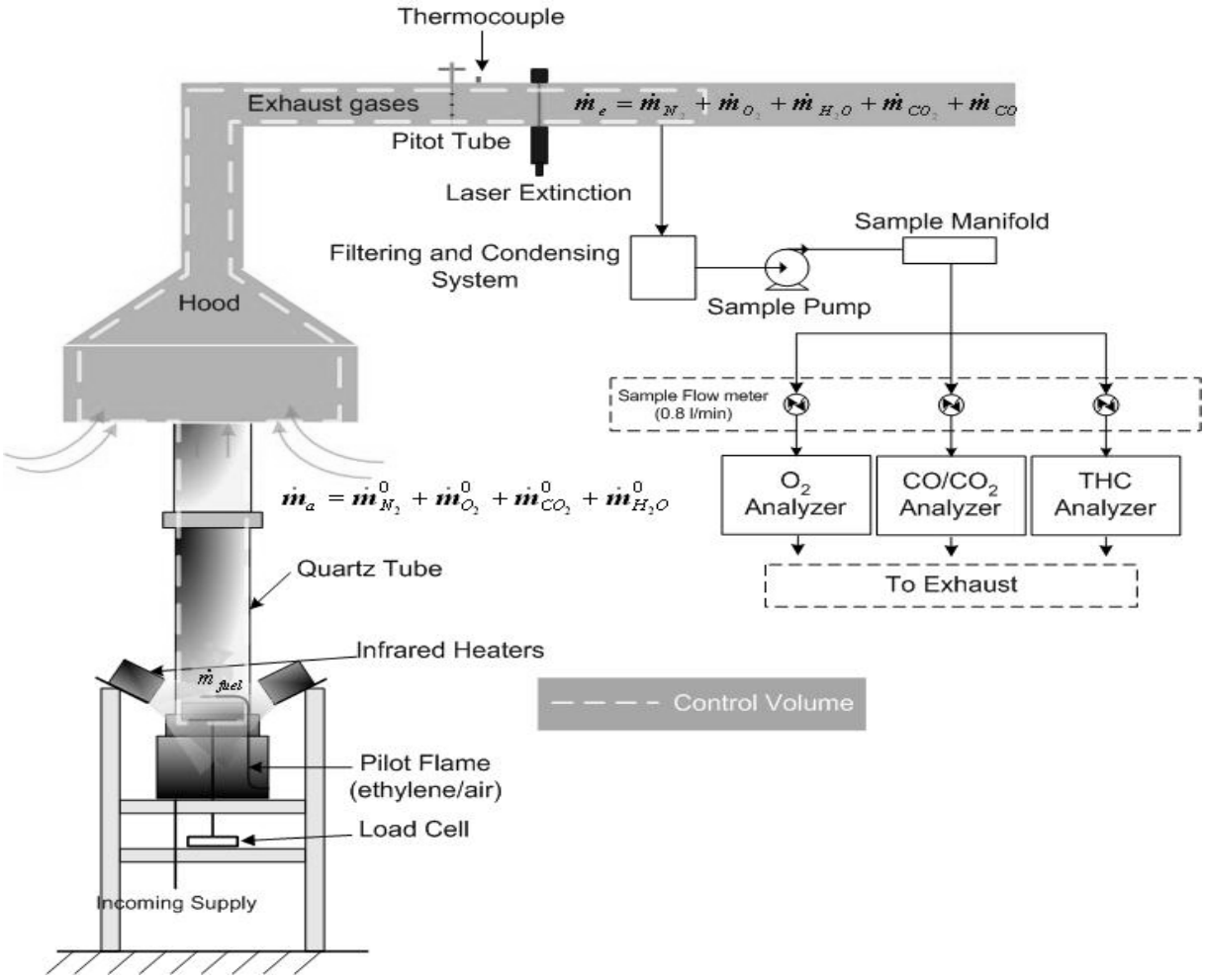

Figure 1. Overview of the FPA system.

(a)

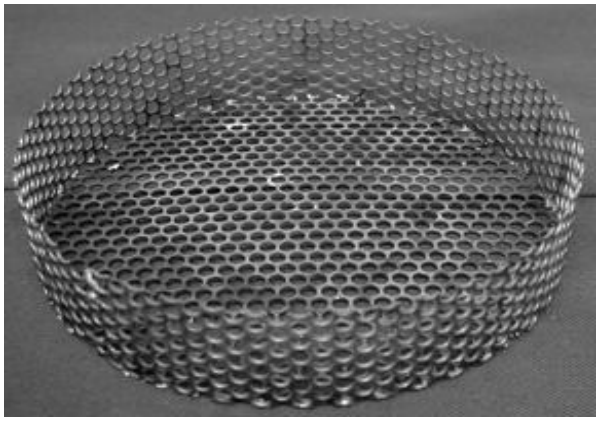

(b)

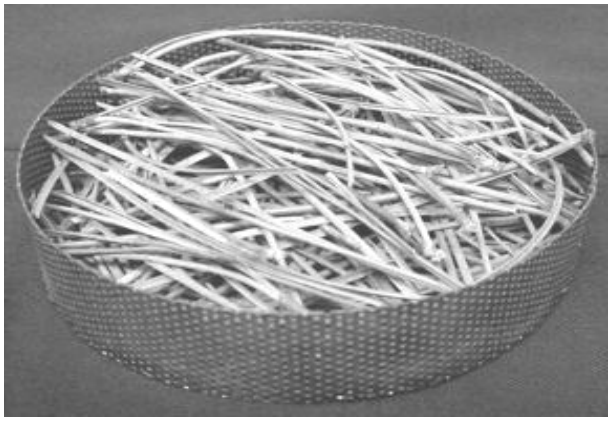

Figure 2. Sample baskets; a) 63% open basket, b) 26% open basket with *Pinus pinaster*

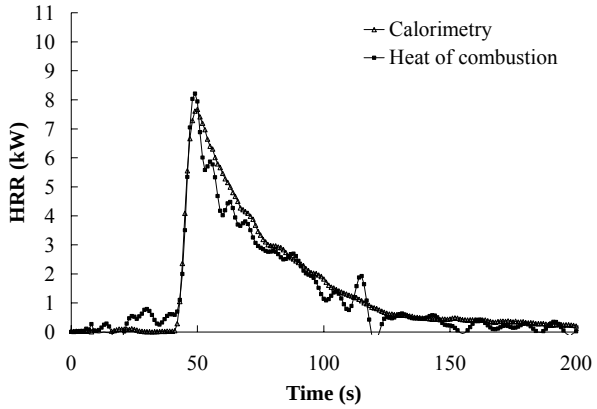

(a)

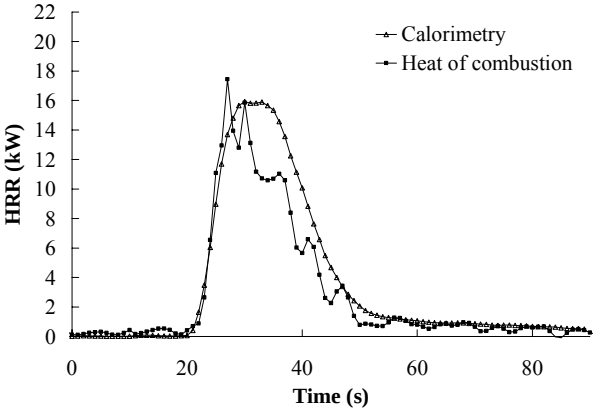

(b)

Figure 3. Mean heat release rates by oxygen consumption calorimetry and total heat
release for *Pinus halepensis* and 26% opening basket – a) no-flow b) flow

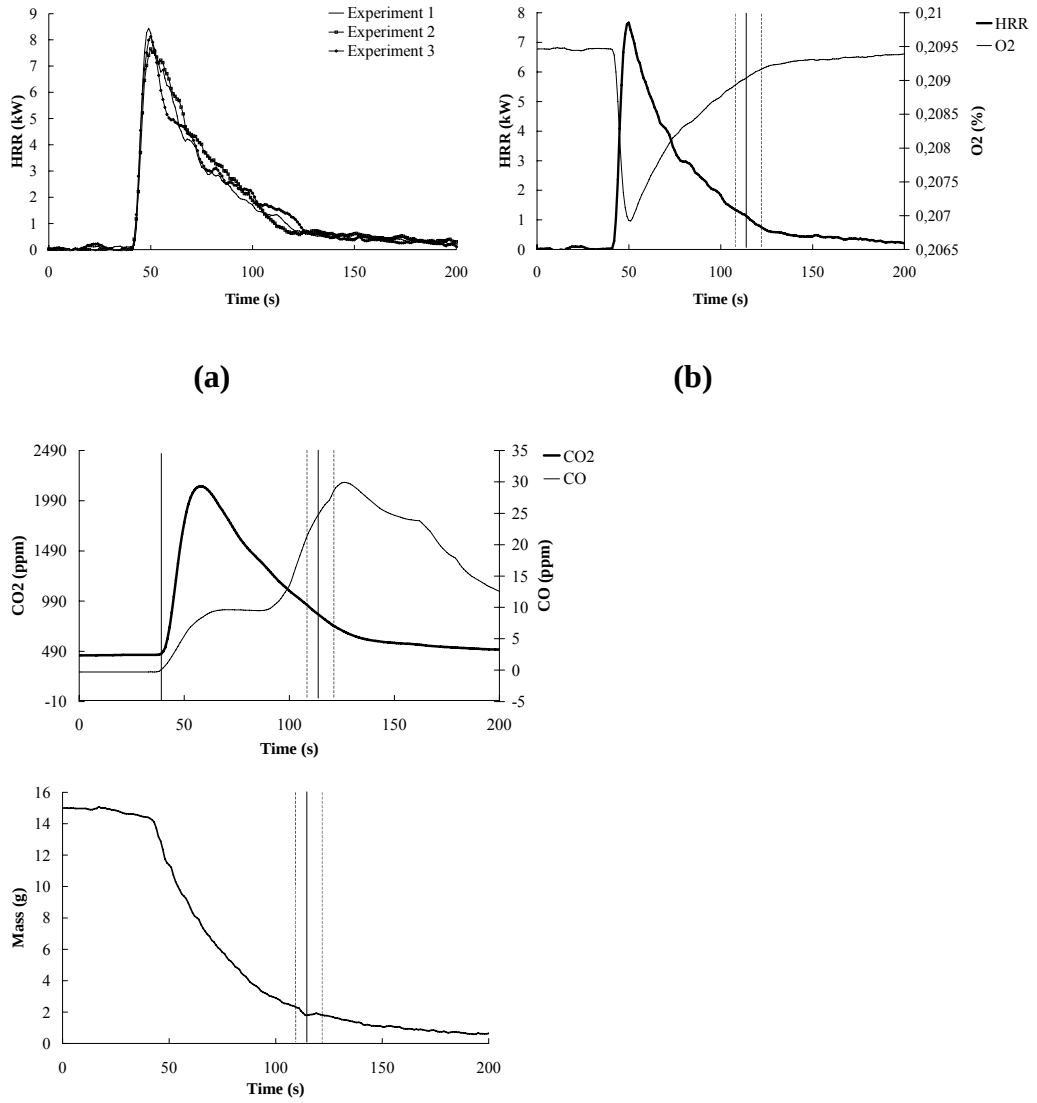

Figure 4. Burning of three samples with no-flow and 26% opening baskets for *Pinus halepensis* needles – a) three repetitions b) mean O_2 consumption and mean heat release rate c) mean CO_2 and CO productions d) mean mass loss. The vertical lines represent ignition and flameout times.

(a)

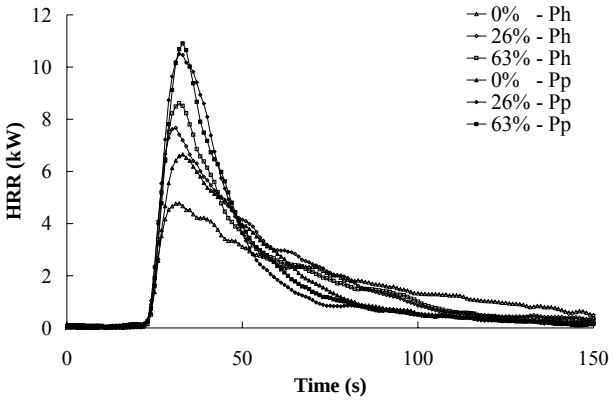

(b)

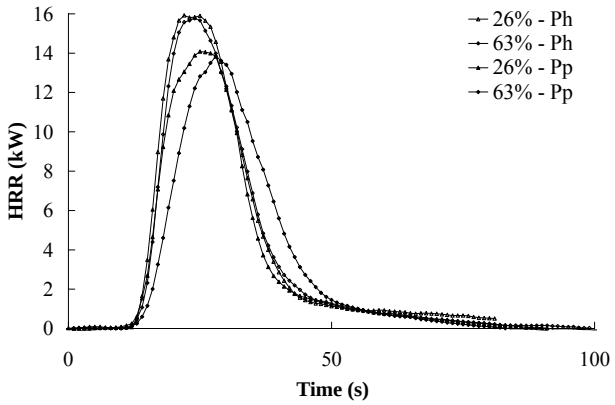

Figure 5. Mean heat release rates for the different baskets with *Pinus halepensis* and *Pinus pinaster* – a) no-flow b) flow conditions

(a)

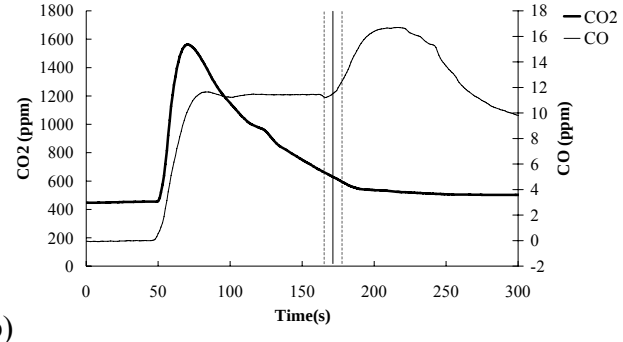

(b)

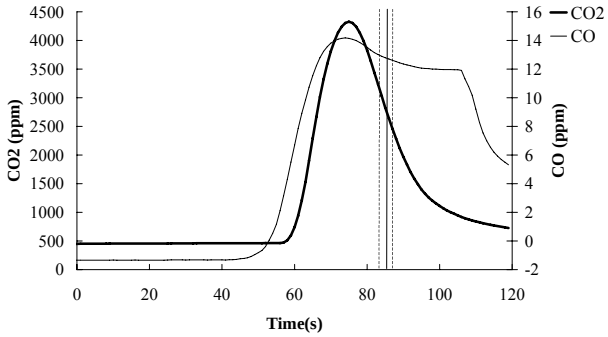

Figure 6. Mean CO_2 and *CO* concentrations for *Pinus halepensis* needles a) no-flow and 0% opening b) flow and 26% opening (vertical lines indicate flameout)

Table 1. Experimental design

Test Number	Fuel Type	Basket Opening	Combustion Air Condition
1-3	*Pinus pinaster*	0%	Natural Convection
4-6	*Pinus halepensis*	0%	Natural Convection
7-9	*Pinus pinaster*	26%	Natural Convection
10-12	*Pinus pinaster*	26%	Forced Flow
13-15	*Pinus halepensis*	26%	Natural Convection
16-18	*Pinus halepensis*	26%	Forced Flow
19-21	*Pinus pinaster*	63%	Natural Convection
22-24	*Pinus pinaster*	63%	Forced Flow
25-27	*Pinus halepensis*	63%	Natural Convection
28-30	*Pinus halepensis*	63%	Forced Flow

Table 2. Factor: Combustion air flow condition effect on peak HRR

Factor(s)/Level	**Mean Value of Peak HRR (SEE) [kw/m^2]**	**N**
Flow	12.893 (0.264)	12
No-flow	8.695 (0.187)	18

Table 3. Combustion air flow, basket opening and fuel effect on time to ignition

Factor(s)/Level	**Mean Value of Time to Ignition (s)**	**Standard Error (s)**	**n**
Combustion Air/ Flow	106	4	12
Combustion Air/ No-flow	53	3	18
Basket/0	79	6	6
Basket/26	68	4	12
Basket/63	90	4	12
Fuel / *Pinus halepensis*	69	4	15
Fuel / *Pinus pinaster*	89	4	15